a Monina

Contents

Introduction

The theoretical framework which describes the strong interaction of quarks and gluons, fundamental constitutes of matter, is the gauge theory of *quantum chromodynamics* (QCD), which enables to calculate not only the properties of protons and neutrons, but in principle also those of atomic nuclei.

Once the QCD has been proposed, it became field of research to study the predictions for nuclear matter in extreme conditions.

The investigation of the confined-deconfined phase transition and of the quark gluon plasma (QGP) is intensively studied and searched experimentally in ultra-relativistic heavy-ion collisions at RHIC in Brookhaven and, in the next feature, at LHC in CERN.

Theoretically, solving the equations of motion of the theory is still a challenge as well as determining simple hadronic properties. A way to solve this problem is based on the observation of a formal mathematical equivalence between statistical mechanics and quantum field theory, written using the *Feynman path integral formulation*. And to give the path integrals a precise meaning has been introduced a space-time lattice, a tool to study the theory non perturbatively.

The lattice approach that we use is based on a Monte Carlo simulations.

Although up today there are powerful computers, simulating the full QCD is very time consuming and rather difficult. For these reasons in these years different kind of approximations have been introduced.

Firstly, the essential features of confinement, of the deconfinement phase transition at finite temperature and of the deconfined phase in QCD can be studied without loss of relevant dynamics in the regime of infinitely massive quarks or, equivalently, in the

pure gauge theory.

Moreover, it has been suggested (and already proved) that some of the main properties of a theory of interest can be studied looking at the more simple models, the spin systems, if these two theories belong to the same *universality class*.

But also a huge contribution to the explanation and comprehension of the theory is given by effective theories which describe phenomena such as high temperature phases (*Polyakov loop Models*).

All of these are subjects of the present Thesis. In particular, after a review of the theoretical background necessary to understand the subsequent work (Introduction), we focus on the Universality between the pure gauge theory which describes the strong interactions and a spin model (Chapter 2), then studying the structure of the hadronic "tube" in the confined and in the deconfined phase (Chapter 3), and finally (Chapter 4), studying a particular tool of the theory with the aim to improve the quality of the description of the effective low energy string theories.

Chapter 1

Theoretical background

1.1 Gauge Theories

Quantum field theories have been successful in predicting physical observables related to the world of elementary particles. In particular, the interactions among elementary particles are described by a particular class of field theories namely by gauge theories. These theories are characterized by the property of invariance under gauge symmetry. Up today, strong, weak and electromagnetic interactions are described by gauge theories; only the gravitational interaction is subtracted from this description.

Gauge field theories are field theories based on the gauge principle. The gauge principle is the requirement that the theory is invariant under local gauge transformations. In a global invariance the same transformation is carried out at all space-time points: it has an 'everywhere simultaneously' character. In a *local invariance* different transformations are carried out at different individual space-time points. In general, a theory that is globally invariant will not be invariant under locally varying transformations. However, by introducing new force fields that interact with the original particles in the theory in a specific way, and which also transform in a particular way under local transformations, a sort of local invariance can be restored. In this sense, one may view these special force fields and their interactions as existing in order to permit certain local invariances to

be true. As an example, the particular local invariance relevant to electromagnetism is the gauge invariance of Maxwell's equations (in the quantum form of the theory this property is directly related to an invariance under local phase transformations of the quantum fields). A generalized form of this phase invariance also underlies the theories of the weak and strong interactions. For this reason they are all 'gauge theories' [1].

When a certain global invariance is generalized to a local one, the existence of a new 'compensating' field is entailed, interacting in a specified way. The first example of dynamical theory 'derived' from a local invariance requirement is the theory of Yang-Mills [2]. Their work was extended by Utiyama [3], who developed a general formalism for such compensating fields.

The strong interactions, responsible for the hadronic and nuclear structure, are described by a quantum field theory, which is a non-Abelian gauge theory called quantum chromodynamics (QCD) and was originally introduced by Yang and Mills [2]. [1]

Non-Abelian gauge field theories are gauge theories similar to quantum electrodynamics though differing from it in that the corresponding gauge symmetries are not Abelian, i.e., generators of the symmetry group are non-commutative.

The non-Abelian gauge theories are generated by symmetries described by a non commutative Lie algebra. The Lie algebra [2] corresponding to the G group is generated by n generators T^a, $a = 1, 2, \cdots, n$, which are subject to the commutation relations

$$[T^a, T^b] = if^{abc}T^c, \tag{1.1}$$

where f^{abc} are the structure constants characterizing the algebra of the group G. The non-Abelian local gauge transformations for a field $\psi(x)$, belonging to a N-dimensional fundamental representation of the G group (thus $\psi(x)$ has N components) under the

[1] Later 't Hooft [4], Gross and Wilczek [5] and Politzer [6] examined non-Abelian gauge field theories using the renormalization group method and found that they satisfied the property called asymptotic freedom.

[2] A Lie group is a group with elements labeled by a finite number of continuous parameters and a multiplication law depending smoothly on the parameters.

operation of the group element U of G is

$$\psi_i^{'} = U_{ij}\psi_j, \quad U = \exp(-iT^a\theta^a) \ , \tag{1.2}$$

where θ^a are parameters which may depend on x as well. The general form of the Lagrangian invariant under the non-Abelian local gauge transformations (1.2) is the following

$$L = -\frac{1}{4}F^a_{\mu\nu}F^{a\mu\nu} + \bar{\psi}(i\gamma^\mu D_\mu - m)\psi \ , \tag{1.3}$$

where D_μ is the covariant derivative

$$D_\mu = \partial_\mu - igT^aA^a_\mu \ , \tag{1.4}$$

g is the coupling of the theory and A^a_μ obeys the transformation rule

$$T^aA^{'a}_\mu = U(T^aA^a_\mu - \frac{i}{g}U^{-1}\partial_\mu U)U^{-1} \ . \tag{1.5}$$

If $G \in SU(2)$ then $T^a = \tau^a/2$ $(a = 1, 2, 3)$ where τ^a are the Pauli matrices and $f^{abc} = \epsilon^{abc}$ is the totally antisymmetric tensor. Otherwise, if $G \in SU(3)$ then $T^a = \tau^a/2$ $(a = 1, 2, \cdots, 8)$ where τ^a are the Gell-Mann matrices.

Gauge theories are characterized by a close interrelation between three conceptual elements: symmetries, conservation laws and dynamics. In fact, it is now believed that the only exact quantum number conservation laws are those which have an associated gauge theory force field.

The Quantum Electrodynamics (QED) and the Quantum Chromodynamics (QCD) posses a local symmetry, in particular, the local symmetry group is a continuous one (for the former $U(1)$, and for the latter $SU(3)$). The action in these theories is obtained by gauging the global symmetry of the free fermions and by adding a kinetic term for the gauge fields.

Let us briefly review how one arrives at the gauge-invariant action in continuum QED (for this section we follow the description of [7]), which is the simplest gauge theory. The starting point is the action of the free Dirac field:

$$S_F^{(0)} = \int d^4x\bar{\psi}(x)(i\gamma^\mu\partial_\mu - M)\psi(x) \ , \tag{1.6}$$

which is invariant under transformations

$$\begin{aligned} \psi(x) &\rightarrow G\psi(x) \\ \bar{\psi}(x) &\rightarrow \bar{\psi}(x)G^{-1} \ , \end{aligned}$$

where G is an element of the abelian $U(1)$ group

$$G = e^{i\lambda} \ ,$$

with λ independent of x. The next step consists in requiring the action to be invariant under local $U(1)$ transformations. This means to introduce the four-vector potential $A_\mu(x)$ and to replace the ordinary four-derivative ∂_μ by the covariant derivative D_μ, defined by

$$D_\mu = \partial_\mu + ieA_\mu \ . \tag{1.7}$$

The action so obtained

$$S_F = \int d^4x \bar{\psi}(x)(i\gamma_\mu D^\mu - M)\psi(x) \ , \tag{1.8}$$

is invariant under the following set of local transformations

$$\begin{aligned} \psi(x) &\rightarrow G(x)\psi(x) \ , \\ \bar{\psi}(x) &\rightarrow \bar{\psi}(x)G^{-1}, \\ A_\mu(x) &\rightarrow G(x)A_\mu(x)G^{-1}(x) - \frac{i}{e}\, G(x)\partial_\mu G^{-1}(x) \ , \end{aligned} \tag{1.9}$$

where

$$G(x) = e^{i\Lambda(x)} \ . \tag{1.10}$$

Having ensured the local gauge invariance of the action (1.8) by introducing a four-vector field A_μ, we must add a kinetic term which allows A_μ to propagate. Also this term must be invariant under the local transformations (1.9), and is given by

$$S_G = -\frac{1}{4}\int d^4x F_{\mu\nu}F^{\mu\nu}, \tag{1.11}$$

where $F_{\mu\nu} = \partial_\mu A_\nu - \partial_\nu A_\mu$ is the gauge invariant field strength tensor. The full gauge invariant action is then

$$S_{QED} = -\frac{1}{4}\int d^4x F_{\mu\nu}F^{\mu\nu} + \int d^4x \bar{\psi}(i\gamma^\mu D_\mu - M)\psi \ . \tag{1.12}$$

Now we pass to the euclidean version of the (1.8) and (1.11); making the following transformations:

$$\begin{aligned} x^0 &\rightarrow -ix_4 \\ A^0 &\rightarrow +iA_4 \ , \end{aligned}$$

then the (1.11) becomes

$$S_G^{(eucl)} = \frac{1}{4}\int d^4x F_{\mu\nu}F_{\mu\nu} \ , \tag{1.13}$$

where a sum over μ and ν ($\mu, \nu = 1, 2, 3, 4$) is understood. For the (1.8) we obtain

$$S_F^{(eucl)} = \int d^4x \bar{\psi}(x)(\gamma_\mu^E \partial_\mu + M)\psi(x) \ . \tag{1.14}$$

Here γ_μ^E is the set of γ matrices which satisfy the following algebra

$$\{\gamma_\mu^E, \gamma_\nu^E\} = 2\delta_{\mu\nu} \ ,$$

with $\gamma_4^E = \gamma^0, \quad \gamma_i^E = -i\gamma^i$. We stress, moreover, that in the euclidean space, the group of Lorentz is substituted with that of four-dimensional rotations.

Since we shall work with the euclidean formulation, to simplify the notation we shall drop the symbols E and $(eucl)$.

1.2 The Lattice Gauge Theories

The lattice represents a mathematical tool [8], which provides a cutoff removing the ultraviolet infinities in the quantum field theory and, as with any regulator, it must be removed after renormalization. We stress that physics can only be extracted in the continuum limit, where the lattice spacing is taken to zero. [3]

[3] For a more detailed description of the continuum limit see the next paragraphs.

Let us briefly recall the renormalization program in continuum perturbation theory. The renormalization of the Green function first requires the regularization of the corresponding Feynman integrals (which will be introduced in the next paragraph) in momentum space. These integrals will depend on one or more parameters which are introduced in the regularization process. Since the effect of any regularization procedure is to render the momentum integrations ultraviolet finite, this step corresponds in the introduction of a momentum cutoff. The second step consists in defining renormalized Green functions, which approach a finite limit as the cutoff is removed. The dependence of the cutoff is "absorbed" by the bare parameters of the theory. This dependence is determined by imposing a set of renormalization conditions.

In the lattice approach this program can be formulated without reference to perturbation theory. Let us see how. The first step (regularization) consists in introducing a space-time lattice at the level of the path integral. The second step of the renormalization corresponds to removing the lattice structure (which means to study the continuum limit). We stress that the introduction of a space-time lattice corresponds to a particular way of regularizing Feynman integrals without introducing a momentum cutoff. In particular the momentum space integrals will indeed be cut off at a momentum of the order of the inverse lattice spacing, but the integrands of Feynman integrals will be modified in a non-trivial way. Just to have an idea of how the lattice-regularization works, let us consider a function $f(x)$ of a single continuous variable. If its absolute value is square integrable, then $f(x)$ has the following Fourier representation:

$$f(x) = \int_{-\infty}^{+\infty} \frac{dk}{2\pi} \tilde{f}(k) e^{ikx} \ . \tag{1.15}$$

If x is restricted to a multiple of a lattice spacing a ($x = na$ with n an integer), then $f(na)$ can be Fourier-decomposed

$$f(na) = \int_{-\frac{\pi}{a}}^{\frac{\pi}{a}} \frac{dk}{2\pi} \tilde{f}_a(k) \ e^{ikna} \ , \tag{1.16}$$

where $\tilde{f}_a(-\frac{\pi}{a}) = \tilde{f}_a(\frac{\pi}{a})$. Here the momentum integration is now restricted to the so-called first Brillouin zone $[-\frac{\pi}{a}, \frac{\pi}{a}]$. This is the cut of the momentum of the order of

the inverse lattice spacing. If $\tilde{f}_a(k)$ satisfies the Dirichlet conditions, then it can be represented by a Fourier series

$$\tilde{f}_a(k) = a \sum_{n=-\infty}^{\infty} f(na)\, e^{-inka} \,, \tag{1.17}$$

which is just the discretized version of the expression for $\tilde{f}$ obtained by inverting the (1.15).

The above formulas are trivially extended to functions depending on an arbitrary number of variables. In particular, in four space-time dimensions, all four components of momenta will be restricted to the interval $[-\frac{\pi}{a}, \frac{\pi}{a}]$.

In the next three paragraphs we will introduce the path integral formulation, the study of the continuum limit and the lattice approach for the case of our interest.

1.2.1 The Path Integrals Formulation

The theory of quantized fields has its origin in the early days of quantum mechanics [9]. After a seminal work of Heisenberg [10], the subsequent article of Born and Jordan [11] already contains a section in which the quantization of the electromagnetic field is sketched.

In the following years the idea of quantizing classical fields was pursued further by P. Jordan [11]. He also aimed at a representation of matter by quantized fields. The Schrödinger wave is considered as classical fields and so he called this procedure *second quantization*.

Quantization is not at all a unique procedure and a variety of quantization methods may exist which lead to the same physical prediction [12].

The path integral method is an alternative formulation of quantum mechanics, which has been reviewed by Feynman [13, 14] and since its introduction has became a very important tool for elementary particle physics.

It was his genius to realize [4] that the propagator of the time-evolution operator can

[4] Surprisingly enough, the same calculus, in the sense of a naïve analytical continuation, was already

be expressed as a sum over all possible paths connecting the points (q,t) and (q',t') with weight factor $\exp[iS(q',t';q,t)]$, where S is the classical action.

Following the description by Rothe [7], we illustrate briefly the principal lines of the so important Feynman's formulation. [5] In quantum mechanics the transition amplitude is given by the Green function:

$$G(q',t';q,t) = \langle q'|e^{-iH(t'-t)}|q\rangle \ , \tag{1.18}$$

where H is the Hamiltonian. For reasons which will be clearer later, we shall need the corresponding representation for the Green function continued to imaginary time (passing from the Minkowski space-time to the euclidean one), which means $t \to -i\tau, \quad t' \to -i\tau'$. So we obtain:

$$G(q',\tau';q,\tau) = \langle q'|e^{-H(\tau'-\tau)}|q\rangle \ . \tag{1.19}$$

To obtain a path integral representation let us split the time interval $[\tau,\tau']$ into N infinitesimal segments of length $\epsilon = (\tau'-\tau)/N$ and assume that the Hamiltonian has the form

$$H = \frac{1}{2}\sum_{\alpha=1}^{n} P_\alpha^2 + V(Q) \ , \tag{1.20}$$

where P_α are the momenta canonically conjugate to Q_α. It is easily showed that, for small ϵ

$$\langle q'|e^{-H(\tau'-\tau)}|q\rangle \approx \left(\frac{1}{\sqrt{2\pi\epsilon}}\right)^{nN} \int \prod_{l'=1}^{N-1} dq^{(l')} e^{-\sum_{l=0}^{N-1}\epsilon L_E(q^{(l)},\dot{q}^{(l)})} \ , \tag{1.21}$$

known to mathematicians due to Wiener in the study of stochastic process. This calculus in the functional space, "Wiener measure", attracted several mathematicians, including Kac and was further developed by several authors, where the best known is the work of Cameron and Martin. The standard reference concerning these achievements is the review paper of Gelfand and Yaglom [15].

[5] In classical physics the time evolution of the system is given by the Lagrange equations of motion which follow from the principle of least action. To quantize the system, one then constructs the Hamiltonian, and writes the equations of motion in term of Poisson brackets. This provides the starting point for the canonical quantization of the theory. Proceeding in this way, one has moved far away from the original action principle. The path integral representation reestablishes the connection with the classical action principle.

where

$$L_E(q^{(l)}, \dot{q}^{(l)}) = \sum_\alpha \frac{1}{2}(\dot{q}_\alpha^{(l)})^2 + V(q^{(l)}),$$
$$\dot{q}_\alpha^{(l)} \equiv \frac{\dot{q}_\alpha^{(l+1)} - q_\alpha^{(l)}}{\epsilon} , \tag{1.22}$$

with $q^{(0)} \equiv q, \quad q^{(N)} \equiv q'$. The subscript "E" is to remind us that we are working on the "euclidean" space-time. Let us pass to the interpretation of the right-hand side of (1.21). Consider an arbitrary path in q-space connecting the space-time points (q, τ) and (q', τ'), consisting of straight line segments in every infinitesimal time interval. The action associated with the path is given by

$$S_E[q] = \sum_{l=0}^{N-1} \epsilon[\sum_\alpha \frac{1}{2}(\dot{q}_\alpha(\tau_l))^2 + V(q(\tau_l))] , \tag{1.23}$$

which is just the expression appearing in the argument of the exponential in (1.21). In conclusion, it is possible to summarize the prescriptions for calculating the Green function for imaginary time in four steps:

1. divide the interval $[\tau, \tau']$ into infinitesimal segments of length ϵ;

2. consider all possible paths connecting the points (q, τ) and (q', τ') and calculate the action (1.23) for each path;

3. weight each path with $e^{-S_E[q]}$ and sum these exponentials over all paths, by integrating over all possible values of the coordinates at intermediate times;

4. multiply the resulting expression with $(\frac{1}{\sqrt{2\pi\epsilon}})^{nN}$, where n is the number of coordinate degrees of freedom and take the limit $\epsilon \to 0, \quad N \to \infty$, keeping the product $N\epsilon = (\tau' - \tau)$ fixed.

The result of this procedure is denoted by

$$(q', \tau'|q, \tau) = \int_q^{q'} Dq e^{-S_E[q]} , \tag{1.24}$$

where

$$S_E[q] = \int_\tau^{\tau'} d\tau'' L_E(q(\tau''), \dot{q}(\tau'')) . \tag{1.25}$$

For convenience we have adopted the following short-hand notation

$$(q', \tau'|q, \tau) \equiv \langle q'|e^{-H(\tau'-\tau)}|q\rangle \ . \tag{1.26}$$

In the real time formulation, the analogous procedure leads to the following path integral representation:

$$\langle q'|e^{-iH(t'-t)}|q\rangle = \int_q^{q'} \ Dqe^{iS[q]} \ , \tag{1.27}$$

where $S[q]$ is the action for the real time. Now we can understand the convenience and geniality of passing to imaginary time. Notice in fact, that since the paths in (1.24) are weighted with e^{-S_E}, the important contributions come from the paths for which the action takes values close to the minimum. As said in the previous note, the Feynman's formalism leads to the principle of least action which in its turn brings, to the classical euclidean equations of motion. In the path integral (1.27) the paths are instead weighted with an oscillating function and for this reason this representation is not suited for numerical calculations. Some comments are now necessary. The first one is that for the path integrals (1.24) or (1.27) an exact evaluation is possible only in a few case (for example the harmonic oscillator in the real time formulation). The second is that the path integral representation of Green function opens the possibility of studying field theories non-perturbatively. If the action is bounded from below, then the (1.24) has the form of a statistical ensemble average with a Boltzmann distribution given by e^{-S_E}. Because of this similarity with the statistical mechanics we call the euclidean Green functions as *correlation functions* and the expression

$$Z = \int \ Dqe^{-S_E[q]} \ , \tag{1.28}$$

as the *partition function*. So to calculate Green functions in theories with a large number of degrees of freedom we will use statistical methods.

For completeness of exposition we report the formalism extended to a field theory [6] (obtained by allowing the number of variables to approach infinity). For bosonic fields

[6] In quantum mechanics all physical information about the quantum system is contained in the Green function (1.18), instead in field theory this information is stored in an infinite set of vacuum expectation values of time-ordered products of Heisenberg field operators.

the Green function in the path integral representation is given by [7]

$$G(x_1, x_2, \cdots, x_l) = \langle 0|T(\hat{\phi}(x_1)\hat{\phi}(x_2)\cdots\hat{\phi}(x_l))|0\rangle = \frac{\int D\phi\ \phi(x_1)\phi(x_2)\cdots\phi(x_l)\ e^{-S_E[\phi]}}{\int D\phi\ e^{-S_E[\phi]}} \tag{1.29}$$

For fermionic fields the path integral is [7]

$$\langle 0|T(\hat{\psi}_{\alpha_1}(x_1)\cdots\hat{\psi}_{\alpha_l}(x_l)\hat{\psi}_{\beta_1}(y_1)\cdots\hat{\psi}_{\beta_l}(y_l))|0\rangle = \frac{\int D(\bar{\psi}\psi)\ \psi_{\alpha_1}(x_1)\cdots\psi_{\alpha_l}(x_l)\psi_{\beta_1}(y_1)\cdots\psi_{\beta_l}(y_l))\ e^{-S_E[\phi]}}{\int D\phi\ e^{-S_E[\phi]}}\ , \tag{1.30}$$

where the integration is over Grassmann variables (anti-commuting c-numbers).

In the traditional canonical operator formalism, one regards fields as operators and sets up canonical commutation relations for them. All Green functions which characterize the quantum theory of fields may be calculated as vacuum expectation values of the product of the field operators. In Feynman functional-integral formalism, the fields are c-numbers and the Lagrangian is of the classical form. The Green functions are obtained by integrating the product of the fields over all of their possible functional forms with a suitable weight. In the stochastic formalism, one notes the similarity between the functional-integral expression of Green functions in Euclidean space and the statistical averaging and regards the field as a stochastic variable. The Green functions are then given by the statistical average of the product of fields in equilibrium.

1.2.2 Gauge Theories on the Lattice

The path integral expression for the Green functions has only a well-defined meaning for systems with a denumerable number of degree of freedom [7]. In field theory, however, the degrees of freedom are an infinite number, and the multiple integrals are only formally defined. To give a precise meaning to the path integrals it is necessary discretize time and space, which leads the introduction of a space-time lattice with lattice spacing a.

In this section we introduce Wilson's formulation of gauge fields on a space-time lattice, following the description of [8].

Every point on the lattice is specified by integers collectively denoted by $n = (n_1, n_2, n_3, n_4)$ (in the case of 3 spatial dimension). By convention the last component will denote euclidean time.

Let us start our description of the lattice gauge theories considering the "construction" of the lattice QED, having dealt with in the previous section this simplest gauge theory (for a more detailed description see [7]).

We want to rewrite the (1.14) in terms of dimensionless lattice variables. This simply means to make the appropriate substitutions for M, ψ e $\bar{\psi}$ with respect the lattice spacing a. The transformations are:

$$\begin{aligned} M &\rightarrow \frac{1}{a}\hat{M} \ , \\ \psi_\alpha(x) &\rightarrow \frac{1}{a^{\frac{3}{2}}}\hat{\psi}_\alpha(n) \ , \\ \bar{\psi}_\alpha(x) &\rightarrow \frac{1}{a^{\frac{3}{2}}}\bar{\hat{\psi}}_\alpha(n) \ , \\ \partial_\mu\psi(x) &\rightarrow \frac{1}{a^{\frac{5}{2}}}\hat{\partial}_\mu\hat{\psi}_\alpha(n) \ , \end{aligned} \tag{1.31}$$

where $\hat{\partial}_\mu$ is defined as

$$\hat{\partial}_\mu\hat{\psi}_\alpha(n) = \frac{1}{2}[\hat{\psi}_\alpha(n+\hat{\mu}) - \hat{\psi}_\alpha(n-\hat{\mu})] \ . \tag{1.32}$$

Then the lattice version of the desired action is

$$S_F = \sum_{\substack{n,m \\ \alpha,\beta}} \bar{\hat{\psi}}_\alpha(n) K_{\alpha\beta}(n,m) \hat{\psi}_\beta(m) \ , \tag{1.33}$$

with

$$K_{\alpha\beta}(n,m) = \sum_\mu \frac{1}{2}(\gamma_\mu)_{\alpha\beta}[\delta_{m,n+\hat{\mu}} - \delta_{m,n-\hat{\mu}}] + \hat{M}\delta_{mn}\delta_{\alpha\beta} \ . \tag{1.34}$$

After making a shift in the summation variable, the corresponding action can be written in the form

$$S_F = \hat{M}\sum_n \hat{\bar{\psi}}(n)\hat{\psi}(n) + \frac{1}{2}\sum_{n,\mu}[\hat{\bar{\psi}}(n)\gamma_\mu\hat{\psi}(n+\hat{\mu}) - \hat{\bar{\psi}}(n+\hat{\mu})\gamma_\mu\hat{\psi}(n)] \ . \tag{1.35}$$

The action (1.35) is invariant under the global transformations

$$\begin{aligned} \psi(n) &\rightarrow G\psi(n) \ , \\ \bar{\psi}(n) &\rightarrow \bar{\psi}(n)G^{-1} \ , \end{aligned}$$

where G is an element of the $U(1)$ group.

Now we require that the theory be invariant under local $U(1)$ transformations, with the group element G depending on the lattice site. Concentrating on the off-diagonal elements of the (1.35), we introduce a factor which depends on the gauge potential $A_\mu(x)$. It is possible to demonstrate that to arrive at a gauge-invariant expression for the fermionic action on the lattice, we have to make the following substitutions in (1.35)

$$\begin{aligned} \hat{\bar{\psi}}(n)\gamma_\mu\hat{\psi}(n+\hat{\mu}) &\rightarrow \hat{\bar{\psi}}(n)\gamma_\mu U_{n,n+\hat{\mu}}\hat{\psi}(n+\hat{\mu}) \\ \hat{\bar{\psi}}(n+\hat{\mu})\gamma_\mu\hat{\psi}(n) &\rightarrow \hat{\bar{\psi}}(n+\gamma_\mu)\gamma_\mu U_{n+\hat{\mu},n}\hat{\psi}(n) \ , \end{aligned} \tag{1.36}$$

where

$$U_{n+\hat{\mu},n} = U^\dagger_{n,n+\hat{\mu}} \ , \tag{1.37}$$

is an element of the $U(1)$ gauge group. It can therefore be written as

$$U_{n,n+\hat{\mu}} = e^{i\phi_\mu(n)} \ , \tag{1.38}$$

where $\phi_\mu(n)$ is restricted to the compact domain $[0, 2\pi]$. We stress that the group element $U_{n,n+\hat{\mu}}$ lives on the links connecting two neighboring lattice sites; we refer them as link variables and sometimes simply as links.

In the continuum limit the (1.35) must be of the form (1.14). This establishes a relation between the link variables and the vector potential $A_\mu(n)$. The vector potential $A_\mu(n)$ at the lattice site n is real-valued and carries a Lorentz index. The same is true for ϕ_μ (which parametrizes the link variable (1.38)). But ϕ_μ takes only values in the interval $[0, 2\pi]$, while the A_μ's values extend over the entire real line. However, A_μ carries the dimension of inverse length, while ϕ_μ is dimensionless. It is so possible to make the following ansatz:

$$\phi_\mu = caA_\mu \ ,$$

where a is the lattice spacing and c is a constant to be determined. Using (1.31) and substituting in $U_{n,n+\hat{\mu}}$ its expression for small a,

$$U_{n,n+\hat{\mu}} \approx 1 + icaA_\mu \ ,$$

equation (1.35) is reduced to (1.14) in the naive continuum limit, if we choose $c = e$. We underline the connection between $U_{n,n+\hat{\mu}}$ and $A_\mu(n)$ using the more suggestive notation

$$U_\mu(n) \equiv U_{n,n+\hat{\mu}} = e^{ieaA_\mu} \ . \tag{1.39}$$

To complete our construction of the lattice action for the QED, we must obtain the lattice version of (1.13), which should be strictly gauge-invariant and be a functional of the link variables only. Such gauge-invariant functionals are constructed by taking the product of link variables around closed loops on the euclidean space-time lattice. Since the integrand of the (1.13) has a local structure, we should focus on the smallest possible loops. It is so defined the path-ordered product of link variables around an elementary plaquette. Let this plaquette lying in the $\mu - \nu$ plane, we then define it as

$$U_{\mu\nu}(n) = U_\mu(n)U_\nu(n+\hat{\mu})U_\mu^\dagger(n+\hat{\nu})U_\nu^\dagger(n) \ . \tag{1.40}$$

Inserting (1.39) in the (1.40), one finds

$$U_{\mu\nu}(n) = e^{iea^2F_{\mu\nu}(n)} \ , \tag{1.41}$$

where $F_{\mu\nu}(n)$ is the discretized version of the field strength tensor:

$$F_{\mu\nu}(n) = \frac{1}{a}[(A_\nu(n+\hat{\mu}) - A_\nu(n)) - (A_\mu(n+\hat{\nu}) - A_\mu(n))] \ .$$

From (1.41) it follows that, for small lattice spacing,

$$\frac{1}{4}\sum_{\substack{n \\ \mu,\nu}} a^4 F_{\mu\nu}(n)F_{\mu\nu}(n) \approx \frac{1}{e^2}\sum_n \sum_{\substack{\mu,\nu \\ \mu<\nu}} [1 - \frac{1}{2}(U_{\mu\nu}(n) + U_{\mu\nu}^\dagger(n))] \ . \tag{1.42}$$

In conclusion, the lattice action for the QED gauge potential in the compact form is

$$S_G[U] = \frac{1}{e^2}\sum_P [1 - \frac{1}{2}(U_P + U_P^\dagger)] \ , \tag{1.43}$$

where U_P (plaquette variable) stands for the product of link variables around the boundary of a plaquette "P" taken in the counterclockwise direction. We want to stress that, with respect to the continuum limit, the coupling now appears as an inverse power in the action for the gauge field.

1.2.3 The QCD on the Lattice

The lattice gauge theory we have discussed since now can be easily extended to the case of non-abelian unitary group, which is the case of the QCD.

We only have to replace the Dirac fields ψ and $\hat{\psi}$ by N-component vectors and the link variables $U_\mu(n)$ by the corresponding group elements of $SU(N)$ in the fundamental (N dimensional) representation.

The simplest way to obtain a gauge-invariant quantity from the group elements $U_\mu(n)$ is to take the trace of the path ordered product of link variables along the boundary of an elementary plaquette,

$$U_{\mu\nu}(n) = U_\mu(n)U_\nu(n+\hat{\mu})U_\mu^\dagger(n+\hat{\nu})U_\nu^\dagger(n) \ . \tag{1.44}$$

In analogy to the abelian case we find

$$S_G[U] = c\mathrm{Tr}\sum_{n,\mu<\nu}\left[1-\frac{1}{2}(U_{\mu\nu}(n)+U_{\mu\nu}^\dagger(n))\right] \ , \tag{1.45}$$

where c is a constant to be determined

Since we are interested in describing the strong interactions, we focus on $SU(3)$ group. Any elements Θ lying in the Lie algebra of $SU(3)$ can be written in the form

$$\Theta = \sum_{B=1}^{8}\Theta^B\frac{\lambda^B}{2} \ ,$$

where the eight group generators λ^B are usually chosen to be the Gell-Mann matrices, satisfying the commutation relations

$$[\lambda^A,\lambda^B] = 2i\sum_{C=1}^{8} f_{ABC}\lambda^C. \tag{1.46}$$

The f_{ABC} are the completely antisymmetric structure constants of the group.

Let us study the continuum limit of the (1.45) for the case $N=3$. To this effect we introduce a dimensioned matrix valued lattice field $A_\mu(n)$ as follows,

$$\phi_\mu(n) = g_0 a A_\mu(n) \ , \tag{1.47}$$

with $\phi_\mu(n)$ defined by an expression analogous to that of the abelian case,

$$U_\mu(n) = e^{i\phi_\mu(n)} \ , \tag{1.48}$$

where g_0 is the bare coupling constant. Since $A_\mu(n)$ is an element of the Lie algebra of $SU(3)$, it is of the form

$$A_\mu(n) = \sum_{B=1}^{8} A_\mu^B(n)\frac{\lambda^B}{2} \ , \tag{1.49}$$

where $A_\mu^B(n)$ are eight real-valued vector fields corresponding to the eight generators of $SU(3)$.

We define, in analogy to (1.41), the matrix-valued lattice field tensor $F_{\mu\nu}(n)$ by

$$U_{\mu\nu}(n) = e^{ig_0a^2F_{\mu\nu}(n)} \ . \tag{1.50}$$

To determine the relation between $F_{\mu\nu}(n)$ and $A_\mu(n)$ we use the Baker-Hausdorff formula

$$e^Ae^B = e^{A+B+\frac{1}{2}[A,B]+\cdots} \ . \tag{1.51}$$

Recalling that for the (1.47), $\phi_\mu(n)$ is proportional to the lattice spacing a (which has to be small), then it will be calculated only the quadratic terms in a of the exponential (1.51). One finds

$$F_{\mu\nu} \overset{a\to 0}{\to} F_{\mu\nu} = \partial_\mu A_\nu - \partial_\nu A_\mu + ig_0[A_\mu, A_\nu] \ . \tag{1.52}$$

Since the (1.52) is again an element of the Lie algebra, it can be written in the form

$$F_{\mu\nu} = \sum_{B=1}^{8} F_{\mu\nu}^B\frac{\lambda^B}{2} \ . \tag{1.53}$$

Making use of the (1.46) and of the orthogonality relation of the Gell-Mann matrices,

$$\mathrm{Tr}(\lambda^A\lambda^C) = 2\delta_{BC} \ , \tag{1.54}$$

one arrives at

$$F_{\mu\nu}^B = \partial_\mu A_\nu^B - \partial_\nu A_\mu^B - g_0f_{BCD}A_\mu^CA_\nu^D \ . \tag{1.55}$$

We now compute the continuum limit of the action S_G. Approximating the (1.50) for small lattice spacing by the first two non-trivial terms in the expansion of the exponential and inserting this expression into (1.45) we find

$$S_G \to c\frac{g_0^2}{2}\frac{1}{2}\mathrm{Tr}\int d^4x F_{\mu\nu}F_{\mu\nu} \ , \tag{1.56}$$

where it is understood a sum over μ and ν. We have obtained the well-known gauge field action of QCD; this leads us to choice $c = 2/g_0^2$.

Following the same procedure for the most general case of $SU(N)$, one finds that the gauge part of the lattice action is

$$S_G^{(SU(N))} = \beta \sum_P [1 - \frac{\mathrm{Tr}}{2N}(U_P + U_P^\dagger)] \ , \tag{1.57}$$

where

$$\beta = \frac{2N}{g_0^2} \ . \tag{1.58}$$

As in the abelian case, the sum in (1.57) extends over all distinct plaquettes on the lattice, and we have introduced the short notation U_P for the path-ordered product (1.44) of link variables around the boundary of a plaquette P. For this product both orientations are taken into account (ensuring the hermiticity of the action). The (1.57) is commonly known as *Wilson action*.

1.2.4 The Wilson Loop

One of the most important test of QCD is whether it accounts for confinement in hadronic phase. Hence one expects that quarks within an hadron are sources of chromoelectric flux, which is concentrated within narrow tubes (strings) connecting the constituents. Since the energy is not allowed to spread, the potential of a quark-antiquark pair will increase with their separation, as long as vacuum polarization effects do not screen their color charge. For sufficiently large separations of quarks, the energy stored in the string will be enough to produce a real quark pair, and the system will lower its energy by going over into a new hadronic state. This phenomenon is known as *hadronization process*.

Many informations can be obtained computing the non perturbative potential between a quark-antiquark pair.

On the lattice, for the QCD case, we define the Wilson loop operator by [7]

$$W_C[U] = \mathrm{Tr} \prod_{l \in C} U_l \ , \tag{1.59}$$

where C is a rectangular contour which spatial length is $\hat{R}$ in the spatial dimension and $\hat{T}$ in the temporal one. The U_l are the links variables taking the ordered product. Its ground state expectation value

$$W(\hat{R},\hat{T}) = \langle W_C[U] \rangle \ , \tag{1.60}$$

is given by

$$W(\hat{R},\hat{T}) = \frac{\int DUD\bar{\psi}D\psi W_C[U]\ e^{-S_{QCD}[U,\psi,\bar{\psi}]}}{\int DUD\bar{\psi}D\psi\ e^{-S_{QCD}[U,\psi,\bar{\psi}]}} \ . \tag{1.61}$$

Let us explain the physical meaning of the Wilson loop.

The Wilson loop essentially measures the response of the gauge fields to an external quarklike source passing around its perimeter. For the timelike loop (as that one we have presented here), this represents the production of a quark pair at the earliest time, moving them along the world lines dictated by the sides of the loop and then annihilating at the latest time. A transfer matrix arguments [8] suggests that for large $\hat{T}$

$$W(\hat{R},\hat{T}) \overset{\hat{T}\to\infty}{\sim} \exp(-E(\hat{R})\hat{T}) \ , \tag{1.62}$$

where $E(\hat{R})$ is the gauge field energy associated with the static quark-antiquark sources separated by distance $\hat{R}$. If the interquark energy for large separations grows linearly

$$E(\hat{R}) \overset{\hat{R}\to\infty}{\to} \hat{\sigma}\hat{R} \ , \tag{1.63}$$

with $\hat{\sigma}$ is the string tension measured in lattice units. Then we expect for large loops of long rectangular shape

$$W(\hat{R},\hat{T}) \sim \exp(-\hat{\sigma}\hat{R}\hat{T}) \ . \tag{1.64}$$

The (1.64) is known as *area law* behavior. Physically this area law represents the action of the world sheet of a flux tube connecting the sources.

1.2.5 Lattice Formulation of QCD at Finite Temperature

An important field of research in lattice QCD is the study on the phase transition from the low temperature confining phase to an high temperature phase where quarks and

gluons are deconfined. The search of signatures of the quark gluon plasma (QGP) is object of experiments which use collisions between large massive ions as that ones at CERN [16, 17, 18].

Hence the subject of this section is the lattice formulation of QCD at finite temperature, which allows us to study the non-perturbative behavior of thermodynamical observables in the transition region.

The thermodynamic of a system at temperature T is described by the partition function

$$Z(T,V) = \mathrm{Tr}\ e^{-\frac{H}{T}}\ , \tag{1.65}$$

where H is the Hamiltonian and V is the volume of the system. For convenience we pone the Boltzmann constant equal to one. The thermal expectation value of any observable O is given by

$$\langle O\rangle = \frac{1}{Z}\mathrm{Tr}(Oe^{-\frac{H}{T}})\ . \tag{1.66}$$

Let us consider the path integral representation for the partition function. For a quantum mechanical system consisting of a finite number of degrees of freedom $q_i (i = 1, \cdots, N)$ we have

$$Z(T,V) = \int \prod_i^N dq_i\ \langle q|e^{-\frac{H}{T}}|q\rangle\ , \tag{1.67}$$

where $q = (q_1, \cdots, q_N)$, and where $|q\rangle$ denotes the simultaneous eigenstates of the coordinate operators Q_i with eigenvalues q_i. The path integral representation of the integrand is

$$\langle q|e^{-\frac{H}{T}}|q\rangle = \int_q^q Dq\ e^{-\int_o^{\frac{1}{T}} d\tau L_E(q,\dot{q})}\ , \tag{1.68}$$

where L_E is the euclidean version of the Lagrangian describing the interacting system, and where the path integral is understood to be a sum over all periodic paths starting from q t time $\tau = 0$, and terminating at q at time $\tau = 1/T$. Inserting (1.68) into the (1.67), we see that the partition function is given by the weighted sum over all periodic paths starting and ending at an arbitrary point in coordinate space.

All we found can be easily obtained for a field theory (we consider only bosonic variables). Details can be found in [7].

Let us introduce β as the inverse of the temperature:

$$\beta = \frac{1}{T} \ . \tag{1.69}$$

In this case the partition function is a weighted sum over all field configurations which live on a euclidean space-time surface compactified along the time direction.

We can summarize that, within the path integral formulation, the concept of temperature is introduced by simply compactifying the euclidean time direction and identifying the inverse temperature with the temporal extension of the space-time manifold.

For completeness of exposition we will report in the following the description of the lattice formulation of QCD at finite temperature, having this formulation a very important physical meaning.

We will consider only the case of pure $SU(3)$ gauge theory, because in our research work we did not use fermions at all (see [7] for the complete description of QCD).

The path integral representation in the continuum formulation of the partition function is

$$Z_G = N \int \ DA e^{-S_G^{(\beta)}[A]} \ , \tag{1.70}$$

where N is a normalization constant and $S_G^{(\beta)}[A]$ is the finite temperature action

$$S_G^{(\beta)}[A] = \frac{1}{2} \int_0^\beta d\tau \int d^3x \mathrm{Tr}(F_{\mu\nu} F_{\mu\nu}) \ . \tag{1.71}$$

The path integral (1.70) is to be carried out over all field configurations which satisfy the periodic boundary conditions

$$A_\mu^B(\vec{x}, 0) = A_\mu^B(\vec{x}, \beta), \quad (B = 1, 2 \cdots, 8) \ . \tag{1.72}$$

The lattice-regularized version of (1.70) is given by:

$$Z_G = N \int DU e^{-S_G^{(\beta)}[U]} \ , \tag{1.73}$$

where the lattice action has the same structure as in (1.57) except that now the sum over the lattice sites is restricted to a lattice whose temporal extension measured in units of lattice spacing a is

$$\hat{\beta} = \frac{1}{\hat{T}} \ , \tag{1.74}$$

with $\hat{T} = Ta$.

1.2.6 The Polyakov Loop

At zero temperature, the potential of a static quark-antiquark pair can be determined, as we mentioned before, by studying the ground state expectation value of the Wilson loop for large euclidean time. At finite temperatures the lattice has finite extension in the time direction, and the Wilson loop no longer plays this role. Which is then the corresponding object to be considered when studying QCD at finite temperature? We can construct a periodic gauge quantity by taking the trace of the product of link variables along loops winding around the time direction, that is

$$L(\vec{n}) = \mathrm{Tr} \prod_{n_4=1}^{\hat{\beta}} U_4(\vec{n}, n_4) \ , \tag{1.75}$$

where $\hat{\beta}$ is the inverse temperature measured in units of the lattice spacing. We refer to $L(\vec{n})$ as Wilson line or *Polyakov loop*. This quantity is invariant under periodic gauge transformations

$$\begin{aligned} U_4(\vec{n}, n_4) &\rightarrow G(\vec{n}, n_4) U_4(\vec{n}, n_4) G^{-1}(\vec{n}, n_4 + 1) \\ G(\vec{n}, 1) &= G(\vec{n}, \hat{\beta} + 1) \ . \end{aligned}$$

In the continuum formulation the expression of the Polyakov loop is given by

$$L(\vec{x}) = P\left(e^{ig \int_0^\beta A_4(\vec{x}, \tau) d\tau} \right) \ , \tag{1.76}$$

where P is the path ordered product, A_4 is the temporal component of the vector potential and g is the coupling constant of the theory. The Polyakov loop in the (1.76) is the product of matrices belonging to $SU(N)$ group (in the most general case) and so it is a element of this group, which means that

$$L^\dagger(x) L(x) = 1 \ , \qquad \det(L(x)) = 1 \ . \tag{1.77}$$

Let us consider the simplest local gauge transformation Ω belonging to $SU(N)$ group. It consists of a factor phase times the unitary matrix:

$$\Omega = e^{i\phi} 1 \ . \tag{1.78}$$

Since (1.78) is an element of $SU(N)$, the determinant must be equal to one this implies that

$$\phi = \frac{2\pi j}{N} \ , \qquad j = 0, 1 \cdots (N-1) \ . \tag{1.79}$$

Since an integer does not change continuously from point to point, the expression (1.79) introduces a global symmetry under $Z(N)$. We introduce the quantity l_1 called sometimes in literature Polyakov loop [19], is defined as the trace of the Wilson line in the fundamental representation

$$l_1 = \frac{1}{N}\mathrm{Tr}L(\vec{x}) \ , \tag{1.80}$$

where L is given by (1.76). Under $Z(N)$ global transformation, the Polyakov loop l is transformed as a field of charge one

$$l_1 \rightarrow e^{i\phi} l_1 \ . \tag{1.81}$$

Let us consider a case of our interest: the group $SU(3)$. In this case, l_1 has global symmetry $Z(3)$. According the (1.79), for $N = 3$, the elements for which there is a global symmetry are $e^{2i\pi j/3} \in Z(3)$, where $j = 0, 1, 2$. These elements of $SU(3)$ belong to the center C of the gauge group.[7]

It is possible to show [7] that the free energy of a system with a single heavy quark, measured relative to that in the absence of the quark, is given by

$$e^{-\beta F_q} = \langle L(\vec{x}) \rangle = \langle L \rangle \ . \tag{1.82}$$

In writing this last equality we have made use of the translational invariance of the vacuum. On the lattice the (1.82) is replaced by $e^{-\hat{\beta}\hat{F}_q}$, with $\hat{\beta}$ and $\hat{F}_q$, inverse of the temperature and the free energy measured in lattice units. Furthermore, the free energy of a static quark and antiquark located at $\vec{x} = \vec{n}a$ and $\vec{y} = \vec{m}a$ can be obtained from the correlation function of two such loops with base at $\vec{n}$ and $\vec{m}$, and having opposite orientations:

$$\Gamma(\vec{n}, \vec{m}) = \langle L(\vec{n}) L^{\dagger}(\vec{m}) \rangle \ . \tag{1.83}$$

[7]The center C of the group G is defined by all the elements z for which $zgz^{-1} = g$, with $g \in G$.

One can put in relation $\Gamma(\vec{n},\vec{m})$ with the free energy $\hat{F}_{q\overline{q}}(\vec{n},\vec{m})$ of a pair quark-antiquark [7]:

$$\Gamma(\vec{n},\vec{m}) = e^{-\hat{\beta}\hat{F}_{q\overline{q}}(\vec{n},\vec{m})} \ . \tag{1.84}$$

and using the fact that

$$\langle L(\vec{n})L^{\dagger}(\vec{m})\rangle \overset{|\vec{n}-\vec{m}|\to\infty}{\to} |\langle L\rangle|^2 \ . \tag{1.85}$$

we can conclude that, if $\langle L\rangle = 0$, then the free energy increases for large separation of the quarks.

We interpret this as a signal of confinement. On the other hand, if $\langle L\rangle \neq 0$, then the free energy of a static quark-antiquark pair approaches a constant for large separations. We interpret this as a signal of deconfinement. The expectation value of the Polyakov loop in a pure gauge theory is an order parameter (see later for more details) by which we can understand if the theory is in a confined or deconfined phase.

In statistical mechanics phase transitions are usually associated with a breakdown of a global symmetry. Since the case of $SU(3)$ is the most physical one, let us deal with this gauge group which also presents a spontaneous breakdown of the global symmetry.

The lattice action of a pure $SU(3)$ gauge theory is invariant under periodic gauge transformation but also posses a further symmetry which is not shared by the Polyakov loop.

Consider the elements of $SU(3)$ belonging to the center C of the group; they are given by $e^{2i\pi l/3} \in Z(3)$ where $l = 0, 1, 2$. The action of $SU(3)$ gauge theory is invariant if we multiply all time-like link variables U_4 between two neighboring spatial sections of the lattice by an element of the center

$$U_4(\vec{n}, n_4) \to zU_4(\vec{n}, n_4) \qquad \forall\ \vec{n}, n_4 \ ,$$

where $z \in C$. These transformations form a global symmetry of the theory to which we will refer as the *center symmetry*. Otherwise the Polyakov loop is not invariant under these transformations since it contains an element which transforms non-trivially:

$$L(\vec{n}) \to zL(\vec{n}) \ .$$

If the ground state of the quantum system respects the symmetry of the classical action, the expectation value of the Polyakov loop must vanish. Indeed, if we call V the operator which realizes the center transformation, $|\Omega\rangle$ the ground state and if $V|\Omega\rangle = |\Omega\rangle$, then we have

$$\langle L\rangle = \langle\Omega|L|\Omega\rangle = \langle\Omega|V^{-1}VLV^{-1}V|\Omega\rangle = \langle\Omega|VLV^{-1}|\Omega\rangle = z\langle\Omega|L|\Omega\rangle = z\langle L\rangle \ ,$$

that is $\langle L\rangle = 0$. But we have interpreted this as a signal of confinement. Hence we expect that the center symmetry is realized in the low temperature regime. On the other hand, if $\langle L\rangle \neq 0$, then the center symmetry is broken. Hence we expect that the deconfined phase transition is accompanied by the breakdown of the center symmetry abd the values of the Polyakov loops cluster around the $Z(3)$ roots. [8]

Svetitsky and Yaffe [20] first in the 1982 argued that the $Z(3)$ symmetry played a crucial role in the confinement. They argued that the critical behavior of the $SU(3)$ pure gauge theory would be comparable with that the $Z(3)$ spin system (the three states Potts model). And since this model undergoes a first order phase transition, they expect that the deconfined phase transition of $SU(3)$ pure gauge theory is first order as well.

1.3 The Continuum Limit

We have just constructed a lattice gauge theory based on the non-abelians group $SU(3)$ and have given arguments which suggest that in the continuum limit it describes the QCD, based on the observation that the lattice action reduces to the correct expression in the naive continuum limit. But there exists an infinite number of lattice actions which have the same naive continuum limit (we have chosen the simplest). What does exactly ensure that the theory have a continuum limit corresponding to QCD? The answer is that the lattice theory must exhibit first of all a critical region in parameter space where correlation lengths diverge.

[8] When quarks are coupled to the gauge fields the action is no longer $Z(3)$ symmetric and the Polyakov loop is no longer the order parameter, even if at least for large quark masses, it is still expected to show a rapid variation across the transition region.

Let us explain this last statement.

To do this let us consider the case of the pure $SU(3)$ gauge theory (the theory without fermions), with the following partition function

$$Z = \int DU e^{\frac{1}{g_0^2}\mathrm{Tr}\sum_P (U_P + U_P^\dagger)} \ . \tag{1.86}$$

Then suppose we want to extract the mass spectrum of the corresponding field theory by studying the appropriate correlation functions for large euclidean times (see later for more details). The fundamental mass is in fact the inverse of the correlation length ξ. So if the corresponding physical mass m is to be finite, then the mass measured in lattice units $\hat{m}$, must vanish in the continuum limit. This implies that the correlation length measured in lattice units $\hat{\xi}$, must diverge. Hence the continuum field theory can only be realized at a critical point of the statistical mechanical system described by the partition function (1.86). It follows that if the above system is not critical for any value of the coupling, it cannot describe QCD.

To study a system near criticality means tuning the parameters accordingly. In our case, the only parameter is the bare coupling g_0. The correlation length $\hat{\xi}$ measured in lattice units will depend only on it. Hence the continuum limit is realized for $g_0 \to g_0^*$, while

$$\hat{\xi}(g_0) \overset{g_0 \to g_0^*}{\to} \infty \ . \tag{1.87}$$

We remember that the physical quantities should be finite in the limit of zero lattice spacing.

The important thing is so to know how the coupling g_0 depends on the lattice spacing a [9]. It is in principle possible to know this dependence, let us see how.

Consider an observable Θ with mass dimension d_θ, and denoting with $\hat{\Theta}$ the corresponding lattice quantity (which may in principle be determined numerically). As

[9] We would underline that is not surprising that the bare parameters will depend on the lattice spacing. Making the lattice finer and finer, the number of lattice sites and links within a given physical volume increases, hence if the physics is to remain the same, the bare parameters must be tuned to a (in a way depending in general on the dynamics of the theory).

above, $\hat{\Theta}$ will depend on the bare parameters of the theory. Let us suppose that there is just one parameter g_0, the existence of a continuum limit then implies that

$$\Theta(g_0, a) = \left(\frac{1}{a}\right)^{d_\Theta} \hat{\Theta}(g_0) \ , \tag{1.88}$$

approaches a finite limit for $a \to 0$, i.e. when g_0 approaches the critical coupling g_0^*. Informally we write

$$\Theta(g_0(a), a) \stackrel{a\to 0}{\to} \Theta_{phys.} \ . \tag{1.89}$$

If we know the functional dependence of $\hat{\Theta}$ on g_0, we can determine $g_0(a)$ from the (1.88) for sufficiently small lattice spacing by fixing the left-hand side at its physical value $\Theta_{phys.}$. In this discussion we did not use any particular observable, but it may appear that the functional dependence of $g_0(a)$ will depend on the observable considered. In that case a universal function $g_0(a)$ should exist, which ensures the finiteness of any observable.

But how do we know whether we are extracting continuum physics when performing calculations on finite lattices? The answer to this question is found in following relations which give the relation between g_0 and the lattice spacing (derived from the first two universal coefficients in the power series expansion of the β-function for N_F flavors of massless quarks) [10]

$$\beta(g_0) = -\beta_0 g_0^3 - \beta_1 g_0^5 + \cdots \ , \tag{1.90}$$

with

$$\beta_0 = \frac{1}{16\pi^2}\left(11 - \frac{2}{3}N_F\right) \ , \qquad \beta_1 = \left(\frac{1}{16\pi^2}\right)^2\left(102 - \frac{38}{3}N_F\right) \ , \tag{1.91}$$

$$a = \frac{1}{\Lambda_L} R(g_0) \ , \tag{1.92}$$

$$R(g_o) = (\beta_0 g_0^2)^{\frac{-\beta_1}{2\beta_0^2}} e^{-\frac{1}{2\beta_0 g_0^2}} \ . \tag{1.93}$$

This relations tell us how the bare coupling constant controls the lattice spacing. Inserting (1.92) into (1.88), the requirement (1.89) implies that for $g_0 \approx g_0^* = 0$, $\hat{\Theta}(g_0)$ must behave as follows:

$$\hat{\Theta}(g_0) \stackrel{g_0\to 0}{\approx} \hat{C}_\Theta \Big(R(g_0)\Big)^{d_\Theta} \ , \tag{1.94}$$

[10] See [7] and [8] for a more detailed description.

where $\hat{C}_\Theta$ is a dimensionless constant. Quantities behaving like (1.94) are said to show *asymptotic scaling*.

On a lattice of finite size there will exist in general only a narrow region in coupling constant space where $\hat{C}_\Theta(g_0)$ scales according to (1.94). This region is called the *scaling region*. (By studying the ratio $\hat{\Theta}(g_0)/(R(g_0))^{d_\Theta}$ as a function of g_0 in the scaling region one determines the constant $\hat{C}_\Theta$.)

This leads us to introduce another important concept for numerical simulations: *finite size effects*. Since the lattice spacing is controlled by the bare coupling according to (1.92), physics will no longer fit on the lattice if g_0 (and hence a) becomes too small.

On the other hand, by increasing the bare coupling, the lattice may become too coarse to account for fluctuations taking place on a small scale.

1.4 Monte Carlo simulations and algorithms used

The lattice formulation reduces the Feynman path formula for the gauge theory into a multiple ordinary integral [8]. However, the high multidimensionality of the integrals makes conventional mesh techniques impractical. We need a statistical treatment, also suggested in the previous paragraphs. The goal of the Monte Carlo approach is to provide a "small" number of configurations which are typical of thermal equilibrium in the statistical analog.

An efficient method to compute the ensemble average

$$\langle O \rangle = \frac{\int DUO[U]e^{-S[U]}}{\int DUe^{-S[U]}} \ , \tag{1.95}$$

is generating a sequence of link variable configurations with a probably distribution given by the Boltzmann factor $\exp[-S(U)]$. This technique is called *importance sampling*. If the sequence generated constitutes a representative set of configurations, then the ensemble average will be given by

$$\langle O \rangle = \frac{1}{N} \sum_{i=1}^{N} O(\{U\}_i) \ , \tag{1.96}$$

where $\{U\}_i$ $(i = 1, ..N)$ indicates the link configurations generated.

1.4.1 Construction principles for algorithms

Henceforth, it is explained the general strategy to calculate the expectation value (1.95), following the [7] description. First we construct an algorithm, that generates a sequence of configurations which will be distributed with the desired probability and then measure the observable using the thermalized configurations (obtained in a time depending on the algorithm used).

As with real experiments, Monte Carlo simulations have a certain inherent source of error. We can divide them in statistical fluctuations, systematic effects and systematic errors. The *statistical fluctuations* are always present and if N is the number of measurements statistically independent, then the error in the mean value will be of the order $1/\sqrt{N}$. In praxis, however, the configurations generated will not be statistically independent, so it will be necessary use appropriate tools to determine the errors. The *systematic effects* may arise from the finite lattice size and spacing. The nature of finite volume effects depends very much on the theory under consideration. A more detailed description of this effects and the technique to control them can be found in [21]. Finally, a *systematic error* arises in determining when equilibrium has been reached.

In the following we discuss some principles for constructing algorithms which ensure for the sequence of configurations generated being a representative ensemble. Let $C_1, C_2, ..$ indicate a countable set of states of the system. We consider a stochastic process in which a finite set of configurations is generated one after the other according to some transition probability $P(C_i \to C_j) \equiv P_{ij}$ for going from configuration C_i to C_j. Let $C_{\tau_1}, C_{\tau_2}...$ be the configurations generated sequentially in this way. The state of the system will be a random variable whose distribution will depend only on the state preceding it, that is, the transition probability is independent of all states except for its immediate predecessor; this defines a Markov chain whose elements are the random variables defined above.

It is possible to show that for a Markov process, to sample the distribution $\exp[-S(C)]$, it is sufficient to require that the transition probability satisfies the *de-*

tailed balance:

$$e^{-S(C)}P(C \to C') = e^{-S(C')}P(C' \to C) \ , \tag{1.97}$$

for every pair C and C'. If we consider a set of configurations $\{C_{\tau_i}\}$ generated by a Markov process and an observable O evaluated on this set of states, we can define a "time" average of O taken over N elements of the Markov chain by

$$\langle O \rangle_N = \frac{1}{N} \sum_{i=1}^{N} O(C_{\tau_i}) \ .$$

It is this quantity which we compute in praxis, and which we want to equal the ensemble average corresponding to a given Boltzmann distribution.

1.4.2 Metropolis Algorithm

This method, proposed by Metropolis et al. [22] in the 1953, is in principle applicable to any system and it has became the most popular in practice. Let C be any configuration which is to be updated and C' the new one with a transition probability $P_0(C \to C')$ which satisfies the following micro reversibility requirement:

$$P_0(C \to C') = P_0(C' \to C) \ . \tag{1.98}$$

We must decide whether the new configuration suggested C' should be accepted. If the transition probability $P(C \to C')$ is to satisfy (1.98), the choice depends on the actions $S(C)$ and $S(C')$. If $e^{-S(C')}/e^{-S(C)}$, i.e. if the action has been lowered, then the configuration C' is accepted. Otherwise, if the action has increased, one accepts the trial configuration only with probability $e^{-S(C')}/e^{-S(C)}$. It is generated a random number R in the interval $[0, 1]$ and it is taken C' as the new configuration if

$$R \leq \frac{e^{-S(C')}}{e^{-S(C)}} \ . \tag{1.99}$$

Otherwise C' is rejected and the old configuration is kept. It is possible to show that this algorithm satisfies the detailed balance [7]. Some other considerations: this algorithm is used to update a single variable at time. Otherwise the updating procedure would involve large changes in the action and consequentially the acceptance rate will be very small. The system will move slowly through the configuration space.

1.4.3 Heat Bath Algorithm

For $SU(2)$ we use the standard Kennedy-Pendleton [23] heat bath algorithm. This is extended to higher groups using the Cabibbo-Marinari [24] algorithm where effectively one updates some of the $SU(2)$ subgroups of the $SU(N)$ matrices.

An important practical question here is how many of these subgroups to update. Clearly the more subgroups one updates the faster we will explore phase space. To determine an appropriate number of these subgroups we have chosen a criterion which involves monitoring how efficiently the action of the $SU(N)$ fields is reduced by cooling the fields [25, 26], when the cooling is applied through different numbers of $SU(2)$ subgroups. We recall that to cool an $SU(2)$ lattice link we simply replace the matrix that is on that link by the matrix which minimizes the action. This matrix is easy to determine [25, 26]. A link appears in 4 plaquettes and hence its contribution to the action can be written as

$$\delta S_l = -\frac{\beta}{2}\mathrm{Tr}\{U_l\Sigma\} \tag{1.100}$$

where the matrix Σ is the sum of the 'staples' enclosing the link l. Each staple is an $SU(2)$ matrix and hence Σ is proportional to an $SU(2)$ matrix. Then it is easy to see that the matrix that minimizes δS_l is given by

$$U_l = \frac{\Sigma^\dagger}{|\Sigma|} \tag{1.101}$$

We note that this is just the choice of matrix that the heat bath algorithm makes if we set $\beta = \infty$. Once we have applied this procedure to every link of the lattice we have performed a cooling sweep. And we can systematically reduce the action by performing a sequence of such cooling sweeps. We can extend this to $SU(N)$ fields by using the Cabibbo-Marinari algorithm and cooling within the chosen $SU(2)$ subgroups. In this case the algorithm no longer exactly minimizes the action. Instead the rate at which it reduces the action is a measure of how rapidly it moves through phase space. So our procedure is to generate some (plausibly) thermalized $SU(N)$ fields, and then to cool these fields using various numbers of $SU(2)$ subgroups. We choose the smallest

number of subgroups that will reduce the action reasonably fast. We then use these same subgroups in the Monte Carlo. In practice we have used 3, 4 and 8 subgroups in the case of $SU(3)$, $SU(4)$ and $SU(5)$ respectively. (There is obviously some ambiguity in the precise choice.)

1.4.4 Over-relaxation

To reduce the correlation between the configurations it is useful to use the *over-relaxation* technique. It consists in updating the link after that the Metropolis updating procedure is done. In this way the action does not change. [9, 27]
In addition to heat-bath sweeps one can also use over-relaxation sweeps [28, 29, 30]. In $SU(2)$ this corresponds to replacing our old link matrix, U_{old}, by a new link matrix, U_{new}, defined by

$$U_{new} = \frac{\Sigma^\dagger}{|\Sigma|} U_{old}^\dagger \frac{\Sigma^\dagger}{|\Sigma|} \ , \tag{1.102}$$

where the notation is as in (1.100). It is easy to see that this change does not alter the action. Moreover it can be extended to $SU(N)$ using the Cabibbo-Marinari algorithm.

An over-relaxation step involves a large change in the link matrix and so it is plausible that it will increase the rate at which we traverse our phase space [28, 29, 30]. We find that for physical quantities, such as masses, a suitable mix of over-relaxation and heat bath sweeps decorrelates field configurations significantly, although not dramatically faster than pure heat bath. There is an additional gain that arises from the fact that an over-relaxation step is faster then a heat bath step, which in any case involves the calculation of all the staples. (This gain is greater in 3 than in 4 dimensions since there are fewer staples to calculate in the former case.)

Thus in the calculations of the works presented we shall typically choose to make 4 or 5 over-relaxation sweeps for each heat bath sweep.

1.4.5 Cooling

Cooling [31, 32] is a well established method for locally suppressing quantum fluctuations in gauge field configurations. The locality of the method allows topologically nontrivial field configurations to survive numerous iterations of the cooling algorithm. Application of such algorithms are central to removing short-distance fluctuations responsible for causing renormalization constants to significantly deviate from one as is the case for the topological charge operator [33].

Cooling [34, 31, 32, 35] consists in freezing the quantum fluctuations of equilibrium field configurations by an upgrading procedure in which only changes are accepted which make the action smaller. All the links of the lattice are upgraded one after the other; a complete sweep over the lattice will be called a cooling step in what follows.

If the changes of the links are kept sufficiently small each cooling step can be viewed as the lattice version of a smooth deformation of a continuum field configuration to a new configuration with smaller action. The effect of cooling will then be to bring smoothly the field configuration to a minimum of the action, which means to a configuration which is a solution of the classical equation of motion. Due to the smoothness of the deformations, the topology of the initial configuration will be preserved during cooling. It is known [36], however, that classical solutions of the equations of motion only correspond to approximate solutions on the lattice: they will therefore be only metastable, instead of stable. Care must be put in controlling the speed of cooling process to avoid possible immediate losses of metastable configurations. Physical observables which are related to topological proprierties will in fact be metastable along cooling. However, if the cooling process is too fast these metastabilities will not be observed, since the corresponding field configurations will be destroyed immediately. The original cooling method [32] was motivated by the study of the topological susceptibility and therefore performed having in mind the instantons [11].

In the follow we illustrate the method we use.

[11] For more details see [34]

At the $SU(2)$ level the algorithm is transparent. An element of $SU(2)$ may be parameterized as, $U = a_0 I + i\,\vec{a}\cdot\vec{\sigma}$, where a is real and $a^2 = 1$. Let $\widetilde{U}_\mu$ be one of the six staples associated with creating the plaquette associated with a link U_μ.

$$\widetilde{U}_\mu = U_\nu(x+\hat{\mu})\,U_\mu^\dagger(x+\hat{\nu})\,U_\nu^\dagger(x)\ . \tag{1.103}$$

We define

$$\sum_{\alpha=1}^{6}\widetilde{U}_\alpha = k\overline{U} \qquad \text{where} \qquad \overline{U}\in SU(2) \quad \text{and} \quad k^2 \equiv \det\left(\sum_{\alpha=1}^{6}\widetilde{U}_\alpha\right)\ . \tag{1.104}$$

The feature of the sum of $SU(2)$ elements being proportional to an $SU(2)$ element is central to the algorithm. The local $SU(2)$ action is proportional to

$$\mathcal{R}e\,\mathrm{Tr}(1 - U\overline{U})\ , \tag{1.105}$$

and is locally minimized when $\mathcal{R}e\,\mathrm{Tr}(U\overline{U})$ is maximized, i.e. when

$$\mathcal{R}e\,\mathrm{Tr}(U\overline{U}) = \mathcal{R}e\,\mathrm{Tr}(I)\,. \tag{1.106}$$

which requires the link to be updated as

$$U \longrightarrow U' = \overline{U}^{-1} = \overline{U}^\dagger = \frac{\left(\sum_{\alpha=1}^{6}\widetilde{U_\alpha}\right)^\dagger}{k}\ . \tag{1.107}$$

At the $SU(3)$ level, one successively applies this algorithm to various $SU(2)$ subgroups of $SU(3)$, with $SU(2)$ subgroups selected to cover the $SU(3)$ gauge group.

1.4.6 Smearing

APE smearing [37] is a gauge covariant [38] prescription for averaging a link $U_\mu(x)$ with its nearest neighbors $U_\mu(x+\hat{\nu}),\ \nu\neq\mu$. The linear combination takes the form:

$$U_\mu(x) \longrightarrow U'_\mu(x) = (1-\alpha)U_\mu(x) + \frac{\alpha}{6}\widetilde{\Sigma}^\dagger(x;\mu)\ , \tag{1.108}$$

where $\widetilde{\Sigma}(x;\mu) = \left(\sum_{\nu=1}^{6}\widetilde{U_\nu}(x)\right)_\mu$, is the sum of the six staples defined in Eq. (1.103). The parameter α represents the smearing fraction. The algorithm is constructed as follows:

(i) calculate the staples, $\widetilde{\Sigma}(x;\mu)$; (ii) calculate the new link variable $U'_\mu(x)$ given by Eq. (1.108) and then reunitarize $U'_\mu(x)$; (iii) once we have performed these steps for every link, the smeared $U'_\mu(x)$ are mapped into the original $U_\mu(x)$. This defines a single APE smearing sweep which can then be repeated.

Since this algorithm is applied simultaneously to all link variables, without any annealing in the process of a lattice update, the application of the algorithm may be viewed as an introduction of higher dimension irrelevant operators designed to improve the operator based on unsmeared links. This approach also leads to the desirable effect of renormalization constants approaching one. The net effect may be viewed as introducing a form factor to gluon vertices [39] that suppresses large q^2 interactions and, as a result, suppresses lattice artifacts at the scale of the cutoff.

The celebrated feature of APE smearing is that it can be realized as higher-dimension operators that might appear in a fermion action for example. Indeed, "fat link" actions based on the APE algorithm are excellent candidates for an efficient action with improved chiral properties [40]. The parameter space of fat link actions is described by the number of smearing sweeps $n_{\rm ape}$ and the smearing coefficient α.

Blocking scheme

In lattice gauge theory physical quantities of interest like masses, potential values, and matrix elements are related to asymptotic properties of exponentially decreasing correlation functions in Euclidean time, and therefore prone to be drowned in noise. So one is forced to improve operators in order to reach the desired asymptotic behavior for the small T region. We will shortly describe our particular improvement technique [41].

We start from the relation between Wilson loops, $W(R,T)$, and the (ground state) potential $V(R)$

$$W(R,T) = C(R)\exp\{-TV(R)\} \quad + \quad \text{excited state contributions.} \tag{1.109}$$

Our aim is to enhance — for each value of R — the corresponding ground state overlap $C(R)$. Since the ground state wave function is expected to be smooth on an ultraviolet

scale we concentrate on reducing noise by applying a *local* smoothing procedure on the spatial links: consider a spatial link variable $U_i(n)$, and the sum of the four spatial staples $\Pi_i(n)$ connected to it:

$$\Pi_i(n) = \sum_{\substack{j=\pm 1,\ldots,3 \\ j\neq i}} U_j(n) U_i(n+\hat{j}) U_j^\dagger(n+\hat{i}) \ . \tag{1.110}$$

We apply a gauge covariant, iterative smoothing algorithm which replaces (in the same even/odd ordering as the Metropolis update) $U_i(n)$ by $U_i'(n)$ minimizing the local spatial action $S_i(n) = -\mathrm{ReTr}\{U_i(n)\Pi_i^\dagger(n)\}$, which is qualitatively a measure for the *roughness* of the gauge field. This is very similar to lattice cooling techniques already invented by previous authors [42, 43] except that we are *cooling* only within time-slices and thus not affecting the transfer matrix. Alternatively, this algorithm may be interpreted as substituting $U_i(n)$ by $\mathcal{P}\left(\Pi_i(n)\right)$ where $\mathcal{P}$ denotes the projection operator onto the *nearest* $SU(3)$ matrix. In this sense it is a variant of the APE recursive blocking scheme [**?**] with the coefficient of the straight link set to *zero*, but with even/odd updating. The latter feature renders the algorithm less memory consuming and seems to improve convergence.

1.5 Data Analysis procedure

Following the description of [9], let us introduce in this section the procedures used in our simulations for the analysis of the data.

In numerical simulations the updating process creates a configuration sample $([\phi_n], \quad n = 1, 2 \cdots, N)$. Some introductional concepts: we define *primary quantities* $A[\phi]$ the quantities that can be directly obtained as averages.

An estimation of their expectation values is given by the sample average

$$\bar{A} \equiv \frac{1}{N} \sum_{n=1}^{N} A[\phi_n] \ .$$

Averaging over an infinite number of sample or over an infinitely large sample gives the ensemble average equal the expectation value

$$\tilde{A} = \langle A \rangle \ .$$

Such a quantities are in distinction to the *secondary quantities*, which are determined by functions of the averages.

In the ideal case, when the configurations of a sample are all statistically independent, the sample average $\bar{A}$ is normally distributed around the mean value $\tilde{A}$, with variance

$$\sigma^2_{\bar{A}} = \frac{\bar{A^2} - \bar{A}^2}{N-1} \ . \tag{1.111}$$

The error so estimated in usually too optimistic, because during the updating process the subsequent configurations are not really independent. This correlation in the sequence of generated configurations is called *autocorrelation*.

Hence the true variance for a primary quantity is given by

$$\sigma^2_{\bar{A}} = \frac{2\tau_{int,A}}{N}(\bar{A^2} - \bar{A}^2) \ , \tag{1.112}$$

where $\tau_{int,A}$ is the integrated autocorrelation time, defined [44]

$$\tau_{int,A} = \frac{1}{2}\sum_{t=1}^{T_{cut}} \frac{C_A(t)}{C_A(0)} \ , \tag{1.113}$$

where $C_A(t)$ is the correlation function:

$$C_A(t) = \frac{1}{N-|t|}\sum_{i=1}^{N-|t|}(A_i - \bar{A})(A_{i+t} - \bar{A}) \ . \tag{1.114}$$

The continuum limit of the lattice quantum field theory is always defined in proximity of critical points as we have said in the previous sections. This causes a difficulty in autocorrelations, because the correlation length ξ diverges near the critical points. This leads to a divergence of the autocorrelation time according to the dynamical scaling law

$$\tau_{int,A} \propto \xi^{z(A)} \ , \tag{1.115}$$

where $z(A)$ is the dynamical critical exponent, which is characteristic of the updating process and may depend on the observed quantity A. (See the next section for the description of critical indices).

Another practical way of obtaining correct error estimates from an updating sequence with autocorrelations is *binning*. Assuming that the sequence is long enough, one can

build blocks of subsequences (called "bins") and average the primary quantities first in the bins. The obtained bin averages themselves can be considered as results of single measurements, and so can be used to estimate the variance according the (1.111).

Jack-knife analysis

The estimate of the value and the errors for the secondary quantities can be obtained using the *jack-knife analysis*. Consider a sample of independent measures of a primary quantity A that can be indicated with $A_1, A_2, \cdots, A_{N_s}$. The sample average is

$$\bar{A} \equiv \frac{1}{N_s} \sum_{s=1}^{N_s} A_s \ . \tag{1.116}$$

Hence the best estimate of a secondary quantity is $\bar{y} = y(\bar{A})$. The error estimate for $\bar{y}$ can be derived from the jack-knife averages obtained by omitting a single measurement from the sample in all possible ways:

$$A_{(J)_s} \equiv \frac{1}{N_s - 1} \sum_{r \neq s} A_r \ . \tag{1.117}$$

The corresponding values of the secondary quantity are the jack-knife estimators

$$y_{(J)_s} \equiv y(A_{(J)_s}) \ ,$$

with an average

$$\bar{y}_(J) \equiv \frac{1}{N_s} \sum_{s=1}^{N_s} y_{(J)_s} \ . \tag{1.118}$$

Finally, the variance of the estimators can be obtained as

$$\sigma_{y_{(J)_s}} \equiv \frac{N_s - 1}{N_s} \sum_{s=1}^{N_s} (y_{(J)_s} - \bar{y}(J))^2 \ . \tag{1.119}$$

1.6 Critical Phenomena and Phase Transitions

We define phase of the matter [45] the states of the matter which can exists simultaneously in mutual equilibrium and can be in contact. We can also say that a phase is

a set of states of a macroscopic physical system that have relatively uniform chemical properties.

In the follow, we report a briefly list of main elements about critical phenomena and phase transition. For a more specific description on these arguments see [46, 47, 48].

According the Paul Ehrenfest classification [46] of the phase transitions, the transitions can be classified according the degrees of non-analyticity of the free energy f. In particular, the transitions are divided in groups of larger order depending on the lower derivative of the free energy which is discontinuous at the transition point. According to this classification, we call a *first order* phase transition, a transition which presents a discontinuity in the first derivative of f, calculated respect to a thermodynamic variable.

We say that a transition is of *second order*, when there is a discontinuity in the second derivative of f, and so on for transition of order larger than two.

In the modern classification scheme, phase transitions are divided into two broad categories, named similarly to the Ehrenfest classes: first-order phase transitions are those that involve a latent heat. During such a transition, a system either absorbs or releases a fixed (and typically large) amount of energy; the second class of phase transitions are continuous phase transitions, also called second order phase transitions. These transitions have not an associated latent heat. Examples of second order phase transitions are the ferromagnetic transition, the superfluid one and the Bose-Einstein condensation. Phenomena associated with the continuous phase transitions are called critical phenomena. [12]

As said in the previous section, a phase transition is accompanied with a symmetry breaking. The presence of symmetry breaking (or non-breaking) is very important. As pointed by Landau [45], given any state of a system, one may unequivocally say whether or not it possesses a given symmetry. Therefore, it cannot be possible to analytically deform a state in one phase into a phase possessing a different symmetry.

To describe quantitatively the change in the structure of a body when it passes

[12] To describe critical phenomena, it has become customary to use the language of magnetic system, although many systems to which the theory applies are non-magnetic [47].

through the phase transition point, we can define a quantity, the *order parameter*. The word order parameter is used [48] to denote a fluctuating variable the average value of which provides a signature of the order or broken symmetry in the system. As said in the previous section, an example of order parameter is the Polyakov loop for the confinement-deconfinement transition in $SU(3)$ pure gauge theory.

In such a way it takes non-zero (positive or negative) values in the unsymmetrical phase and is zero in the symmetric one. A passage through a phase transition point of the second kind has a continuous change of the order parameter to zero.

To extend the meaning of order parameter, it is useful to introduce another concept: the *range of correlations*, that is the distance over which fluctuations in one region of space are correlated or affected by those in another region. If two points are separated by a distance larger than that range, then the different fluctuations at these two points will be uncorrelated from each other.

It turns out that continuous phase transition can be characterized by parameters known as *critical exponents*. Critical exponents are defined, examining the power law behavior of a measurable physical quantity near the phase transition and they are related by *scaling relations*.

It is a remarkable fact that phase transitions arising in different systems often possess the same set of critical exponents. This phenomenon is known as *universality*. Such systems are said to be in the universality class [20]. Universality is a prediction of the renormalization group theory of the phase transitions, which states that thermodynamic properties of a system near a phase transition depend only on a small number of features, such as dimensionality and symmetry, and is insensitive to the underlying microscopic properties of the system.

Let us conclude our brief summary about the phase transition, introducing the critical exponents ν and μ (which will be subject of next arguments). They describe the properties of fluctuation of the order parameter, determining the dependence from the temperature of the correlation length ξ. Without going into details (see [46]), we intro-

duce the expression

$$\xi \sim |\epsilon|^{-\nu} \ , \tag{1.120}$$

where

$$\epsilon \equiv \frac{T - T_c}{T_c} = \frac{T}{T_c} - 1 \tag{1.121}$$

with T_c critical temperature.

Chapter 2

The $SU(3)$ pure gauge theory. Screening masses and universality

A new state of the matter, the Quark Gluon Plasma (QGP) should appear at very high temperature. In this phase one uses the plasma picture because it is characterized by an interacting gas of essentially massive quasiparticle. While this description applies well above the critical temperature T_c, it may not very useful near T_c. Recently an effective theory [49], which is better situated near the critical temperature, was proposed; there, in a mean field approximation, the free energy is expressed in terms of Polyakov loops and the deconfined phase is described by a condensate of $Z(N)$ spins. The role of a global $Z(N)$ symmetry, and its relationship with the confinement, was firstly introduced by 't Hooft [50].

2.1 The $SU(3)$ pure gauge theory at finite temperature

The essential features of confinement, of the deconfinement phase transition at finite temperature and of the deconfined phase in QCD can be studied without loss of relevant dynamics in the regime of infinitely massive quarks or, equivalently, in the $SU(3)$ *pure*

gauge theory.

The (3+1)d $SU(3)$ pure gauge theory at finite temperature undergoes a confinement/deconfinement phase transition associated with the breaking of the center of the gauge group, $Z(3)$ [51, 52]. This transition is *weakly* first order [53, 54, 55, 56, 57] and the order parameter is the thermal Wilson line, also called Polyakov loop [51, 52], a gauge invariant quantity defined as the trace of the product of the link variables along topologically non-trivial loops winding around the time direction:

$$L(\vec{n}) = \mathrm{Tr} \prod_{n_4=1}^{\hat{\beta}} U_4(\vec{n}, n_4) \ , \tag{2.1}$$

where $\hat{\beta}$ is the inverse temperature measured in units of the lattice spacing.

2.2 The Svetitsky-Yaffe conjecture. Universality

The deconfinement transition in the $(d+1)$-dimensional $SU(N)$ pure gauge theory at finite temperature can be put in relation with the order/disorder [78] phase transition of the d-dimensional Z(N) spin model through the Svetitsky-Yaffe conjecture [59]. According to this conjecture, when the transition is *second order* the gauge theory and the spin model belong to the same universality class and therefore share critical indices, amplitude ratios and correlation functions at criticality. There are so many numerical evidences in favor of this conjecture – see, for instance, Refs. [60, 61, 62, 63, 64, 65, 66] and, for a review, Ref. [67] – that there is no residual doubt about its validity.

In the case of *first order* phase transitions, as for the (3+1)d $SU(3)$ pure gauge theory, the Svetitsky-Yaffe conjecture is not applicable in strict sense, since the correlation length keeps finite at the transition point and a universal behavior, independent of the details of the microscopic interactions, cannot be established. Therefore there are no *a priori* reasons why the critical dynamics of (3+1)d $SU(3)$ and of its would-be counterpart spin model, 3d $Z(3)$ or 3-state Potts model [76, 77], should look similar. It turns out, however, that for both these theories the phase transition is *weakly* first order, which means that the correlation length at the transition point, although finite, becomes much

larger than the lattice spacing. This leads to the expectation that the two theories may have some long distance aspects in common and that some specific issues of $SU(3)$ in the transition region can be studied taking the $3d$ 3-state Potts model as an effective model.

Since there are no critical indices to compare, a test of this possibility could be based on the comparison of the spectrum of massive excitations of the $3d$ 3-state Potts model in the broken phase near the transition at zero magnetic field with the spectrum of the inverse decay lengths of Polyakov loop correlators in the (3+1)d $SU(3)$ gauge theory in the deconfined phase near the transition. If universality would apply in strict sense, these spectra should exhibit the same pattern, as suggested by several numerical determinations in the $3d$ Ising class [70, 71, 72, 73].

We determine the low-lying masses of the spectrum of the (3+1)d $SU(3)$ pure gauge theory at finite temperature in the deconfined phase near the transition [74] in two different sectors of parity and orbital angular momentum, 0^+ and 2^+, and compare their ratio with that of the corresponding massive excitations in the phase of broken $Z(3)$ symmetry of the $3d$ 3-state Potts model, determined in Ref. [75].

In fact, we extend our numerical analysis to temperatures far away from the transition temperature T_t in order to look for possible "scaling" of the fundamental masses with temperature.

2.3 The $3d$ 3-state Potts model

The 3-d 3-states Potts model [76, 77] is a spin theory in which the fundamental degree of freedom, s_i, defined in the site i of a 3-dimensional lattice, is an element of the $Z(3)$ group, *i.e.*

$$s_i = e^{i\frac{2}{3}\pi\sigma_i}, \quad \sigma_i = \{0, 1, 2\} \quad . \tag{2.2}$$

The Hamiltonian of the model is

$$H = -\frac{2}{3}\beta \sum_{\langle ij \rangle} (s_i^\dagger s_j + s_j^\dagger s_i) = -\beta \sum_{\langle ij \rangle} \delta_{\sigma_i,\sigma_j} \ , \tag{2.3}$$

up to an irrelevant constant. Here, β is the coupling in units of the temperature and the sum is done over all the nearest-neighbor pairs of a cubic lattice with linear size L.

The Hamiltonian (2.3) is invariant under the $Z(3)$ transformation

$$s_i \longrightarrow s_i' = e^{i\frac{2\pi}{3}\sigma} s_i \ , \tag{2.4}$$

where σ is fixed at any of the values $\{0, 1, 2\}$. It is well known that this system undergoes a *weakly* first order phase transition [78], associated with the spontaneous breaking of the $Z(3)$ symmetry. The order parameter of this transition is the magnetization,

$$\langle S \rangle = \langle \frac{1}{L^3} \sum_i s_i \rangle \ , \tag{2.5}$$

which, in the thermodynamic limit, is zero above the transition temperature T_t (or below the transition coupling β_t) and takes a non-zero value below T_t (or above β_t).

In presence of an external magnetic field it is convenient to work with an Hamiltonian written in terms of the σ_i degrees of freedom, instead of the s_i ones. For a uniform magnetic field along the direction σ_h with strength h in units of the temperature, the Hamiltonian is

$$H = -\beta \sum_{\langle ij \rangle} \delta_{\sigma_i,\sigma_j} - h \sum_i \delta_{\sigma_i,\sigma_h} \equiv -\beta E - hM \ , \tag{2.6}$$

where E is the internal energy and M is the magnetization. The magnetic field breaks explicitly the $Z(3)$ symmetry. However, first order transitions still occur for values of the magnetic field strength h below a critical value h_c, the transition temperature increasing with increasing h. The line of first order phase transitions ends in a second order critical point $P_c = (T_c, h_c)$ (see Fig. 2.1), belonging to the $3d$ Ising class [79]. The Hamiltonian in the scaling region of the critical point P_c can be written as

$$H = -\tau \tilde{E} - \xi \tilde{M} \ , \tag{2.7}$$

where $\tilde{E}$ and $\tilde{M}$ are the Ising-like energy and magnetization operators and τ and ξ the corresponding temperature-like and symmetry-breaking-like parameters. This means that $\langle \tilde{M} \rangle$ is the new order parameter. Close enough to P_c, the following relations hold,

$$\tilde{M} = M + sE \ , \qquad \tilde{E} = E + rM \ , \tag{2.8}$$

where the mixing parameters (r, s) have been determined numerically for several lattice sizes L in Ref. [79]. The τ-direction identifies the first order line. In Ref. [79] the location of the critical point P_c has been accurately determined: $P_c = (\beta_c, h_c)$=(0.54938(2),0.000775(10)) or, equivalently, $P_c = (\tau_c, \xi_c)$=(0.37182(2),0.25733(2)).

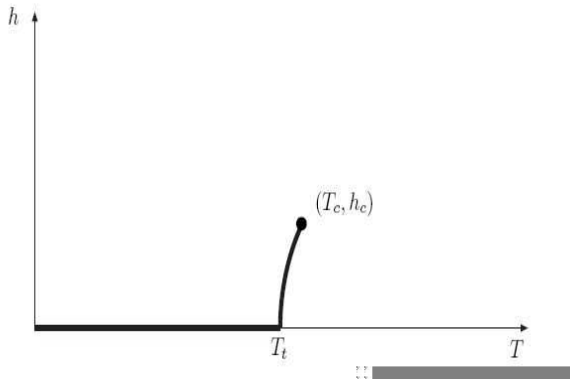

Figure 2.1: Qualitative phase diagram of the $3d$ 3-states Potts model in the (β, h)-plane: ξ and τ are the symmetry-breaking and the temperature parameters of the Ising theory (2.7).

2.4 The Polyakov loop Models

We consider also the screening masses resulting from correlators of the real parts and of the imaginary parts of the Polyakov loop. These determinations can represent useful benchmarks for effective models of the high-temperature phase of $SU(3)$, such as those based on mean-field theories of the Polyakov loop, suggested by R. Pisarski [49].

The finite temperature confinement transition may be viewed as a transition in which the global center symmetry is spontaneously broken; the expectation value of the Polyakov loop $\langle l \rangle$ is an order parameter for this symmetry, as introduced in the previous chapter. Integrating out all degree of freedom of a theory, except this order parameter, generates an effective scalar field theory $S[l]_{eff}$ for the order parameter,

globally invariant under the center symmetry:

$$Z = \int [dU] e^{-S[U]} = \int [dU] e^{-S[U]} \prod \int dl(\vec{x}) \delta\Big(l(\vec{x}) - \prod_{\tau=1}^{N_\tau} U_4(\vec{x},\tau) \Big) = \int [dl] e^{-S[l]_{eff}} \ ,$$

where we have used the following relations

$$\int dl(\vec{a}) \delta\Big(l(\vec{a}) - \prod_{\tau=1}^{N_\tau} U_4(\vec{x},\tau) \Big) = 1 \qquad \int [dl] = \prod_{\vec{x}} \int dl(\vec{x}) \ .$$

The effective theory, for an initial $(d+1)$-dimensional gauge theory, may be study working on the d-dimensional scalar field theory or a spin system. The finite temperature transition in the gauge theory precisely corresponds to an order-disorder phase transition in the effective spin system [80]. The effective theory possesses only short-range interactions [20].

For four or more colors, the importance of Polyakov loop was considered in [81]. Polyakov loops with higher $Z(N)$ charge are easy to construct. We introduce the traceless part of L:

$$\tilde{L} = L - l_1 1 \ .$$

Then we define the charge-two Polyakov loop

$$l_2 = \frac{1}{N} \mathrm{Tr} \tilde{L}^2 \ ,$$

where

$$l_2 \to e^{2i\phi} l_2 \ .$$

There are two operators with charge-two l_2 and l_1^2. Continuing on,

$$l_3 = \frac{1}{N} \mathrm{Tr} \tilde{L}^3 \ ,$$

has charge three under the global $Z(N)$ symmetry. Other charge-three operators are l_1^3 and $l_1 l_2$. The construction of operators with higher $Z(N)$ charge proceeds similarly.

Effective theories for $l(x)$ are dictated by symmetry gauge of the Polyakov loop. In the following we discuss about effective theories for three colors [49].

We construct a potential for the Polyakov loop, taking the simplest form consistent with the global $Z(3)$ symmetry:

$$\mathcal{V}(\ell) = -\frac{b_2}{2}|\ell|^2 - \frac{b_3}{3}\left(\ell^3 + (\ell^*)^3\right) + \frac{1}{4}\left(|\ell|\right)^2 \ . \tag{2.9}$$

The coefficient of the quartic term is chosen to simplify further results. At the minimum of the potential, which we assume occurs for real ℓ, $\partial\mathcal{V}/\partial\ell = 0$,

$$\ell_0 \equiv \langle\ell\rangle = b_3 + \sqrt{b_2 + b_3^2}\ . \tag{2.10}$$

At high temperatures, b_2 is adjusted so that $\ell_0 \approx 1$; then b_4 is adjusted to give the proper value of the ideal gas term. Away from infinite temperature, in the spirit of mean field we take the quantities b_3 and b_4 to be approximately constant with temperature. Given the pressure, the dependence of b_2 upon the temperature is then fixed.

While ℓ_0 is the standard variable measured on the lattice, this is the bare value. Single insertions of the Polyakov loop are regularized by introducing a renormalization constant; the natural condition to fix the value of that constant is to require that the renormalized Polyakov loop is unity at infinite temperature. If a lattice regulator is used instead of dimensional regularization, though, one has to deal with divergences $\sim g^2/(aT)$, *etc.*, which are most singular as the lattice spacing $a \to 0$.

For $SU(3)$, the Polyakov loop is a complex number, with real, $\ell_r = \mathrm{Re}\ell$, and imaginary, $\ell_i = \mathrm{Im}\ell$, parts. By a global $Z(3)$ rotation, we can assume that the vacuum expectation value of ℓ, ℓ_0, is real. Computing second derivatives, the mass squared for the real part is:

$$m_r^2 = \frac{\partial^2\mathcal{V}}{\partial\ell_r^2} = -b_2 - 4b_3\ell_0 + 3\ell_0^2\ , \tag{2.11}$$

while that for the imaginary part is:

$$m_i^2 = \frac{\partial^2\mathcal{V}}{\partial\ell_i^2} = -b_2 + 4b_3\ell_0 + \ell_0^2\ . \tag{2.12}$$

When $b_3 \neq 0$, the transition is necessarily of first order. The transition occurs when the nontrivial minimum is degenerate with the trivial minimum; *i.e.*, when $\mathcal{V}(\ell_0) = 0$. Putting in the expression for ℓ_0, we find

$$b_2(T_c^+) = -\frac{8}{9}b_3^2 \quad , \quad \ell_0(T_c^+) = \frac{4}{3}b_3\ . \tag{2.13}$$

This is all trivial algebra, done in detail to avoid any possible confusion. The full effective Lagrangian can then be computed. Besides the potential term, given above, there is also the kinetic term, with a nonstandard normalization:

$$\mathcal{Z}_W T^2 |\vec{\partial}\ell|^2 \quad , \quad \mathcal{Z}_W = \frac{3}{g^2}\left(1 - .08\frac{g^2}{4\pi} + \ldots\right) . \tag{2.14}$$

The first term in $\mathcal{Z}_W$ appears at the classical level, while the second arises from one loop corrections, as computed by Wirstam [82].

Over large distances, $x \to \infty$, the two point functions of the Polyakov loop are

$$\langle \ell_r(x)\ell_r(0)\rangle - \langle \ell\rangle^2 \sim \frac{\exp(-\widetilde{m}_r x)}{x} \quad , \tag{2.15}$$

$$\langle \ell_i(x)\ell_i(0)\rangle \sim \frac{\exp(-\widetilde{m}_i x)}{x} . \tag{2.16}$$

The two fields, ℓ_r and ℓ_i, do not mix to the order at which we work. The masses which enter into the correlation functions are

$$\widetilde{m}^2_{r,i} = \frac{b_4}{\mathcal{Z}_W} m^2_{r,i} T^2 . \tag{2.17}$$

For two colors, the Polyakov loop is real, and one can only measure one mass. Then, without knowing both the coupling constant and the wave function renormalization constant $\mathcal{Z}_W$, there is no firm prediction.

This is not true for three colors. Then one can form the *ratio* of the masses for the real and imaginary parts of the Polyakov loop. The constants b_4 and $\mathcal{Z}_W$ drop out, and one has a unique relation between this ratio of masses and the pressure. In particular, at the point of transition, using the previous results we find that

$$\frac{\widetilde{m}_i}{\widetilde{m}_r} = 3 \quad , \quad T = T_c^+ . \tag{2.18}$$

It is dependent upon the assumed form of the potential for $\mathcal{V}(\ell)$, and would change if terms such as $\sim (|\ell|^2)^3$ were included.

These two point functions in the Polyakov Loop Model are very different from those of ordinary perturbation theory. In perturbation theory, ℓ_0 is near unity, and correlations

are determined by multiple exchanges of A_0 fields. The mass of the A_0 field is the Debye mass, $m_D^2 \sim g^2 T^2$. Expanding the exponentials, the real part of the Polyakov loop couples to $\sim \mathrm{Tr} A_0^2$, while that for the imaginary part couples to $\sim \mathrm{Tr} A_0^3$. Thus over large distances, $x \to \infty$,

$$\langle \ell_r(x) \ell_r(0) \rangle - \langle \ell \rangle^2 \sim \frac{\exp(-2 m_D x)}{x^2} \; , \tag{2.19}$$

$$\langle \ell_i(x) \ell_i(0) \rangle \sim \frac{\exp(-3 m_D x)}{x^3} \; . \tag{2.20}$$

Notice that the prefactors in front differ markedly from those of the Polyakov Loop Model; instead of $1/x$, they are $1/x^2$ and $1/x^3$, respectively, with the power of $1/x$ measuring the number of quanta exchanged.

If we ignore the difference in prefactors, even so the perturbative result for the mass ratio of (2.18) is not 3, but 3/2.

Measurements of the two point function of the real part of the Polyakov Loop have been carried out by Kaczmarek *et al.* [57]. From the two point function of Polyakov loops, which is presumably dominated by that for the real part, the mass drops by about a factor of ten, from $m/T \sim 2.5$ at $T = 2T_c$, to perhaps $m/T \sim .25$ at T_c^+. We are not aware of any measurements of the imaginary part close to T_c.

There are also measurements by Bialas *et al.* for a $SU(3)$ gauge theory in $2+1$ dimensions [83]. While the critical behavior in this model is that of a two dimensional system, and so can have characteristics special to a low dimension, for the Polyakov Loop Model in mean field theory, our predictions remain the same. These authors find that the ratio $\widetilde{m}_i / \widetilde{m}_r$ does increase from 3/2 as the temperature approaches T_c.

In fact, the Polyakov Loop Model must be inapplicable at some temperature not too far above T_c. At high temperature, where $\ell_0 \approx 1$, the above formula give $b_2 = 1 - 2b_3$, and

$$\frac{\widetilde{m}_i}{\widetilde{m}_r} = \sqrt{\frac{3 b_3}{1 - b_3}} \quad , \quad T \to \infty \; . \tag{2.21}$$

The constant b_3 is not well determined, but for $b_3 < 3/7$, the above ratio is less than the perturbative value of 3/2.

They propose [84] that the two point function of Polyakov loops can be used as a measure of the regime in which the Polyakov Loop Model applies, and the regime where perturbation theory applies.

What if the ratio of masses, (2.18), is wrong even at T_c? Besides including terms of higher order in the potential, it may also be necessary to include the charge-two Polyakov loop, ℓ_2. Since $Z(3)$ is a cyclic symmetry, a field with charge-two is the same as one with charge minus one. The couplings of this loop with itself are identical to the couplings of the usual Polyakov loop, since the sign of the charge does not matter. Unlike the charge-one Polyakov loop, however, the charge-two loop should always have a positive mass squared, in order to avoid condensation which breaks $SU(3) \to SU(2)$ [85]. Thus one would assume that the charge-two field, as a massive field, can be ignored. Nevertheless, the following coupling is $Z(3)$ symmetric:

$$\ell_1 \ell_2 + \ell_1^* \ell_2^* \ . \tag{2.22}$$

This term mixes the charge-one and charge-two Polyakov loops, $\sim \mathrm{Tr}\mathbf{L}\mathrm{Tr}\mathbf{L}^2 + \ldots$. Its coupling constant is directly measurable; if small, the charge-two Polyakov loop can be ignored, and our prediction should hold.

Lastly, they note that the Polyakov loop may well couple weakly to other operators. Thus while in principle it should dominate all correlation functions at large distances (if it is the lightest state), this may be very difficult to see unless the operator couples strongly.

2.5 Screening masses from Polyakov loop correlators

We define the general procedure for extracting screening masses in (3+1)d $SU(3)$ at finite temperature from correlators of the Polyakov loop,

$$P(x,y,z) = \mathrm{Tr} \prod_{n_t=1}^{N_t} U_4(x,y,z,n_t a) \ , \tag{2.23}$$

where N_t is the number of lattice sizes in the temporal direction and a is the lattice spacing.

The point-point connected correlation function is defined as

$$\Gamma_{i_0}(r) = \langle P_i^\dagger P_{i_0} \rangle - \langle P_i^\dagger \rangle \langle P_{i_0} \rangle \ , \tag{2.24}$$

where i and i_0 are the indices of sites and r is the distance between them. The large-r behavior of the point-point connected correlation function is determined by the correlation length of the theory, ξ_0, or, equivalently, by its inverse, the fundamental mass. In order to extract the fundamental mass it is convenient to define the wall-wall connected correlation function, since numerical data in this case can be directly compared with exponentials in r, without any power prefactor.

The 0^+-channel connected wall-wall correlator in the z-direction is defined as

$$G(|z_1 - z_2|) = \mathrm{Re}\langle \bar{P}(z_1) \bar{P}(z_2)^\dagger \rangle - |\langle P \rangle|^2 \ , \tag{2.25}$$

where

$$\bar{P}(z) = \frac{1}{N_x N_y} \sum_{n_x=1}^{N_x} \sum_{n_y=1}^{N_y} P(n_x a, n_y a, z) \ , \tag{2.26}$$

represents the Polyakov loop averaged over the xy-plane at a given z. Here and in the following, N_i $(i = x, y, z)$ is the number of lattice sites in the i-direction. The wall average implies the projection at zero momentum in the xy-plane.

The correlation function (2.25) takes contribution from all the screening masses in the 0^+ channel. In fact, the general large distance behavior for the function $G(|z_1 - z_2|)$, in an infinite lattice, is:

$$G(|z_1 - z_2|) = \sum_n a_n e^{-m_n |z_1 - z_2|} \ , \tag{2.27}$$

where m_0 is the fundamental mass, while m_1, m_2, ... are higher masses with the same angular momentum and parity (0^+) quantum numbers of the fundamental mass. On a periodic lattice the above equation must be modified by the inclusion of the so called "echo" term:

$$G(|z_1 - z_2|) = \sum_n a_n \left[e^{-m_n |z_1 - z_2|} + e^{-m_n (N_z - |z_1 - z_2|)} \right] . \tag{2.28}$$

The fundamental mass in a definite channel can be extracted from wall-wall correlators by looking for a plateau of the effective mass,

$$m_{\rm eff}(z) = \ln \frac{G(z-1)}{G(z)} \tag{2.29}$$

at large distances. For the 2^+-channel, we used the variational method [86, 87], which consists in defining several wall-averaged operators with 2^+ quantum numbers and in building the matrix of cross-correlations between them. The eigenvalues of this matrix are single exponentials of the effective masses in the given channel. The variational method is usually adopted to determine massive excitations above the fundamental one in the given channel. In our case, however, it turned out that this method improved the determination of the fundamental mass in the 2^+-channel, but did not lead to determine higher excitations. Our choice of wall-averaged operators in the 2^+-channel is inspired by Ref. [88] and reads

$$\bar{P}_n(z) = \frac{1}{N_x N_y} \sum_{n_x=1}^{N_x} \sum_{n_y=1}^{N_y} P(n_x a, n_y a, z) \Big[P(n_x a + na, n_y a, z) - P(n_x a, n_y a + na, z) \Big] \ . \tag{2.30}$$

In most cases we have taken 8 operators, corresponding to different values of n, with the largest n almost reaching the spatial lattice size N_x. We have determined the 0^+ and the 2^+ fundamental masses in lattice units, $\hat{m}_{0^+}$ and $\hat{m}_{2^+}$, over a wide interval of temperatures above the transition temperature T_t of (3+1)d $SU(3)$ and have studied

- the extent of the region above T_t over which the fundamental correlation length $\hat{\xi}_0 = 1/\hat{m}_{0^+}$ scales with the temperature with the appropriate critical exponent for a first order phase transition, $\nu = 1/3$ [89];

- if $\hat{m}_{2^+}$ has the same scaling behavior as $\hat{m}_{0^+}$;

- how the ratio m_{2^+}/m_{0^+} compares with the ratio of the corresponding excitations in the broken phase of $3d$ 3-state Potts model near the transition, $m_{2^+}/m_{0^+} = 2.43(10)$, found in Ref. [75] on a 48^3 lattice.

We consider also correlators of the (wall-averaged) real and imaginary parts of the Polyakov loop, defined as

$$G_R(|z_1 - z_2|) \ = \ \langle {\rm Re}\bar{P}(z_1) {\rm Re}\bar{P}(z_2) \rangle - \langle {\rm Re}\bar{P}(z_1) \rangle \langle {\rm Re}\bar{P}(z_2) \rangle \ , \tag{2.31}$$

$$G_I(|z_1 - z_2|) \;=\; \langle \mathrm{Im}\bar{P}(z_1)\mathrm{Im}\bar{P}(z_2)\rangle \; . \tag{2.32}$$

The corresponding screening masses, $\hat{m}_R$ and $\hat{m}_I$, can be extracted in the same way as for the 0^+ mass.

We have studied the ratio m_I/m_R over a wide interval of temperatures above the transition temperature T_t of (3+1)d $SU(3)$ and seen how it compares with the prediction from high-temperature perturbation theory, according to which it should be equal to 3/2 [90, 91], and with the prediction from the mean-field Polyakov loop model of Ref. [84], according to which it should be equal to 3 in the transition region. The interplay between the two regimes should delimit the region where mean-field Polyakov loop models should be effective.

2.6 Numerical results

We used the Wilson lattice action and generated Monte Carlo configurations by a combination of the modified Metropolis algorithm [24] with over-relaxation on $SU(2)$ subgroups [92]. The error analysis was performed by the jackknife method over bins at different blocking levels. We performed our simulations on a $16^3\times 4$ lattice, for which $\beta_t = 5.6908(2)$ [93], over an interval of β values ranging from 5.69 to 9.0.

Screening masses are determined from the plateau of $m_{\mathrm{eff}}(z)$ as a function of the wall separation z. In each case, the *plateau mass* is taken as the effective mass (with its error) belonging to the *plateau* and having the minimal uncertainty. We define *plateau* the largest set of consecutive data points, consistent with each other within 1σ. This procedure is more conservative than identifying the plateau mass and its error as the results of a fit with a constant on the effective masses $m_{\mathrm{eff}}(z)$, for large enough z.

Just above the critical value β_t we find a large correlation length, which is not of physical relevance. It is instead a genuine finite size effect [78] related to *tunneling* between degenerate vacua. This effect disappears by going to larger lattice volumes or moving away from β_t in the deconfined phase. Indeed, by increasing β one can see that the symmetric phase becomes less and less important in the Monte Carlo ensemble, up

to disappearance; then, for large enough β, also the structure with three-degenerate $Z(3)$ sectors disappears, leaving only the real sector of $Z(3)$. This is illustrated in Fig. 2.2 where the scatter plot of the Polyakov loop is shown for three representative β values.

Tunneling can occur between the symmetric and the broken phase, and between the three degenerate vacua of the deconfined phase. The former survives only in a short range of temperatures around β_t, and at $\beta \simeq 5.71$ has almost completely disappeared, as we can see from Fig. 2.2(b). When tunneling is active, the correlation function has the following expression [78]:

$$G(|z_1 - z_2|) \sim a_0 e^{-m_0|z_1-z_2|} + b_0 e^{-m_t|z_1-z_2|} \ , \tag{2.33}$$

where m_t is the inverse of the tunneling correlation length and is generally much smaller than the fundamental mass m_0 and therefore behaves as a constant additive term in the correlation function. In (2.33) we have taken into account only the lowest masses in the spectrum and omitted the "echo" terms. The dependence on m_t in the correlation function can be removed by extracting the effective mass by use of the combination

$$m_{\rm eff}(z) = \ln \frac{G(z) - G(z+1)}{G(z+1) - G(z+2)} \ . \tag{2.34}$$

For $\beta \geq 5.71$ the only active tunneling is among the three broken minima. However, the separation among them is so clear (see, for instance, Fig. 2.3(a)), that it is possible to "rotate" unambiguously all the configurations to the real sector (see Fig. 2.3(b)) and to treat them on the same ground.

We have performed simulations for several values of β in the deconfined phase, up to $\beta = 9.0$, with a statistics of a few hundred thousand "measurements" at each β value. Simulations have been performed on the PC cluster "Majorana" of the INFN Group of Cosenza.

As discussed in the Introduction and in Section 2.5, our typical observable is a screening mass in a given channel of angular momentum and parity, identified as the plateau value in the plot of the effective mass as a function of the separation z between two-dimensional walls. The procedure to determine the plateau value has been illustrated

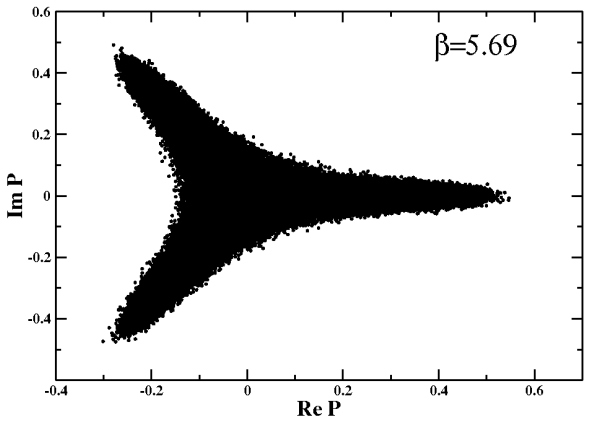

(a)

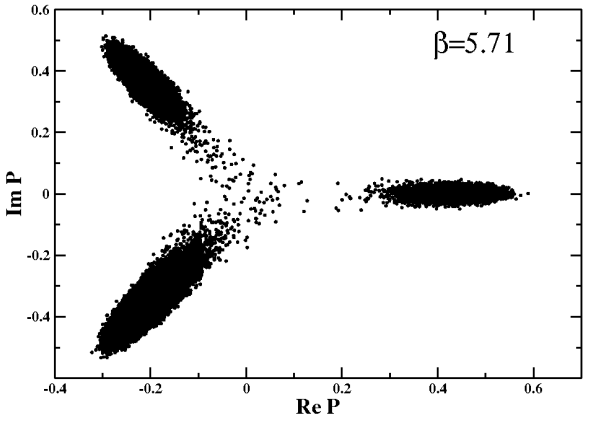

(b)

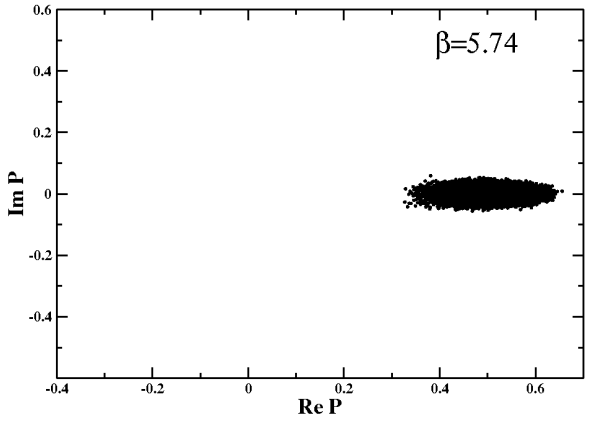

(c)

Figure 2.2: Scatter plots of the real and imaginary part of the Polyakov loop at (a) $\beta = 5.69 \simeq \beta_t$, (b) $\beta = 5.71$ and (c) $\beta = 5.74$.

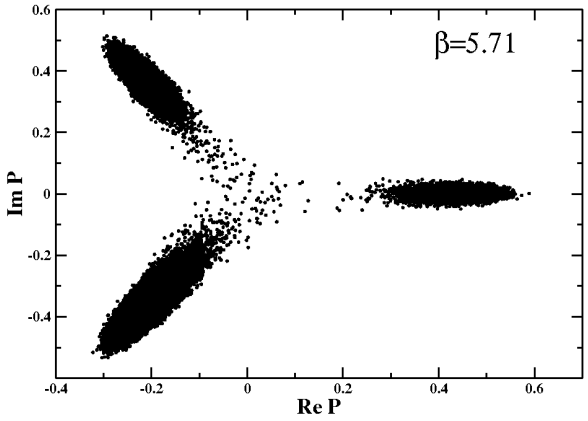

(a)

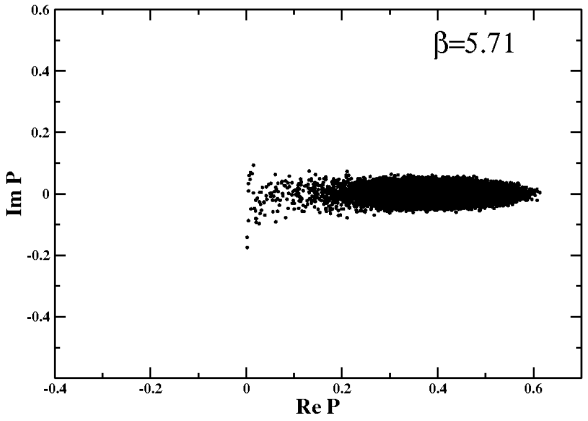

(b)

Figure 2.3: (a) Typical scatter plot of the complex order parameter P for β larger than 5.705 on a $16^3 \times 4$ lattice. There are no states in the symmetric phase, but tunneling survives between the three broken minima.

(b) Same as (a) with the tunneling between broken minima removed by the "rotation" to the real phase.

in Section 2.5. A typical example of the behavior of the effective mass with z is shown in Fig. 2.4 for the 0^+ and the 2^+ channels and in Fig. 2.5 for the masses $\hat{m}_I$ and $\hat{m}_R$ ext

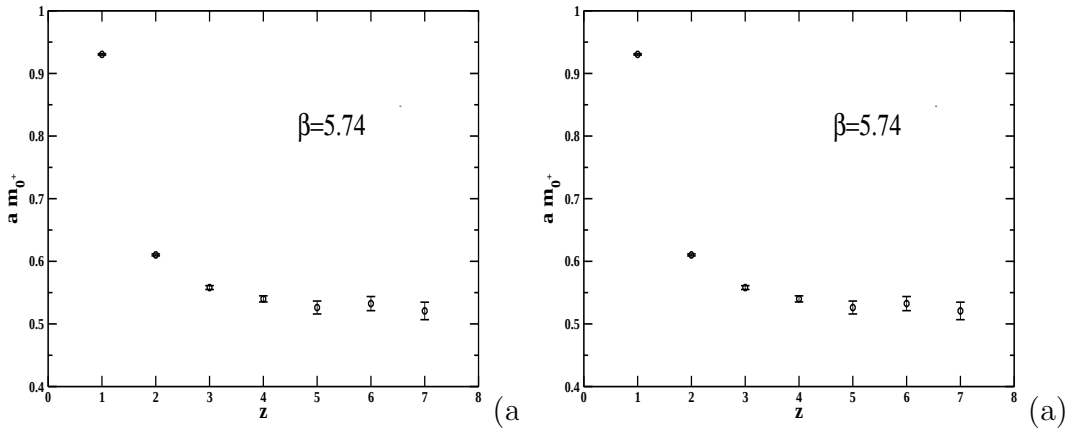

Figure 2.4: Effective mass in the 0^+ (a) and the 2^+ (b) channel as a function of the separation between walls on the (x, y) plane at $\beta = 5.74$.

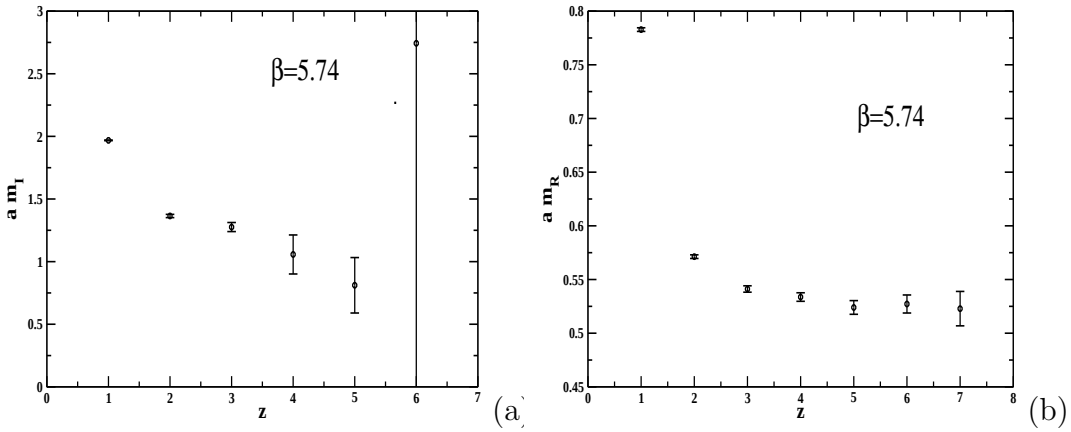

Figure 2.5: Effective mass $\hat{m}_I$ (a) and $\hat{m}_R$ (b) as a function of the separation between walls on the (x, y) plane at $\beta = 5.74$.

The deviation from the plateau value at small z can be attributed to lattice artifacts and to the possible effect of other states with excited masses in the same channel. Our determinations refer only to the fundamental masses in a given channel. The behavior with β of the fundamental masses in the 0^+ and the 2^+ channels is given in Fig. 2.6.

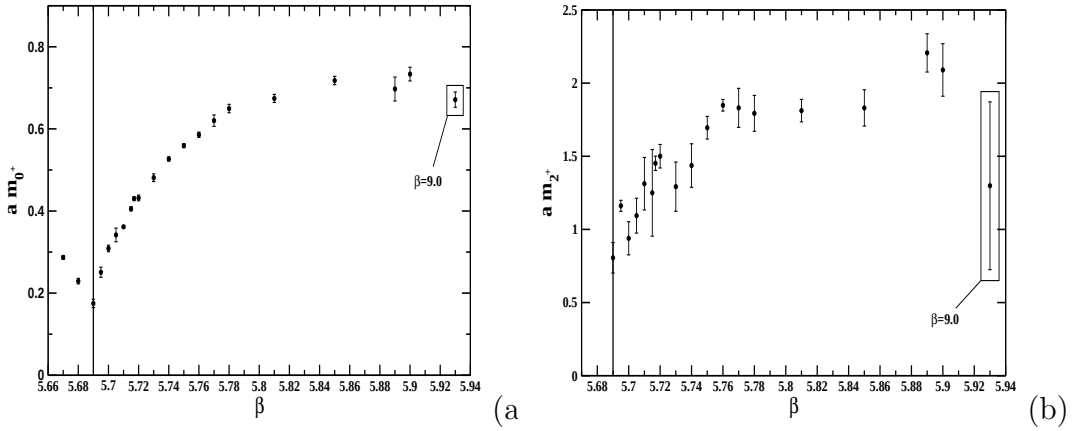

Figure 2.6: Screening mass in the 0^+ (a) and in the 2^+ (b) channel as a function of β.

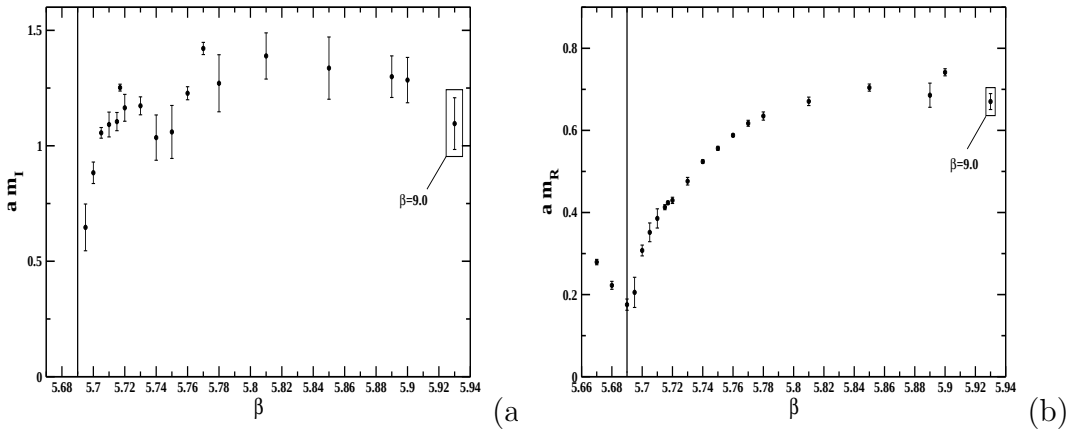

Figure 2.7: Screening mass $\hat{m}_I$ (a) and $\hat{m}_R$ (b) as a function of β.

A summary of all our results is presented in Table 2.1. We observe from Table 2.1 that $\hat{m}_{0^+}$ and $\hat{m}_R$ are consistent within statistical errors, this indicating that the Polyakov loop correlation is dominated by the correlation between the real parts. Our results for $\hat{m}_{0^+}$ at $\beta = 5.70$ and $\beta = 5.90$ ($T \simeq 3T_t/2$) can be compared with the corresponding determinations on a $4 \times 8^2 \times 16$ lattice of Ref. [94], which give $0.27^{+0.01}_{-0.02}$ and 0.64(1), respectively. The $\sim$15% disagreement can be taken as a measure of the systematic effects involved in the whole procedure for the determination of masses. We cannot make a direct comparison with the determination for $\hat{m}_{0^+}$ at $\beta = 5.93$ on a $16^3 \times 4$ lattice of

Ref. [95], since we did not perform simulations at this value of β. We observe, however, that the determination of Ref. [95], which gives 0.73(5) according to our definition of plateau mass value, agrees with the results for the two adjacent β values in our Table, $\beta = 5.90$ and $\beta = 9.0$.

We can see that the fundamental mass in the 0^+ channel, as well as $\hat{m}_R$, becomes much smaller than 1 at β_t, as expected for a weakly first order phase transition. In the cases of $\hat{m}_{0^+}$ and of $\hat{m}_{R,I}$ we have made some determinations even *below* β_t (see Figs. 2.6 and 2.7), where the concept of "screening" does not apply. It turns out, as it must be, that masses in lattice units take their minimum value just at β_t, where there is a "cusp" in the β-dependence. Such a behavior was observed also by the authors of Ref. [94], whose results, when the comparison is possible, agree with ours.

2.6.1 Scaling behavior and comparison with the Potts model

In order to estimate the extension of the scaling region, we have compared our data with the scaling law for first order phase transitions,

$$\left(\frac{\beta_1 - \beta_t}{\beta_2 - \beta_t}\right)^{\nu} \sim \frac{\hat{m}_{0^+}(\beta_1)}{\hat{m}_{0^+}(\beta_2)} \ , \tag{2.35}$$

where $\nu = 1/3$ [89] and $\hat{m}_{0^+}(\beta_1)$ and $\hat{m}_{0^+}(\beta_2)$ are the fundamental masses in the 0^+ channel at β_1 and β_2, respectively. One can use the scaling law (2.35) instead of the correct one

$$\left(\frac{T_1 - T_t}{T_2 - T_t}\right)^{\nu} \sim \frac{\hat{m}_{0^+}(T_1)}{\hat{m}_{0^+}(T_2)} \ , \tag{2.36}$$

in an interval around T_t short enough that the linear approximation $T_1 - T_t \propto \beta_1 - \beta_t$ holds. We have chosen $\beta_1 = 5.72$ and varied β_2 from β_t to $\beta = 9.0$.

Fig. 2.8 shows that the scaling region extends at least up to $\beta \simeq 5.78$. We would like to stress that we have found here a scaling with exponent $\nu = 1/3$ using *connected* correlation functions, although in Ref. [89] it is noted that this exponent should apply to the *standard* correlation function.

Then, we have considered the β-dependence of the ratio m_{2^+}/m_{0^+}, shown in Fig. 2.9. We can see that this ratio is roughly constant in the scaling region, thus suggesting that

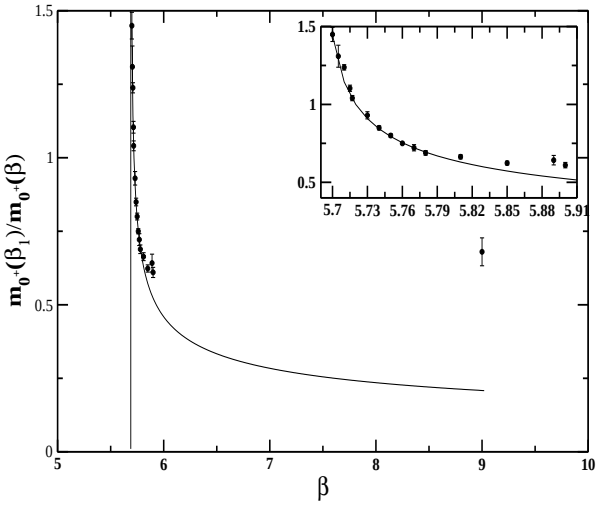

Figure 2.8: Comparison between the scaling function $[(\beta_1-\beta_t)/(\beta-\beta_t)]^{1/3}$ and the mass ratio $m_{0^+}(\beta_1)/m_{0^+}(\beta)$ for varying β, with β_1=5.72.

$\hat{m}_{2^+}$ scales similarly to $\hat{m}_{0^+}$. Moreover, this ratio is in rough agreement with the ratio between the lowest massive excitations in the same channels in the broken phase of the $3d$ 3-state Potts model. This suggests that, at least as far as screening effects are concerned, the $3d$ 3-state Potts model in the broken phase near the transition can be taken as an approximate description of (3+1)d $SU(3)$ pure gauge theory at finite temperature in the deconfined phase near transition.

2.6.2 Comparison with Polyakov loop models

We have calculated the ratio m_I/m_R for β ranging from 5.695 up to 9.0, which means that we have considered this ratio also across the transition temperature. We observe from Fig. 2.10 that this ratio is compatible with 3/2 at the largest β values considered, in agreement with the high-temperature perturbation theory. Then, when the temperature is lowered towards the transition, this ratio goes up to a value compatible with 3, in agreement with the Polyakov loop model of Ref. [84], which contains only quadratic, cubic and quartic powers of the Polyakov loop, i.e. the minimum number of terms required in order to be compatible with a first order phase transition.

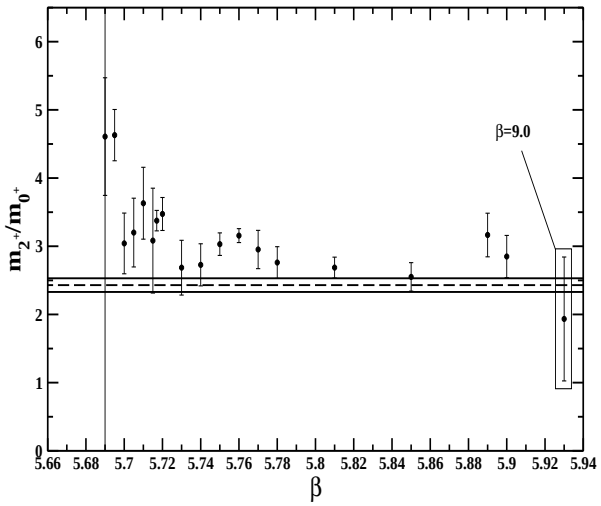

Figure 2.9: Ratio m_2^+/m_0^+ as a function of β in the deconfined phase, compared with the $3d$ 3-state Potts model value [75] (horizontal line with its error).

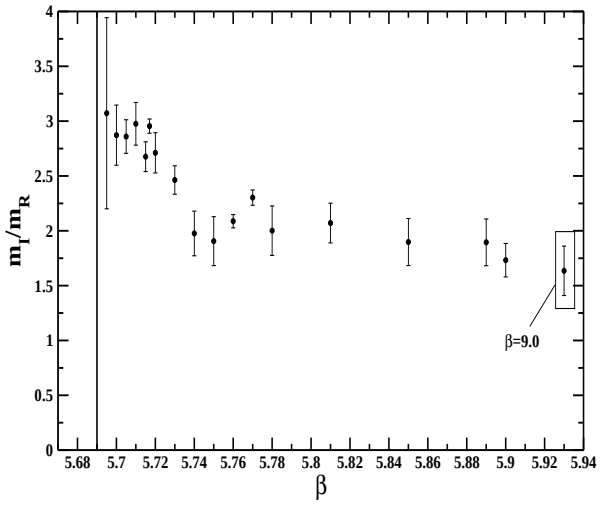

Figure 2.10: Ratio m_I/m_R as a function of β in the deconfined phase. The vertical line corresponds to the critical β value.

2.7 Conclusions

We have studied some screening masses of the (3+1)d $SU(3)$ pure gauge theory from Polyakov loop correlators in a large interval of temperatures above the deconfinement transition.

In particular, we have considered the lowest masses in the 0^+ and the 2^+ channels of angular momentum and parity and the screening masses resulting from the correlation between the real parts and between the imaginary parts of the Polyakov loop.

The behavior of the ratio between the masses in the 0^+ and the 2^+ channels with the temperature suggests that they have a common scaling behavior, in agreement with a (weakly) first order phase transition, above the transition temperature. Moreover, this ratio is in fair agreement with the ratio of the lowest massive excitations in the same channels of the $3d$ 3-state Potts model in the broken phase. This suggests that the Svetitsky-Yaffe conjecture, valid in strict sense only for continuous phase transitions, can play some role also for (3+1)d $SU(3)$ at finite temperature.

The dependence on the temperature of the ratio between the screening masses from the correlation between the real parts and between the imaginary parts of the Polyakov loop shows a nice interplay between the high-temperature regime, where perturbation theory applies, and the transition regime, where mean-field effective Polyakov loop models could apply, except for a sudden drop very close to the transition for which we could not find any explanation.

Table 2.1: Summary of the results for the fundamental masses in the 0^+ and 2^+ channels, for $\hat{m}_I$ and $\hat{m}_R$ and for some mass ratios.

β	$\hat{m}_{0^+}$	$\hat{m}_{2^+}$	m_{2^+}/m_{0^+}	$\hat{m}_I$	$\hat{m}_R$	m_I/m_R	stat.
5.67	0.2870(46)	-	-	-	0.2793(65)	-	750k
5.68	0.2293(67)	-	-	-	0.2226(97)	-	250k
5.69	0.175(10)	0.81(10)	4.61(86)	-	0.176(14)	-	770k
5.695	0.251(12)	1.161(38)	4.63(38)	0.65(10)	0.205(37)	3.07(87)	320k
5.70	0.3088(80)	0.94(11)	3.04(45)	0.883(47)	0.307(13)	2.87(27)	770k
5.705	0.342(17)	1.09(12)	3.20(50)	1.056(23)	0.352(23)	2.86(15)	750k
5.71	0.3615(30)	1.31(18)	3.63(53)	1.092(54)	0.386(23)	2.98(19)	770k
5.715	0.4054(51)	1.25(30)	3.08(77)	1.105(40)	0.4129(61)	2.68(14)	250k
5.717	0.4301(46)	1.452(49)	3.38(15)	1.252(15)	0.4237(43)	2.955(65)	320k
5.72	0.4319(69)	1.500(80)	3.47(24)	1.164(58)	0.4296(76)	2.71(18)	770k
5.73	0.4811(92)	1.29(17)	2.69(40)	1.173(39)	0.4762(92)	2.46(13)	170k
5.74	0.5267(52)	1.44(15)	2.73(31)	1.035(98)	0.5241(44)	1.98(20)	770k
5.75	0.5592(50)	1.695(77)	3.03(17)	1.06(11)	0.5562(49)	1.91(22)	770k
5.76	0.5857(65)	1.849(39)	3.16(10)	1.227(28)	0.5880(36)	2.087(61)	770k
5.77	0.620(14)	1.83(13)	2.95(28)	1.421(26)	0.6173(73)	2.303(70)	60k
5.78	0.650(10)	1.79(12)	2.76(23)	1.27(12)	0.635(10)	2.00(23)	60k
5.81	0.6742(99)	1.812(77)	2.69(15)	1.39(10)	0.671(10)	2.07(18)	190k
5.85	0.718(10)	1.83(12)	2.55(21)	1.34(13)	0.7042(87)	1.90(21)	110k
5.89	0.697(29)	2.21(13)	3.17(32)	1.299(90)	0.686(29)	1.89(21)	190k
5.90	0.734(17)	2.09(18)	2.85(31)	1.284(98)	0.7415(87)	1.73(15)	215k
9.0	0.671(19)	1.30(57)	1.93(91)	1.10(11)	0.670(19)	1.64(23)	200k

Chapter 3

The $SU(3)$ pure gauge theory. Flux tubes in confined and deconfined phases

Quark confinement in QCD is a central phenomenon in the particle physics, which has continued to intrigue people for many years. Much insight has already been obtained from different approaches to the problem. A satisfying solution would be to set up an approximate vacuum state which confines color charges. In this way one could derive an effective action which describes the long-distance properties of QCD [96]. We have at our disposal a framework in which we can do non-perturbative calculations, namely the lattice discretization of gauge theories. Since a typical Monte Carlo simulation generates vacuum configurations, one expects to gain information on the non-perturbative vacuum structure.

At the end of 1975 G. 't Hooft [97] and S. Mandelstam [98] proposed that the confining vacuum of QCD behaves as a coherent state of color magnetic monopoles. This is equivalent to say that the vacuum of QCD is a magnetic (dual) superconductor. This fascinating proposal offers a picture of confinement whose physics can be clearly extracted. As a matter of fact, the dual Meissner effect causes the formation of chromo-

electric flux tubes between chromoelectric charges leading to a linear rising potential. It is worthwhile to discuss briefly the 't Hooft's proposal [1].

3.1 A magnetic (dual) superconductivity scenario

In the usual electric superconductor the corresponding solution of Ginzburg-Landau equations was first found by Abrikosov [99], which was later revived in field theory [100] and became known as Abrikosov-Nielsen-Olesen vertex. In the "dual superconductor" picture of the QCD vacuum properties of the QCD confining string and the resulting heavy quark potentials have been discussed extensively: see e.g. reviews by M. Baker [101], and more recently by G. Ripka [102] (with exhaustive list for further references).

Lattice studies (e.g. [103]) provided substantial support to these works. Flux tube behavior at finite T was also extensively discussed: in particular Polyakov [80] has shown how exponential growth of flux tube entropy leads to vanishing of the effective tension in free energy $F(r,T)$ and Hagedorn-like phase transition. This scenario would predict gradual deconfinement with the string tension vanishing at T_c: in fact for $N_c > 2$ it jumps to zero. Deconfinement transition for various number of colors N_c was studies in detail: see e.g. [104] where N_c up to 12 was studied. Working with metastable "overheated" confined phase it was found that the Hagedorn-like transition (at which the string tension of the free energy vanishes $\sigma(T) \to 0$) can be approximately located at a universal (N_c independent) $T_H/T_c = 1.116(9)$.

Heating usual superconductors above the critical temperature destroys not only the condensate but also Cooper pairs themselves. Although normal (metallic) phase is a plasma of electric objects (electrons), but their characteristic momenta $p \sim p_F$ are orders of magnitude larger than momenta of Cooper pairs, thus there is no analog of Abrikosov vortexes in the normal phase. This does not happen because presence of a quantum condensate is that necessary for flux tube's existence: a counterexample can be provided

[1] This point is thoroughly discussed in the second paper [50].

e.g. by quite spectacular magnetic flux tubes in solar plasma [2]. Whether charges are Bose-condensed or not, their scattering on a flux tube may provide a pressure which may lead to its stabilization. It is just a matter of certain quantitative condition for tube stabilization being met.

The investigation of the dual superconductivity hypothesis in pure $SU(2)$ lattice gauge theory was done by [105]. They focus on the dual Meissner effect by analyzing the distribution of the color fields due to a static quark-antiquark pair finding evidence of the dual Meissner effect both in the maximally Abelian gauge and without gauge fixing. Their results suggest that the London penetration length is a physical gauge-invariant quantity.

We continue their work, using the same technique for the more interesting case of $SU(3)$ pure gauge theory, studying the chromoelectric distribution at zero and at a finite temperature.

3.2 Strongly coupled plasma with electric magnetic charges

In 2006 J.Liao and E. Shuryak [106] proposed a different approach, which does not put $confinement$ phenomenon at the center of the discussion. In the traditional one, the temperature regimes are divided into two basic phases: (i) confined or hadronic phase at $T < T_c$, and (ii) deconfined or quark-gluon plasma (QGP) phase at $T > T_c$.

They, on the other hand, focus on the competition of electrically and magnetically quasiparticles (EQPs and MQPs, respectively) and divide the phase diagram differently, into (i) the "magnetically dominated" region at $T < T_{E=M}$ and (ii) "electrically dominated" one at $T > T_{E=M}$. In their opinion, the key aspect of the physics involved is the *coupling strength* of both interactions. So, a divider is some *E-M equilibrium* region at

[2] They have very large fluxes and sizes, and thus a macroscopic theory – magnetohydrodynamics – can be used for their description, which unfortunately it is not applicable in our case, for microscopically small tubes.

intermediate T-μ. Since it does *not* correspond to a singular line, one can define it in various ways: the most direct one is to use a condition that electric (e) and magnetic (g) couplings are equal

$$e^2/\hbar c = g^2/\hbar c = 1/2 \ . \tag{3.1}$$

The last equality follows from the celebrated Dirac quantization condition [107]

$$\frac{eg}{\hbar c} = \frac{n}{2} \ , \tag{3.2}$$

with n being an integer, put to 1 from now on.

Besides equal couplings, the equilibrium region is also presumably characterized by comparable densities as well as masses of both electric and magnetic quasiparticles [3].

The "magnetic-dominated" low-T (and low-μ) region (i) can in turn be subdivided into the *confining* part (i-a) in which electric field is confined into quantized flux tubes surrounded by the condensate of MQPs, forming t'Hooft-Mandelstamm "dual superconductor" [108], and a new *"postconfinement"* region (i-b) at $T_c < T < T_{E=M}$ in which EQPs are still strongly coupled (correlated) and still connected by the electric flux tubes. They believe this picture better corresponds to a situation in which string-related physics is by no means terminated at $T = T_c$: rather it is at its maximum there. Then if leaving this "magnetic-dominated" region and passing through the equilibrium region by increase of T and/or μ, we enter either the high-T "electric-dominated" QGP or a color-electric superconductor at high-μ replacing the dual superconductor (with diquark condensate taking place of monopole condensate). A phase diagram explaining this viewpoint pictorially is shown in Fig. 3.1. In this scenario, when heated slightly above T_c, the monopole condensate changes into a non-condensed ensemble of monopoles, which is roughly twice less dense. Yet it is still capable of supporting flux tubes survived from vacuum, and only around $T = 1.3T_c$ the density of monopoles drops so low that there will not be flux tube any more. At very high temperature the electric sector becomes

[3]Let us however remind the reader that the E-M duality is of course not exact, in particular EQPs are gluons and quarks with spin 1 and 1/2 while MQPs are spherically symmetric "hedgehogs" without any spin.

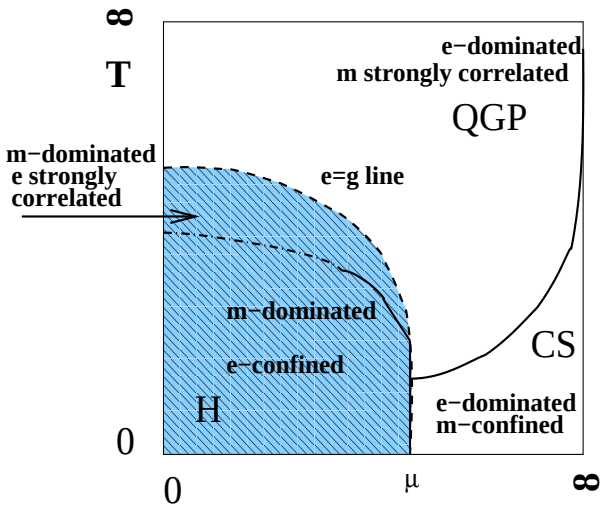

Figure 3.1: A schematic phase diagram on a ("compactified") plane of temperature and baryonic chemical potential $T - \mu$. The (blue) shaded region shows "magnetically dominated" region $g < e$, which includes the e-confined hadronic phase as well as "postconfined" part of the QGP domain. Light region includes "electrically dominated" part of QGP and also color superconductivity (CS) region, which has e-charged diquark condensates and therefore obviously m-confined. The dashed line called "e=g line" is the line of electric-magnetic equilibrium. The solid lines indicate true phase transitions, while the dash-dotted line is a deconfinement cross-over line.

more and more dominant until eventually small number of heavy monopoles become embedded in the perturbative electric plasma.

This picture, among many other new viewpoints, opens a completely new perspective on the role of electric flux tubes: they should not disappear at $T = T_c$ but are rather at their maximum.

However, in a previous work [109] the field distributions around a static $q\bar{q}$ pair at finite temperature have been studied using Polyakov loop plaquette correlations at physical quark separations up to 1.4fm. From the profiles at various T they found that the physical width of the flux tube decreases when T increases. Their conclusion is that the fall of the width and height with the temperature at the same time shows the gradual disappearance of the flux tube when the temperature approaches T_c.

3.3 Lattice determination of the Flux Tube

At $T = 0$ static potential between heavy quarks is the sum of the Coulomb and the confining $\sim \sigma(T = 0)r$ potentials. At nonzero T expectations of the Polyakov loops with a static quark pair define the free energy potential $F(T, r)$, which at the deconfinement point $T = T_c$ has vanishing string tension $\sigma(T_c) = 0$.

However [80] the *energy* or *entropy* separately [4] continue to have linear part in the "postconfinement" domain $T_c < T < T_{E=M}$, as follows from lattice data [110]. These lattice studies reveal that energy and entropy associated with a static quark pair are strongly peaked exactly at the transition temperature (see Fig. 3.2). Quite shockingly, the tension term in $E(T = T_c, r)$ is not smaller but actually twice larger than the zero temperature tension $\sigma(T = 0)$! The total energy added to a pair till it finally breaks into two objects is surprisingly large: $E(T = T_c, r \to \infty) \sim 4$ GeV, while the corresponding entropy as large as $S(T = T_c, r \to \infty) \sim 20$.

Where all these huge energy and entropy come from, at T_c and in the "postconfinement" domain? Linear dependence on r hints that it must still be a string-like object

[4] Related as usual by $F = E - TS$, $S = -\partial F/\partial T$.

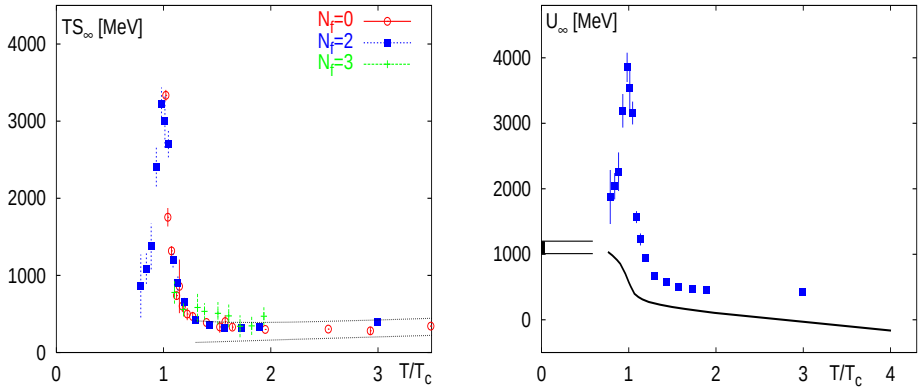

Figure 3.2: (left) The contribution $TS_\infty(T)$ appearing in the free energy, $F_\infty(T) = U_\infty(T) - TS_\infty(T)$, calculated in 2-flavour QCD as function of T/T_c. They also show results from 3-flavour QCD for $T \geq 1.1T_c$ [111] and quenched QCD [112]. (right) The internal energy $U_\infty(T)$ versus T/T_c calculated in 2-flavour QCD. The corresponding free energy, $F_\infty(T)$, calculated in 2-flavour QCD is also shown as solid line. They again indicate in this figure the energy at which string breaking is expected to take place at $T = 0$, $V(r_{\rm breaking}) \simeq 1000 - 1200$ MeV (dashed lines), using $r_{\rm breaking} = 1.2 - 1.4$ fm [113].

connecting two static charges. Can it be that magnetically dominant plasma admits (metastable) electric flux tubes solutions? The answer to this question was given in a recent paper [114]. Indeed, whether monopoles are condensed or not is not so crucial: what is important is the relation between their energy and the repulsive potential of the flux tube. At high enough T flux tube solution disappears, and the critical condition they found roughly does correspond to the upper limit of the "postconfinement" domain.

3.3.1 Zero temperature

According to Ref. [34, 115], one can explore the field configurations produced by the quark-antiquark pair by measuring a suitable connected correlation function (Fig. 3.3). For the $SU(3)$ case it holds:

$$\rho_W = \frac{\left\langle \mathrm{Tr}\left(W L U_P L^\dagger\right)\right\rangle}{\langle \mathrm{Tr}(W)\rangle} - \frac{1}{3}\frac{\langle \mathrm{Tr}(U_P)\mathrm{Tr}(W)\rangle}{\langle \mathrm{Tr}(W)\rangle}\ , \tag{3.3}$$

where $U_P = U_{\mu\nu}(x)$ is the plaquette in the (μ,ν) plane and W is the Wilson loop. The plaquette is connected to the Wilson loop by a Schwinger line L (see Fig. 3.3). Note that the correlation function (3.8) is sensitive to the field strength rather than to the square of the field strength [116]:

$$\rho_W \overset{a\to 0}{\to} a^2 g\left[\langle F_{\mu\nu}\rangle_{q\bar{q}} - \langle F_{\mu\nu}\rangle_0\right]\ . \tag{3.4}$$

According to Eq. (3.4) we define the color field strength tensor as:

$$F_{\mu\nu}(x) = \frac{\sqrt{\beta}}{2}\,\rho_W(x)\ . \tag{3.5}$$

By varying the distance and the orientation of the plaquette U_P with respect to the Wilson loop W, one can scan the color field distribution of the flux tube.

The main advantage of using the connected correlator (3.8) resides in the fact that the connected correlators are sensitive to the field strength rather than to the square of the field strength. As a consequence we are able to detect a sizeable signal even with

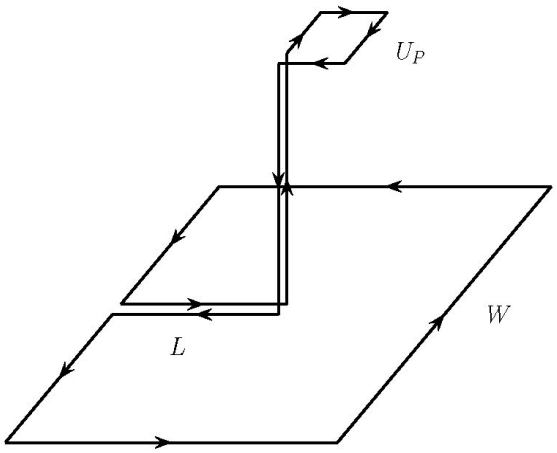

Figure 3.3: The connected correlator 3.8 between the plaquette U_p and the Wilson loop. The subtraction appearing in the definition of correlator is not explicitly drawn.

relatively low statistics. It turns out that the flux tube color fields is composed by the chromoelectric component parallel to the line joining the static charges. Moreover the longitudinal chromoelectric field is almost constant far from the color sources, and it decreases rapidly in the directions transverse to the line connecting the charges. As a matter of fact we found that the transverse distribution of the longitudinal chromoelectric field behaves in accord with the dual Meissner effect. This allows us to determine the London penetration length.

We performed numerical simulations with Wilson action and periodic boundary conditions using an overrelaxed Metropolis algorithm. Our data refer to 12^4 and 16^4 lattices. To evaluate the correlator Eq. (3.8) we used square Wilson loop $L_W \times L_W$, with $L_W = L/2$ (L being the lattice size).

In order to reduce the quantum fluctuations we adopted the controlled cooling algorithm [33], described in the chapter 1. It is known [117] that by cooling in a smooth way equilibrium configurations, quantum fluctuations are reduced by a few orders of magnitude, while the string tension survives and shows a plateau.

The cooling technique allows us to disentangle the signal from the noise with a relatively small statistics. After discarding about 2000 sweeps to insure thermalization

we collect measurements on configurations for different values of β. Firstly we checked how many cooling sweeps assure a good signal. In Fig. 3.4 we report our results for the field strength tensor $F_{\mu\nu}(x_l, x_t)$, where the coordinates x_l, x_t measure respectively the distance from the middle point between quark and antiquark (which corresponds to the center of the spatial side of the Wilson loop W in Eq. (3.8)) and the distance out of the plane defined by the Wilson loop. The entries in Fig. 3.4 refer to measurements

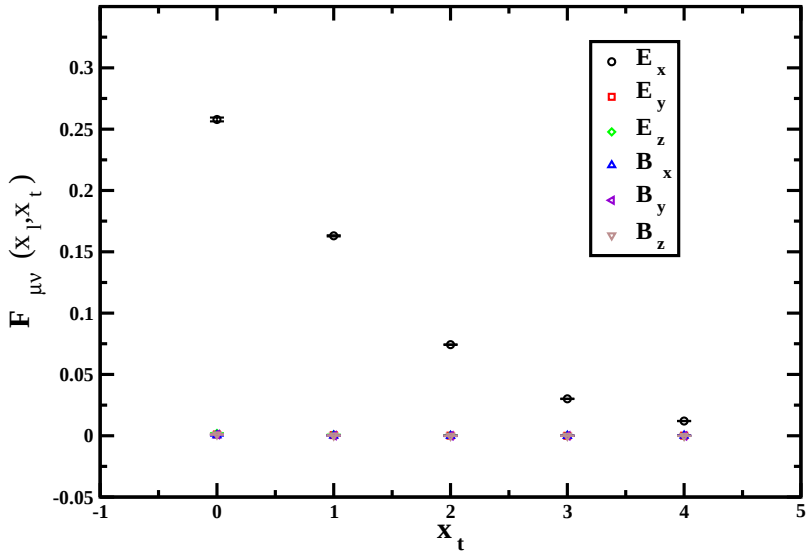

Figure 3.4: The field strength tensor $F_{\mu\nu}(x_l, x_t)$ evaluated at $x_l = 0$ on a 12^4 lattice at $\beta = 6.0$, using Wilson loops of size 4×4 in Eq. (3.8).

of the field strength tensor (actually of the components of the electric and magnetic fields) taken in the middle of the flux tube ($x_l = 0$) with 10 cooling steps at $\beta = 6.0$ on the 12^4 lattice, using a square Wilson loop W of size 4×4. Our results show that ρ_W is sizeable when U_p and W are in parallel planes. This corresponds to measure the component E_l of the chromoelectric field directed along the line joining the $q\bar{q}$ pair (E_x in Fig. 3.4). Moreover we see that $E_l(x_l, x_t)$ decreases rapidly in the transverse direction x_t. In Fig. 3.5 we display the transverse distribution of the longitudinal chromoelectric field along the flux tube for a lattice of 16^4 and a beta value of 6.0. The static color

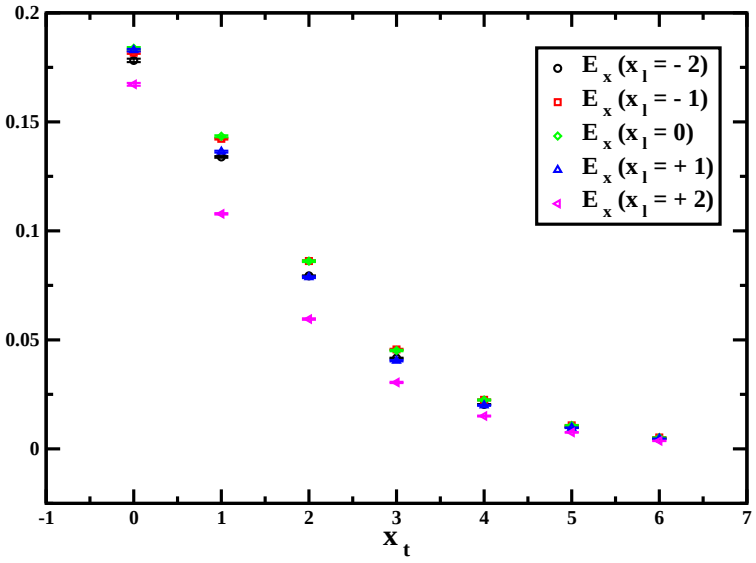

Figure 3.5: The x_l-dependence of the transverse profile of the longitudinal chromoelectric field $E_x(x_l, x_t) \equiv E_l(x_l, x_t)$, ($6 \times 6$ Wilson loop, lattice 16^4).

sources are at $x_l = +2$ and $x_l = -2$ (in lattice units). Fig. 3.5 shows that the effects of the color sources on the chromoelectric fields extends over about two lattice spacings. Remarkably, far from the sources the longitudinal chromoelectric field is almost constant along the $q - \overline{q}$ line. Thus, the color field structure of the $q - \bar{q}$ tube which emerges from our results is quite simple: the flux tube is almost completely formed by the longitudinal chromoelectric field which is constant along the flux tube (if x_l is not too close to the static color sources) and decreases rapidly in the transverse direction.

We find a clear evidence of the chromoelectric flux tube configurations between a static $q\bar{q}$. [5]

If the dual superconductor scenario holds, the transverse shape of the longitudinal chromoelectric field E_l should resemble the dual version of the Abrikosov vortex field

[5]Previous analysis was also made by [118] calculating the squared energy density in the chromoelectric and chromomagnetic flux distribution generated by a static pair for separations of the source up to $R = 4$.

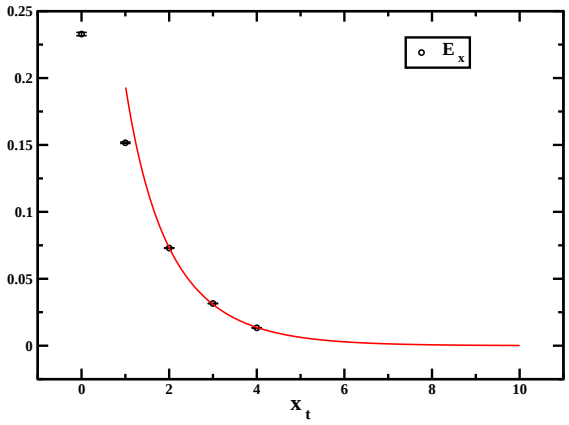

Figure 3.6: The London fit (3.6) to the data for the longitudinal chromoelectric field (12 cooling sweeps).

distribution. Hence we expect that $E_l(x_t)$ can be fitted according to

$$E_l(x_t) = \frac{\Phi}{2\pi}\mu^2 K_0(\mu x_t) \ , \ x_t > 0 \tag{3.6}$$

where K_0 is the modified Bessel function of order zero, Φ is the external flux, and $\lambda = 1/\mu$ is the London penetration length. Equation (3.6) is valid if $\lambda \gg \xi$, ξ being the coherence length (type-II superconductor). The length ξ measures the coherence of the magnetic monopole condensate (the dual version of the Cooper condensate). We fit Eq. (3.6) to our data for $x_t \geq 2$ (in lattice units) obtaining $\chi^2/f \leq 1$ (we used the MINUIT code from the CERNLIB). In Fig. 3.6 we show $E_l(x_t)$ measured in the middle of the flux tube together with the result of our fit. The fit results into the two parameters Φ and μ. Data obtained from the gauge-invariant correlator with cooled gauge configurations lead to a parameter μ which does not show a clear plateau versus the number of cooling steps (see Fig. 3.7). About this new simulations are running.

Our expectation is that the long range physics is unaffected by the cooling procedure. On the other hand, Fig. 3.8 indicates that the overall normalization of the transverse distribution of the longitudinal chromoelectric field is affected by the cooling. In fact the parameter Φ does not stay constant with the cooling. We feel that this is an indication

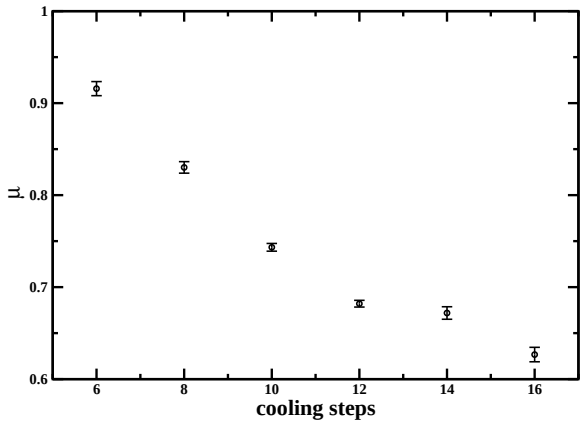

Figure 3.7: The inverse of the penetration length μ versus the number of the cooling steps obtained by fitting the transverse profile of the longitudinal chromoelectric field at $x_l = 0$ (4×4 Wilson loop, lattice 12^4).

that the flux Φ is strongly affected by lattice artefacts [119].

Bresenham algorithm

To study the geometry of the colour flux tube between Q and $\bar{Q}$ sources, one needs an increase both in *resolution* of the underlying lattice and in the *linear extent*, r, of the string [120]. This is achieved by squeezing maximal information out of each vacuum configuration through rotational invariance and comprehensive utilization of *all possible* R*-values* on the lattice [121].

Our aim is to increase statistics in the regime of colour screening, i.e. for large quark antiquark separations, R. Obviously, on such a length scale, a given QCD vacuum configuration contains plenty of information that can be exploited for self averaging and thus for error reduction: firstly, one can realize, on a hypercubic lattice, a fairly dense set of R values; secondly, for a given large value of $R = |\mathbf{R}|$, there are many different three-vector realizations $\mathbf{R}$ on the lattice.

We wish to make use of this fact by a systematic construction of off-axis Wilson loops, $W(R,T)$, in the range $R_{\min} \leq R \leq R_{\max}$. The construction proceeds by choosing

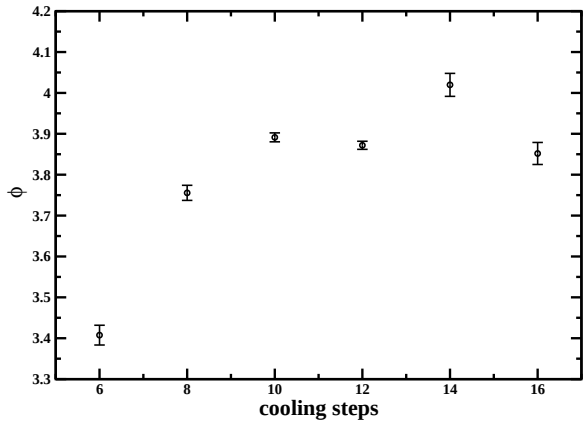

Figure 3.8: The parameter Φ in Eq. (3.6) obtained by fitting the transverse profile of the longitudinal chromoelectric field at $x_l = 0$ versus the number of cooling steps (4×4 Wilson loop, lattice 12^4).

all possible vectors, $\mathbf{R}$, with integer components $C_{\rm min}$, $C_{\rm mid}$, and $C_{\rm max}$ (in any order of appearance) that obey the inequalities,

$$R^2_{\rm min} \leq R^2 = C^2_{\rm min} + C^2_{\rm mid} + C^2_{\rm max} \leq R^2_{\rm max} \ , \tag{3.7}$$

where $|C_{\rm min}| \leq |C_{\rm mid}| \leq |C_{\rm max}|$.

Subsequently, the set of solutions to the constraint eq. (3.7) is sorted according to the corresponding values of R. These technique is used in [122, 123, 124, 125] and moreover they find that ARA reduces the statistical errors on potential values by factors around two.

We shall briefly discuss the construction of the gauge transporters connecting the quark and antiquark locations, $\mathbf{R}_Q$ and $\mathbf{R}_{\bar{Q}} = \mathbf{R}_Q + \mathbf{R}$, that appear within the ARA non-planar Wilson loops. In order to achieve a large overlap with the physical ground state we would like to construct lattice paths that follow as close as possible the straight line connecting $\mathbf{R}_{\bar{Q}}$ with $\mathbf{R}_Q$. This task can be accomplished by a procedure which is known as the Bresenham algorithm [126] in computer graphics. There one wishes to map a straight continuous line between two points, say $\mathbf{0}$ and $\mathbf{C} = (C_{\rm max}, C_{\rm min})$, onto discrete

pixels on a 2-d screen. Then one has to find the explicit sequence of pixel hoppings in max- and min-directions such that the resulting pixel set mimics best the continuum geodesic between points **0** and **C**. The Bresenham prescription is simply to move in max-direction unless a step in min-direction brings you closer to the geodesic from **0** to **C**, where we assume $|C_{\max}| \geq |C_{\min}|$. It can easily be embodied into a fast algorithm based on local decision making only (see Fig. 3.9), by means of a characteristic lattice function χ that incorporates the aspect ratio $C_{\max}/C_{\min}$.

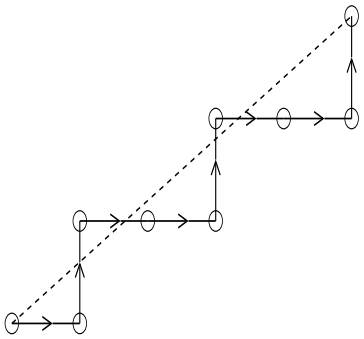

Figure 3.9: Illustration of a path construction by the Bresenham algorithm, for $\mathbf{C} = (5, 3)$.

3.3.2 At finite temperature

At finite temperature the correlator is suggested by [34], and it is:

$$\rho_P = \frac{\left\langle \mathrm{Tr}\left(P(x,t) L U_P L^\dagger\right) \mathrm{Tr} P(y)\right\rangle}{\langle \mathrm{Tr}P(x)\mathrm{Tr}P(y)\rangle} - \frac{1}{N}\frac{\langle \mathrm{Tr}(U_P)\mathrm{Tr}P(x)\mathrm{Tr}P(y)\rangle}{\langle \mathrm{Tr}P(x)\mathrm{Tr}P(y)\rangle}\ , \tag{3.8}$$

where $P(x,t)$ is the Polyakov loop starting from the same site, (x,t), from which the Schwinger line L starts, and using the periodicity of the lattice.

We show examples of the correlator for a plaquette in the plane of the Polyakov loops for the $SU(2)$ gauge theory for a lattice $16^3 \times 4$ ($\beta_c = 2.3$), below the critical temperature in Fig. 3.10 ($\beta = 2.1, 2.2, 2.25$), and above ($\beta = 2.35, 2.37, 2.4, 2.5$) in Fig. 3.11, Fig. 3.12.

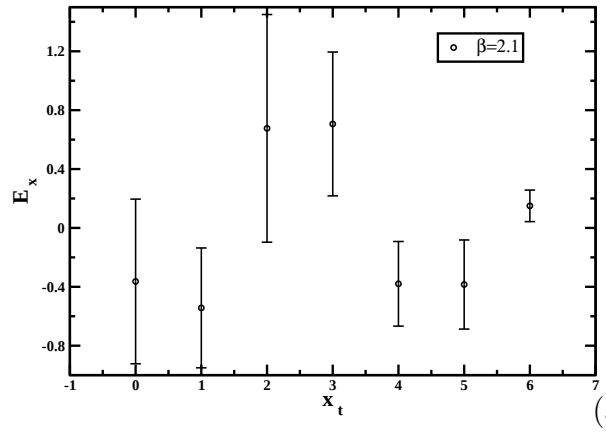

(a)

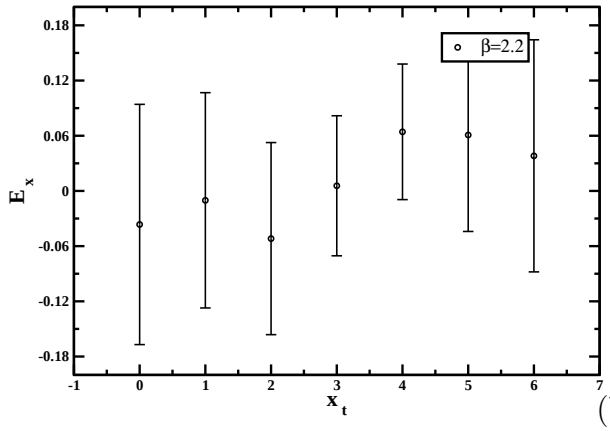

(b)

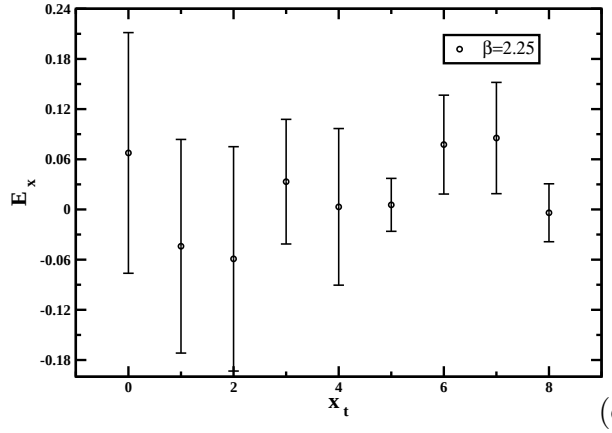

(c)

Figure 3.10: The transverse profile of the longitudinal chromoelectric field $E_x(x_l, x_t)$ evaluated at $x_l = 0$ on a $16^3 \times 4$ lattice at $\beta = 2.1$ (a), $\beta = 2.2$ (b), $\beta = 2.25$ (c) for $SU(2)$ gauge theory.

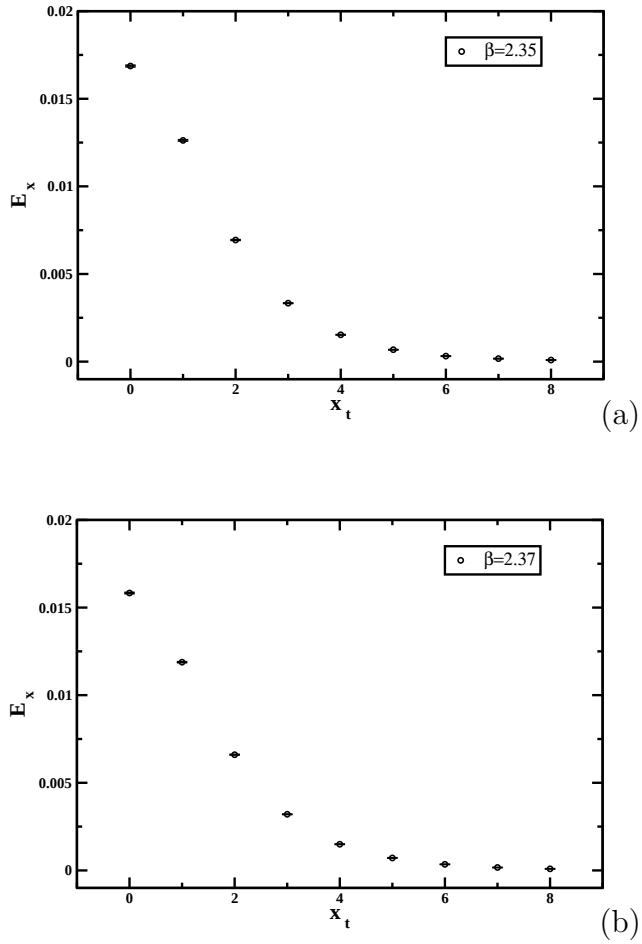

Figure 3.11: The transverse profile of the longitudinal chromoelectric field $E_x(x_l, x_t)$ evaluated at $x_l = 0$ on a $16^3 \times 4$ lattice in the deconfined phase, at $\beta = 2.35$ (a) and $\beta = 2.37$ (b) for $SU(2)$ gauge theory.

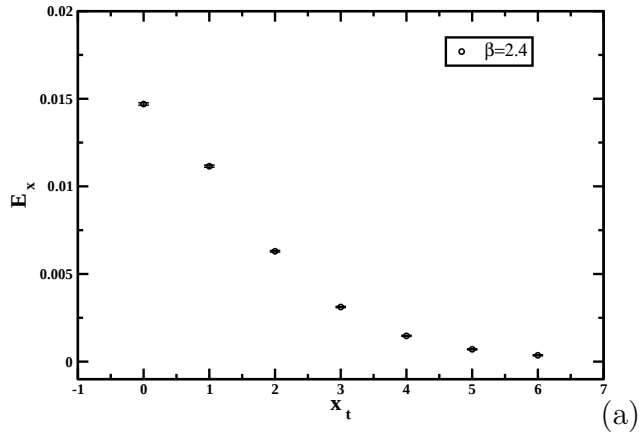

(a)

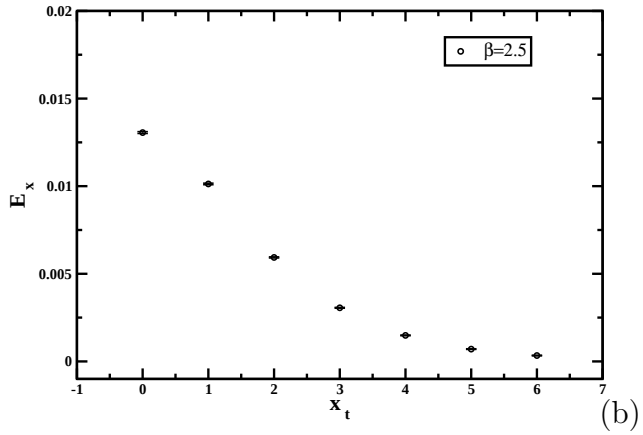

(b)

Figure 3.12: The transverse profile of the longitudinal chromoelectric field $E_x(x_l, x_t)$ evaluated at $x_l = 0$ on a $16^3 \times 4$ lattice in the deconfined phase, at $\beta = 2.4$ (a) and $\beta = 2.5$ (b) for $SU(2)$ gauge theory.

We guess that the bad signal in Fig. 3.10 is caused by the fact that the Polyakov loop at $T < T_c$ is not a good operator (since its expectation value is zero in the confined phase).

3.4 Work in progress

What we have presented since here is still in a preliminary stage. The final aim will be to improve the knowledge both in the $SU(2)$ and, in the more physically interesting case, of the $SU(3)$ pure gauge theory, investigating the flux tube in the confined and in the deconfined phase with a probe which has never been used since up to now.

However there is already something to underline.

Studying the case of $SU(2)$ pure gauge theory at zero (lattice 16^4, $\beta = 2.5$) and at finite temperature (lattice $16^3 \times 4$, $\beta = 2.35, 2.37, 2.4, 2.5$), it seems that we can have a preliminary estimate of the width of the flux tube in the deconfined phase (see Figs. 3.11, 3.12 and Fig. 3.13).

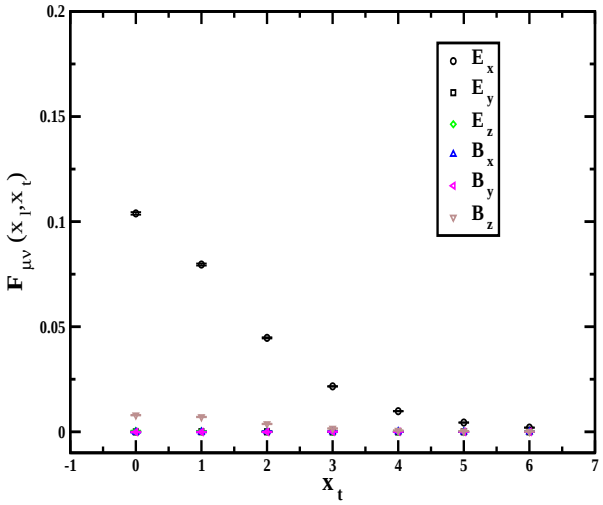

Figure 3.13: The field strength tensor $F_{\mu\nu}(x_l, x_t)$ evaluated at $x_l = 0$ on a 16^4 lattice at $\beta = 2.5$ for $SU(2)$ gauge theory.

Chapter 4

$SU(N)$ pure gauge theories

It is 30 years since it was proposed that it might be useful to think of QCD as a perturbation in $1/N$ around the $N = \infty$ theory [127]. In particular, from an analysis of Fenyman diagrams to all orders one finds that the $N \to \infty$ limit of $SU(N)$ theories is smooth if we vary the coupling as $g^2 \propto 1/N$. This suggests that it should be possible to describe $SU(N)$ gauge theories as perturbations in powers of $1/N$ around $SU(\infty)$ [127] at least for large enough N. Moreover if one assumes confinement for all N, then one can easily show [127, 128] that the phenomenology of the $SU(\infty)$ quark-gluon theory is strikingly similar to that of (the non-baryonic sector of) QCD. This makes it conceivable that the physically interesting $SU(3)$ theory could be largely understood by solving the much simpler $SU(\infty)$ theory. If all the $SU(N)$ theories down to $SU(3)$ can be treated in this way, then this represents an elegant and enormous theoretical simplification.

However we still do not have a quantitative control of the $SU(N = \infty)$ theory and the phenomenology needs to assume, for example, that it is confining and, of course, 'close to' SU(3). Lattice simulations can attempt to answer such questions directly (albeit never exactly) and there has been substantial progress in doing so this last decade, first in $D = 2 + 1$ dimensions [129], and then in the physically interesting case of $D = 3 + 1$. (For a review of work in the earlier 80's, when lattice calculations were not yet precise enough to be so useful, see e.g. [130]).

4.1 $SU(N)$ pure gauge theories and the t'Hooft expansion

Following the guidelines of [131], we will enunciate some motivations for these calculations. A gluon loop on a gluon propagator comes with a factor of g^2N. One easily sees that g^2 is in fact the smallest power of the coupling that comes with a factor of N. So if one wants an $N \to \infty$ limit that is not given by either a free field theory or by infinite order diagrams on all length scales (in neither case would we get something like QCD), then one needs to take the limit keeping g^2N fixed [127]. Using 't Hooft's double-line notation for gluons, diagrams can be categorized as lying on surfaces of different topology, with more handles corresponding to higher powers of $1/N$, so that in the $N = \infty$ limit only planar diagrams survive [127]. As the coupling g^2N becomes strong, the vertices of the diagram fill the surface more densely, defining a world-sheet of the kind one might expect in a string theory. This suggests that perhaps as $N \to \infty$ the gauge theory can be described as a weakly interacting string theory [127]. If the theory is, as one expects, linearly confining then the confining flux tube will behave like a string at long distances, described by some effective string theory. At large N this will presumably coincide with the string theory that describes the $SU(N)$ gauge theory. These 'old' string theory ideas [132] have been recently complemented by the realization that at $g^2N \to \infty$ and $N \to \infty$ gauge theories have a dual string description that is analytically tractable [133]. Determining the effective string theory numerically should provide useful hints about what the dual theory might be in the physical weak-coupling limit, $g^2N \to 0$.

In a confining theory there are no decays at $N = \infty$. This is in contrast to what would happen in a non-confining theory where a coloured state could have a finite decay width into other coloured states. But once we constrain states to be colour singlet we reduce the density of final states by factors of N so that all decay widths vanish. In addition there is no scattering between the colour singlet states. Think of two propagating mesons. A meson propagator is like a closed quark loop. Exchange

two gluons between these two closed loops and you clearly gain (up to) a factor of N, but at the cost of $g^4 \propto 1/N^2$. So, no scattering at $N = \infty$. However it is also easy to see that within a single closed loop, planar interactions give factors of g^2N, are not suppressed, and so there are non-trivial bound states. So we have what looks like a free theory, but it has a complex bound state spectrum and so is non-trivial. If one is going to find room in $D = 3 + 1$ for notions of e.g. integrability, it is here in the $N = \infty$ limit that they might find a suitable home.

This theory with no decays and no scattering is similar to the observed world of the strong interactions. In particular the $SU(\infty)$ theory is linearly confining [131, 129]. Now we can ask: is this confining theory close to $SU(3)$? Always in [131], the lightest masses in the spectrum have been calculated for several values of N, and found that the $SU(3)$ mass spectrum is indeed very close to the (extrapolated) spectrum at $N = \infty$. This provides support for the phenomenological relevance of the $SU(\infty)$ theory. And this provides motivation for trying to understand that theory much better. Moreover the effective string theory describing long confining flux tubes appears to be in the bosonic string universality class (see again [131]). More surprisingly, the energy of shorter strings is close to the Nambu-Goto prediction and at smaller N, where this question can be addressed, the string condensation temperature is very close to that of the Nambu-Goto string action.

The large-N gauge theory deconfines as well, and the transition is robustly first order [131] [1].

[1] In Ref. [26] the properties of $SU(N)$ gauge theories have been calculated for several values of N and determined explicitly how the physics varies as N increases, looking at the pure gauge theory, but there are good reasons for believing that the inclusion of quarks will not alter any of our conclusions (except in some obvious ways).

4.2 The Nambu-Goto string theory

The action of the NG model [134] is the area of the worldsheet swept by the propagation of the string. Due to the Weyl anomaly this model is quantum-mechanically consistent only in the critical dimension $D = 26$ (see for example [135]), but since this anomaly is suppressed for long strings [136] it can still be considered as an effective low energy model.

The single string states can be characterized by the number of times w that the string winds around the torus. The spectrum in each case corresponds to the transverse oscillations of the worldsheet that correspond to movers that travel clockwise and anti-clockwise along the string. Thus the string states are characterized by w, by the occupation number $n_{L(R)}(k)$ of left(right) movers that carry energy k, and also by the center of mass momentum $\vec{p}_{\rm c.m.}$. By projecting to zero transverse momentum $(\vec{p}_{\rm c.m.})_\perp$ we are left only with the momentum along the string axis which is quantized in units of $2\pi q/l$ with $q = 0, \pm 1, \pm 2, \ldots$ for a string of length l. These quanta are not independent of $n_{L,R}$ and obey the level matching constraint [2]

$$N_L - N_R \;=\; qw \;, \tag{4.1}$$

where $N_{L(R)}$ enumerates the momentum contribution of the left(right) movers in a certain state as follows

$$N_L = \sum_{k>0} \sum_{n_L(k)>0} n_L(k)\, k, \qquad N_R = \sum_{k'>0} \sum_{n_R(k')>0} n_R(k')\, k' \;. \tag{4.2}$$

It is customary to characterize the string states as irreducible representations of the $SO(D-2)$ symmetry that rotates the spatial directions transverse to the string axis. In our $D = 2+1$ dimensional case, this group becomes the transverse parity P and acts by assigning a minus sign for each mover on the worldsheet. As a result the string states are eigenvectors of P with eigenvalues

$$P = (-1)^{\sum_{i=1} n_L(k_i) + \sum_{j=1} n_R(k'_j)} \;. \tag{4.3}$$

[2] This condition constraints the physical states to be invariant under the gauged diff-invariance of the action [135], and is effectively momentum conservation.

Finally, the energy of a closed-string state with the above quanta is (here we write it for a general number of spacetime dimensions D)

$$(E_{N_L,N_R,q,w})^2 \;=\; (\sigma\, lw)^2 + 8\pi\sigma\left(\frac{N_L+N_R}{2}-\frac{D-2}{24}\right)+\left(\frac{2\pi q}{l}\right)^2 \ . \qquad (4.4)$$

4.2.1 Effective string theories

Since in $2+1$ dimensions the NG string is at best an [137] effective low-energy string theory, it makes sense to generalize it and write the most general form of an effective string action $S_{\rm eff}$ consistent with the symmetries of the flux-tube system. This was done some time ago for the $w=1$ and $q=0$ in [138] and the spectrum obtained for a general number of space-time dimensions D was

$$E_n = \sigma l + \frac{4\pi}{l}\left(n-\frac{D-2}{24}\right)+O(1/l^2)\ , \qquad (4.5)$$

with $n=0,1,2,\ldots$. Here the second term on the right hand side of (4.5) is known as the Lüscher term and is expected to be universal and independent of the particulars of IR-irrelevant interactions of the low energy effective string theories. Indeed, it can be easily verified that the NG model obeys this universality by expanding the square-root of (4.4) to leading order in $1/l$.

The work [138] was more recently extended in [139], where the authors established and used a certain open-closed string duality of the effective string theory. Using this duality they showed that for any number of spacetime dimensions the $O(1/l^2)$ is absent from (4.5), and that in $D=2+1$ the $O(1/l^3)$ has a universal coefficient. Consequently, in $2+1$ dimensions, (4.5) is extended to

$$E_n = \sigma l + \frac{4\pi}{l}\left(n-\frac{1}{24}\right)-\frac{8\pi^2}{\sigma\, l^3}\left(n-\frac{1}{24}\right)^2+O(1/l^4)\ . \qquad (4.6)$$

In the context of the covariant string description, (4.6) implies that

$$E_n = \sqrt{(\sigma l)^2+8\pi\sigma\left(n-\frac{1}{24}\right)+O(1/l^3)}\ , \qquad (4.7)$$

which is a particularly convenient form since the two first terms under the square root are the prediction of the NG model for the energy squared, that we find to be a very good

approximation (see below). A different approach that also leads to similar conclusions is the Polchinski-Strominger effective string theory [140]. While it originally yielded (4.5), it was used recently in [141] to extend the analysis to higher powers of $1/l$ and leads to the same conclusions as [139], but for all values of D.

Establishing what is the structure of the action is of fundamental interest, and so we study the energy spectrum of the flux tube. In particular, we want to determine the spectrum of the adjoint closed string spectrum.

The Nambu-Goto ansatz for the fundamental representation has been already verified with a good accuracy. See Figures 4.1 and 4.2 for an example and references [137] for more details [3].

4.3 $D = 2 + 1 \sim D = 3 + 1$?

We do our calculations in $(2+1)$ dimensions. In the following we report the motivations of this choice, like they were given by [129].

The $D = 2 + 1$ theory shares with its $D = 3 + 1$ homologue four important properties [129].

• Both theories become free at short distances. In 3 dimensions the coupling, g^2, has dimensions of mass so that the effective dimensionless expansion parameter on a scale l will be

$$g_3^2(l) \equiv lg^2 \stackrel{l\to 0}{\longrightarrow} 0 \tag{4.8}$$

In 4 dimensions the coupling is dimensionless and runs in a way we are all familiar with:

$$g_4^2(l) \simeq \frac{c}{\ln(l\Lambda)} \stackrel{l\to 0}{\longrightarrow} 0 \tag{4.9}$$

In both cases the interactions vanish as $l \to 0$, although they do so much faster in the super-renormalizable $D = 2 + 1$ case than in the merely asymptotically free $D = 3 + 1$ case.

[3] The details of the simulations will be presented in the next section.

(a)

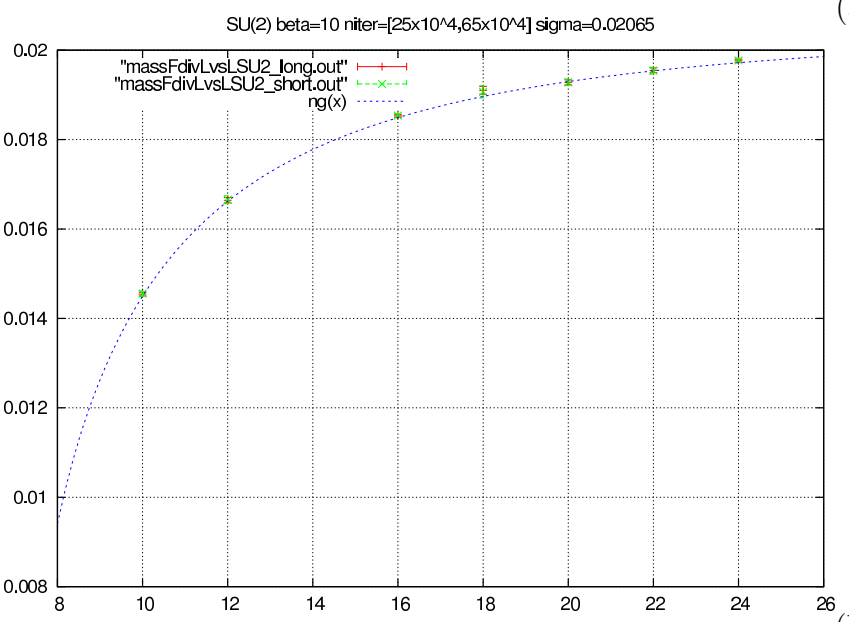

(b)

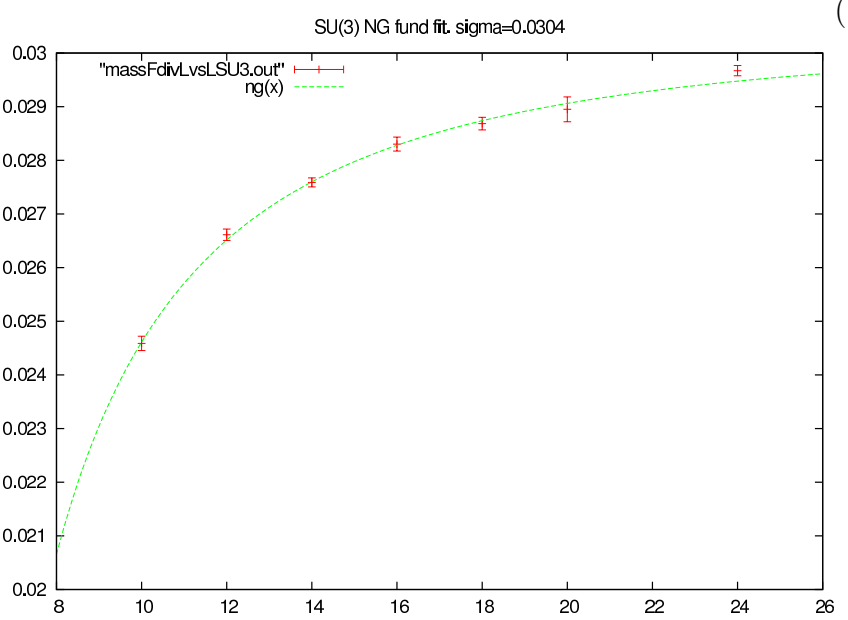

Figure 4.1: The ground state energy per unit length, in lattice units, vs. the string length for $SU(2)$ and $\beta = 10$ (a) and for $SU(3)$ and $\beta = 21$ (b). The blue lines are the results of using the Nambu-Goto fitting ansatz (4.4) for the fundamental representation.

(a)

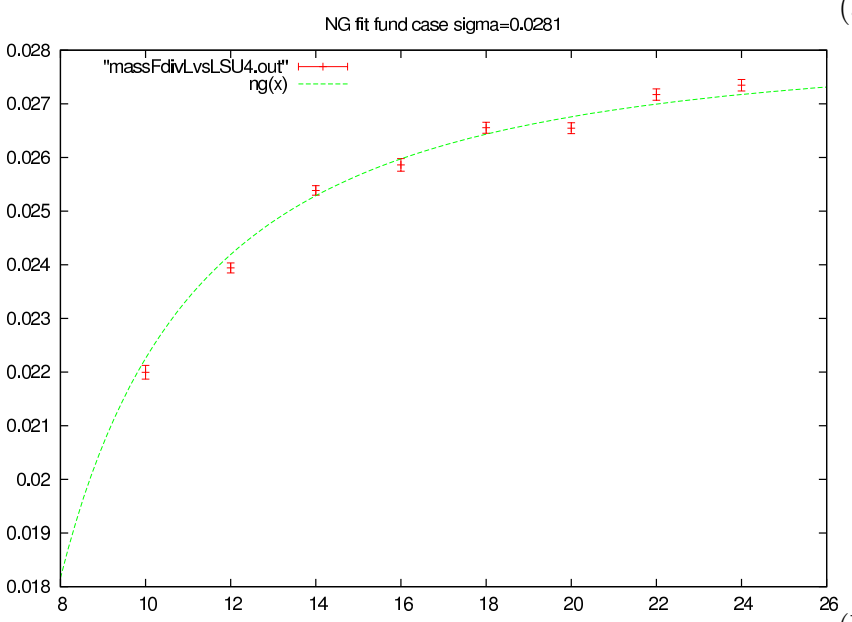

(b)

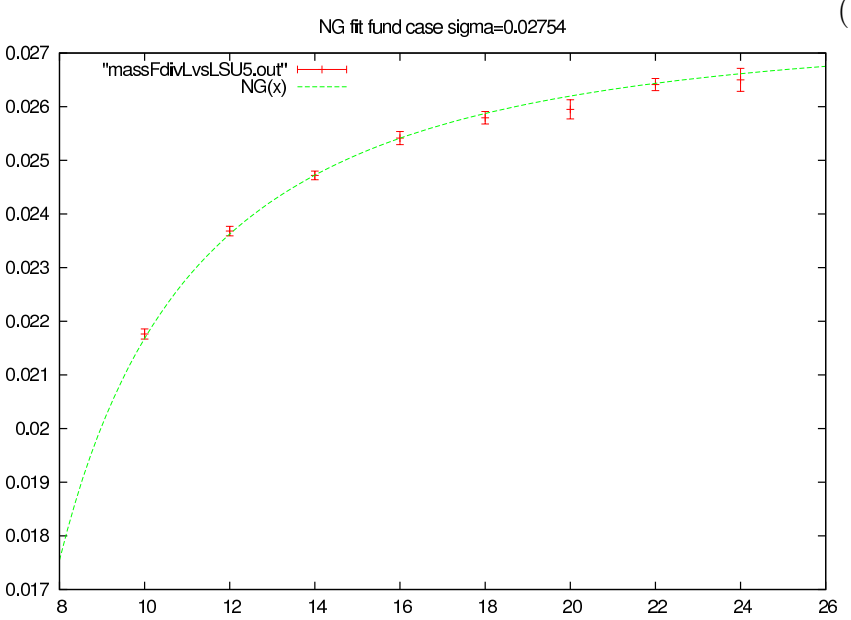

Figure 4.2: The ground state energy per unit length, in lattice units, vs. the string length for $SU(4)$ and $\beta = 40$ (a) and for $SU(5)$ and $\beta = 64$ (b). The blue lines are the results of using the Nambu-Goto fitting ansatz (4.4) for the fundamental representation.

• Both theories become strongly coupled at large distances. Thus in both cases the interesting physics is nonperturbative.

• In both theories the coupling sets the mass scale. In 3 dimensions it does so explicitly:

$$m_i = c_i g^2 \tag{4.10}$$

In 4 dimensions it does so through the phenomenon of dimensional transmutation: the classical scale invariance is anomalous, the coupling runs and this introduces a mass scale through the rate at which it runs:

$$m_i = c_i \Lambda \tag{4.11}$$

• Both theories confine with a linear potential. Lattice simulations provide convincing evidence that this is indeed the case [131]. The $D = 2 + 1$ Coulomb potential is already confining, this is a weak logarithmic confinement, $V_C(r) \sim g^2 \ln(r)$, which has nothing to do with the nonperturbative linear potential, $V(r) \simeq \sigma r$, that one finds at large r.

In addition to these theoretical similarities, the calculated spectra also show some striking similarities [129].

• In both theories the lightest glueball is the scalar 0^{++} with a similar mass $m_{0^{++}} \sim 4\sqrt{\sigma}$. In the $C = +$ sector, the 2^{++} is the next lightest glueball (ignoring any excited scalars) with $m_{2^{++}}/m_{0^{++}} \sim 3/2$ in both cases.

All this has motivated the physicists to believe that a unified treatment makes sense.

Of course there are significant differences as well. For example:

◦ There are no instantons in $D = 2 + 1$ non-Abelian gauge theories. This probably implies quite different quark physics.

◦ The rotation group is Abelian.

◦ The details of the mass spectrum are very different in 3 and 4 dimensions.

The calculations in 3 dimensions are performed in the same way as in 4 dimensions except that the computational problem is much more manageable (lattices grow as L^3 rather than as L^4).

4.4 Numerical simulations

In a gauge-invariant lattice calculation, glueball and string operators are composed of ordered products of link matrices around closed loops [142]. If a is small then we would expect that a good wave-functional for any of the lightest states will be smooth on scales of the order of an appropriate physical length scale and so certainly smooth on the scale of a. One can achieve this by summing over paths between sites and using these, rather than the original link matrices, as the basic components of the operator. By iterating the procedure one can efficiently sum vast numbers of paths, producing operators smooth on physical length scales.

Traditionally there have been two common variants of this procedure, often referred to as 'blocking' [143] and 'smearing' [144] respectively. We only consider loops and links that are space-like, so that the positivity of correlation functions is preserved. Thus all indices will run from 1 to 3.

The smearing and the blocking techniques were described in the previous chapter. For our simulations we used $\alpha = 0.75$ in the smearing algorithm.

4.4.1 unitarisation

There is no fundamental reason why the smeared or blocked matrices should be unitary. However in practice one finds [142] that projecting back to $SU(N)$ produces eventual overlaps that are as good as with any other normalization (and better than most). Thus it is convenient to unitarise. We unitarise by finding the $SU(N)$ matrix U^b that maximizes

$$\mathrm{ReTr}\{\tilde{U}^{b\dagger}U^b\} \tag{4.12}$$

and similarly for smearing. This can be done by using the $\beta = \infty$ limit of the Cabibbo-Marinari heat bath, just as one does when 'cooling' lattice fields to calculate their topological charge [25]. This is an iterative procedure which needs to start with some initial value for U^b, call it U^b_s. Typically one will choose U^b_s to be some very crude unitarisation of $\tilde{U}^b$. After one or two iterations one obtains a good approximation to

U^b in (4.12). The fact that this is an approximation means that one does not maintain exact gauge invariance. However all this will do is to increase slightly the statistical noise in the calculation of correlators. A second potential problem arises in the choice of the crude starting point, U^b_s. Typically this will not be the same for U^b and for $U^{b\dagger}$. For example if one obtains U^b_s by orthonormalising the columns of $\tilde{U}^b$ one by one, as we do, one gets a different matrix than if one started by orthonormalising the rows.

4.4.2 variational calculation

We can calculate the string tension by calculating the energy of the lightest state composed of a static q and $\bar{q}$ a distance R apart. (Any fundamental charges will do; we use q for quarks because they are so familiar.) If we have linear confinement then this energy, $E_{min}(R)$, provides our definition of the string tension, σ, as well as providing us with a definition of the static quark "potential", $V_{q\bar{q}}(R)$,

$$E_{min}(R) \equiv V_{q\bar{q}}(R) \stackrel{R\to\infty}{\simeq} \sigma R \ . \tag{4.13}$$

For large R one thinks of this state as being composed of the dressed static quarks with a confining flux tube of length $\simeq R$ joining them.

As Ref. [129] notes, the usual potential that enters phenomenological discussions of the string tension [145] is essentially based on the Schrödinger equation and the relationship with our definition is not a simple one; this is apparent if one considers, for example, the case of QCD. Vacuum quark fluctuations break the string, so the potential as defined in (4.13) will flatten off for larger R. The phenomenological potential, on the other hand, continues to rise, although it may acquire a modest imaginary part to incorporate the decay of the confining flux tube. Effectively it incorporates information about the time-scales associated with the different dynamical processes that contribute. The two definitions differ most dramatically in the large-N, narrow-width limit of QCD.

We follow for the operators the construction method of [129].

To project onto this $q\bar{q}$ state we define the gauge-invariant operator

$$\phi(t) = \bar{q}(0) \prod U_l q(R) \ , \tag{4.14}$$

where we can suppose that the quarks are separated along the x-direction and the the product of link matrices is along the shortest path joining them. The correlation function of this operator, taken from $t = 0$ to $t = T$, will, for large enough T, be $\propto \exp\{-E_{min}(R)T\}$. This correlation function involves two quark propagators; one from $(x = R, t = 0)$ to $(x = R, t = T)$ and the other from $(x = 0, t = T)$ to $(x = 0, t = 0)$. In the $m_q \to \infty$ limit (which is how one implements static quarks dynamically) the quark hops along the shortest available route: that is to say its propagator is equal to the product of links along the straight line joining its end-points. Thus the correlation function is equal (up to some irrelevant factor) to the expectation value of the Wilson loop, $\langle W(R,T)\rangle$. If we have linear confinement, as in (4.13), then $\langle W(R,T)\rangle \propto \exp\{-E_{min}(R)T\} \propto \exp\{\sigma RT\}$, the usual confining area decay of Wilson loops. This calculation was improved [129].

We use Polyakov loops rather than Wilson loops. Construct a product of link matrices that closes on itself through a spatial boundary; for example

$$\phi_P(x,t) = \mathrm{Tr} \prod_{n=1}^{L} U_y(x, y + n\hat{y}, t) \tag{4.15}$$

on a $L \times L$ spatial lattice. This non-contractible loop is what one gets if one stretches our operator in (4.14) till the q and $\bar{q}$ meet and annihilate. It couples to the corresponding state: a flux tube of length L that encircles the torus. Such an operator has zero overlap onto any contractible loop. One can readily prove this using the symmetry of the action and measure under the transformation $U_y(x, y_0, t) \to z_N U_y(x, y_0, t), \forall t$ where y_0 is an arbitrarily chosen value of y and z_N is a non-trivial element of the center. A contractible loop is obviously invariant under this symmetry while the Polyakov loop is not. This argument breaks down if the symmetry is spontaneously broken; which occurs, for example, in the high temperature deconfining phase.

If we sum over x to make ϕ translation invariant ($\vec{p} = 0$) and form the correlation function, we obtain at large t the mass, $m_P(L)$, of the lightest state containing a periodic flux loop of length aL

$$\langle \phi_P^\dagger(t)\phi_P(0)\rangle \quad \overset{t\to\infty}{\propto} \quad e^{-m_P(L)t}$$

$$= \quad e^{-\{\sigma aL - \frac{\pi}{6aL} + \ldots\}t} \tag{4.16}$$

Here we have explicitly included the first correction term which is the translation to Polyakov loops [146] of the usual Lüscher correction [147] for Wilson loops. This correction is 'universal', but obviously one needs to test whether the physical flux tube does indeed fall into this particular universality class.

Using Wilson loops produces a heavy-quark potential. This contains a Coulomb term which is long range $\propto g^2 \log r$ in $D = 2 + 1$. This term will of course be screened, but having to disentangle it from the linear piece, at the intermediate values of r where the calculations are accurate, can decrease the accuracy of the estimate of σ. In $D = 3{+}1$ the Coulomb term is $\propto 1/r$ and its presence makes it difficult to identify the $\pi/12r$ universal string correction. By contrast, in using as we do correlators of $\vec{p} = 0$ sums of *spatial* Polyakov loops, we have completely dispensed with any charges and have transformed the problem into a standard mass calculation. Because there are no charges, there is no longer a Coulomb contribution. This benefit has of course been achieved at a price: we no longer have a calculation of the heavy quark potential, but only of the string tension.

Two technical asides. When using link matrices at a blocking level N_B, the sites are spaced a distance $2^{N_B-1}a$ apart. A given product of blocked links, that starts at say $y = 1$, is not quite invariant under translations in the y-direction because the blocked links themselves are not completely invariant. One can remedy this by summing products that start at $y = 1, 2, .., 2^{N_B-1} - 1$ respectively; and this does in fact improve the operator overlap slightly. A second point is that L need not be divisible by the length of the blocked link. In that case we include links of a lower blocking level, averaged with staples that include transverse links blocked to the level of interest. (In practice this extra smearing with staples is of marginal utility in getting a good overlap.)

The procedure to extract the masses are entirely conventional [129]. The starting point is the observation that

$$\begin{aligned} \langle \phi^\dagger(t)\phi(0)\rangle \quad &= \quad \sum_n |\langle \mathrm{vac}|\phi|n\rangle|^2 \exp\{-E_n t\} \\ &\stackrel{t\to\infty}{\longrightarrow} \quad |\langle \mathrm{vac}|\phi|0\rangle|^2 \exp\{-E_0 t\} \end{aligned} \tag{4.17}$$

where $|0\rangle$ is the lightest state that couples to the operator ϕ and E_0 is its energy. (We use operators that are localized within a single time-slice.) So if we want the mass of the lightest colour singlet state with quantum numbers J, P, C we simply construct a $\vec{p} = 0$ operator with those quantum numbers, calculate its correlation function and then obtain the mass ($=E_0$) using (4.17). If the quantum numbers are trivial, the lightest state might be the vacuum, in which case we use vacuum subtracted operators.

On the lattice [4] $t = na$ and so what we obtain, not surprisingly, is aE_n, the energy in lattice units. Note that if we are on a lattice with a finite periodic temporal extent, then the expression in (4.17) needs to have an additional term for the propagation around the 'back' of the torus. Such a term will always be included in the numerical calculations, although we shall, for simplicity, persist in writing all our expressions as though the temporal extent were infinite. We also note that the temporal extent of our lattice, $T \equiv aL_t$, will always be chosen large enough for the partition function, Z, to be accurately given by its vacuum contribution: $Z \simeq \exp\{-E_{\rm vac}T\}$. Thus the energies we calculate will always be with respect to the energy of the vacuum.

In principle we can obtain from (4.17) any number of excited states as well. In practice, however, fitting sums of exponentials to a function is a badly conditioned problem. So one needs to develop a more sophisticated strategy [129].

Again in principle, one can use in (4.17) any operator with the desired quantum numbers. However, a numerical calculation has finite statistical errors and because the function $\langle\phi^\dagger(t)\phi(0)\rangle$ is decreasing roughly exponentially in t it will, at large enough t, disappear into the statistical noise. Thus in practice we need to be able to extract E_0 from (4.17) at small values of t. This requires the coefficient $|\langle{\rm vac}|\phi|0\rangle|^2$ to be large. That is to say, we need to use operators that are close to the wave-functional of the state in question.

If we want to use good operators, we obviously need some simple way to decide which operator is in fact better.

[4] We use the Wilson action. The Monte Carlo consists of a mixture of heat bath and over-relaxation sweeps.

Thus it would be useful to have a simple practical criterion to decide, early on in a calculation, which operator is the best. Such a criterion is immediately suggested (see again [129]) by considering the normalized correlation function:

$$C(t) \equiv \frac{\langle \phi^\dagger(t)\phi(0)\rangle}{\langle \phi^\dagger(0)\phi(0)\rangle} = \frac{\langle \phi^\dagger e^{-Ht}\phi\rangle}{\langle \phi^\dagger\phi\rangle} \tag{4.18}$$

Clearly if we were using a complete basis of operators, then the best operator would be the one that maximized $C(t)$: it would be the wave-functional of the lightest state and we would have $C(t) = \exp\{-m_G t\}$. If the basis is not complete, this suggests a variational criterion: the 'best' operator, ϕ, is the one which maximizes $C(t)$.

Our strategy for obtaining estimates of the ground state and excited state masses is the standard procedure [148]. It can be summarized in the following steps:

• we contract a set of M lattice operators, $\phi_i : i = 1, .., M$, with desired quantum numbers;

• we define the $M \times M$ correlation matrix $C(t)$ by

$$C_{ij}(t) = \langle {\phi_i}^\dagger(t)\phi_j(0)\rangle \quad . \tag{4.19}$$

• let the eigenvectors of the matrix $C^{-1}(0)C(a)$ be $\vec{v}^i; i = 1, \ldots, M$. Then

$$\Phi_i = c_i \sum_{k=1}^{M} v_k^i \phi_k \equiv \sum_{k=1}^{M} a_{ik}\phi_k \tag{4.20}$$

where the constant c_i is chosen so that Φ_i is normalized to unity.

• we extract the correlator for each state $\Gamma_n(t) = \sum_{ij} v_i^{*(n)} v_j^{(n)} C_{ij}(t)$

• for each correlation function we look for a 'plateau' in the effective masses. We so extract the mass (energy) for each state

$$m_n = -\ln\frac{\Gamma_n(t)}{\Gamma_n(t-1)} \ .$$

For the excited states we expect, with our incomplete basis, to have some admixture of lighter eigenstates, and so the initial plateau should be finite and will eventually drop to the masses of the lighter states. That is to say, for excited states the mass estimate can be lower than the mass of the state whose mass is being estimated. This

undoubtedly means that there is a larger systematic error on our estimate of the mass of an excited state than on that of a ground state. We do not know how to estimate this error (for either type of state).

There are of course many variations possible on the above procedure.

At this preliminary stage we have studied $N = 2, 3, 4, 5$. In particular we have studied [129]: $SU(2)$ with $a\sqrt{\sigma} \sim 0.1622(4)$ ($\beta = 10$), $SU(3)$ with $a\sqrt{\sigma} \sim 0.17479(38)$ ($\beta = 21$), $SU(4)$ with $a\sqrt{\sigma} \sim 0.1680(30)$ ($\beta = 40$) and $SU(5)$ with $a\sqrt{\sigma} \sim 0.1664(4)$ ($\beta = 64$) [5].

We have used different operators (with 4 or 5 blocking levels, depending on the length of the string). In particular, we have used the fundamental operator

$$\phi(x,t) = \prod_{k=1}^{L_y} U(x, y + n\hat{y}, t) \ , \tag{4.21}$$

but also with transverse momentum different from zero

$$\phi(p) = (\mathrm{Tr}\phi) e^{ipx_{xy}} \qquad p = \frac{2\pi}{L_y} n, \quad n = \pm 1, \pm 2, \pm 3, \pm 4 \ , \tag{4.22}$$

and the adjoint operator [6]:

$$\phi^{\mathrm{adj}} = (|\mathrm{Tr}\phi|^2 - 1) \ . \tag{4.23}$$

In Figs. 4.3 and 4.4 we present our very preliminary results. In Fig. 4.5 it is an example of Nambu-Goto fit for the adjoint ground state if the $SU(3)$ ($\beta = 21$).

4.5 Work in progress

At this stage the work is not complete, since we want to increase the number of operators for the variational technique. The determination of the excited masses of the spectrum for the adjoint string is not an easy calculation, since they have quite big values, other elements of the spectrum have to be considered.

[5] All values are referred to $L = 24$.

[6] To increase the overlap we have added also glueball states, for 0^+ quantum numbers.

(a)

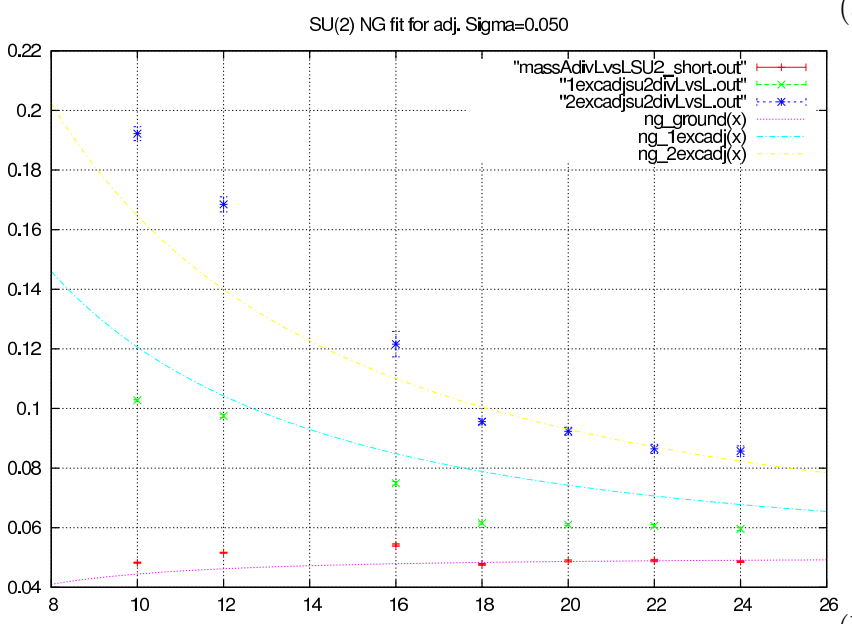

(b)

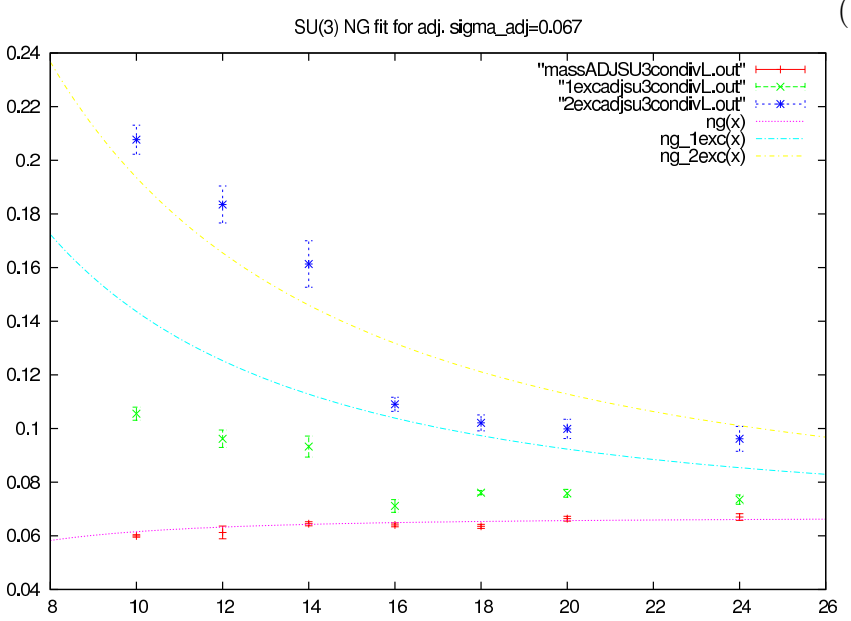

Figure 4.3: The energy of the ground, 1st and the 2st excited states per unit length, divided by $\sqrt{\sigma}l$, for $SU(2)$ (a) and $SU(3)$ (b) ($\beta = 10$ and $\beta = 21$ respectively). The dashed lines are the NG prediction for the adjoint string.

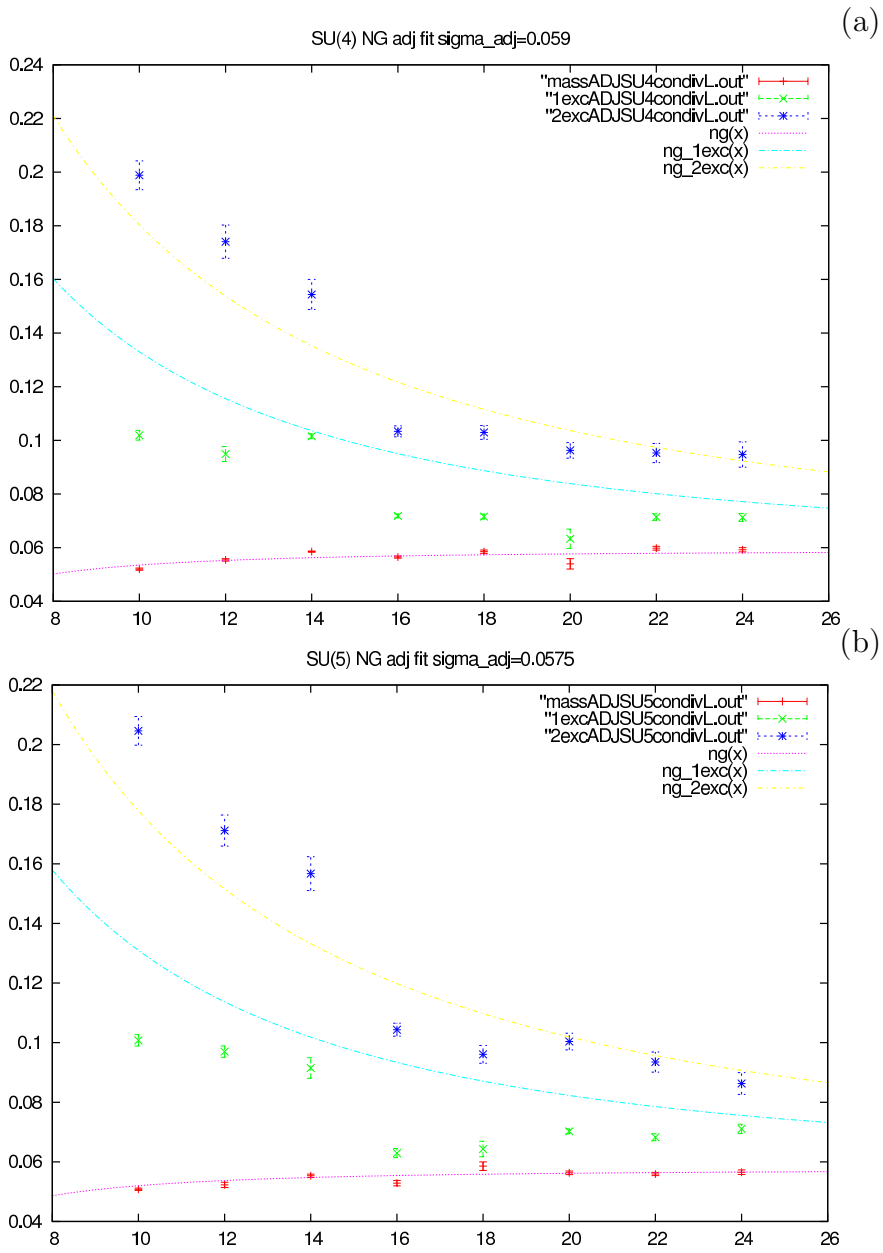

Figure 4.4: The energy of the ground, 1st and the 2st excited states per unit length, divided by $\sqrt{\sigma}l$, for $SU(4)$ (a) and $SU(5)$ (b) ($\beta = 40$ and $\beta = 64$ respectively). The dashed lines are the NG prediction for the adjoint string.

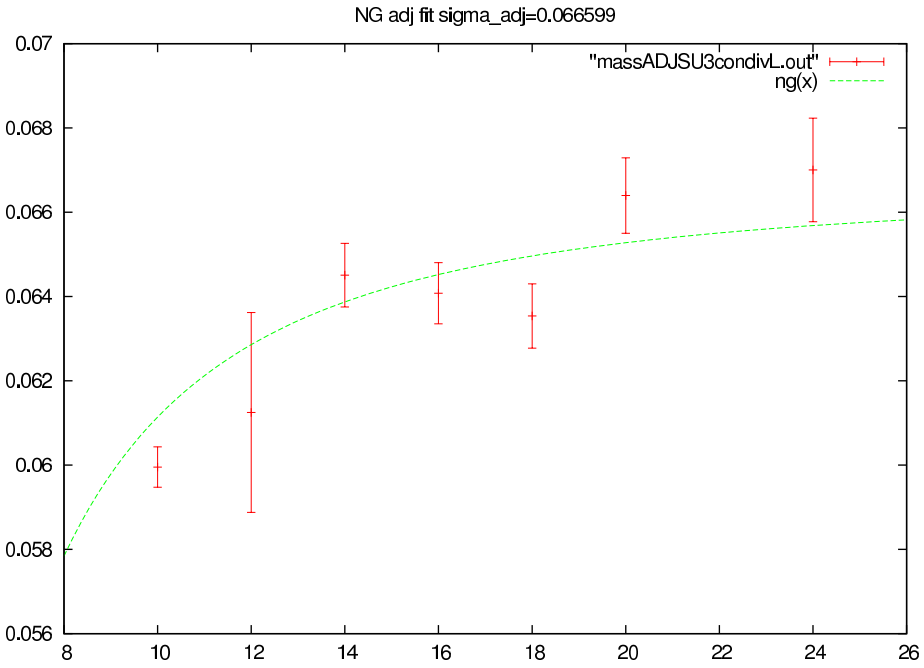

Figure 4.5: Example of NG fit for the ground state of adjoint string for $SU(3)$, $\beta = 21$.

Bibliography

[1] Aitchison H., *Gauge Theories In Particle Physics - Vol I*, Taylor and Francis (2002)

[2] Yang C.N. and Mills R.L., Phys. Rev. **96**, 191 (1954)

[3] Utiyama R., Phys. Rev. **101**, 1597 (1955)

[4] 't Hooft G., Nucl. Phys. **B33**, 173 (1971)

[5] Gross D.J. and Wilczek F., Phys. Rev. Lett. **30**, 1434 (1973)

[6] Politzer H.D., Phys. Rev. Lett. **30**, 1346 (1973)

[7] Rothe H. J., *Lattice Gauge Theories An Introduction*, World Scientific (1992)

[8] Creutz M. J., *Quarks, gluons and lattices*, Cambridge University Press (1983)

[9] Montvay I. and Münster G, *Quantum Fields on a Lattice*, Cambridge Monographs on Mathematical Physics (1994)

[10] Heisenberg W., Z. Phys. **33**, 877 (1925)

[11] Born M. and Jordan P., Z. Phys. **34**, 858 (1925)

[12] Muta T., *Foundations of quantum chromodynamics. Second edition*, World Sci. Lect. Notes Phys. **57** (1998)

[13] Feynman R.P., Rev. Mod. Phys. **20**, 367 (1948)

[14] Feynman R.P., Hibbs A.R. *Quantum Mechanics and Path Integrals*, New York, USA, McGraw-Hill (1965)

[15] Gelfand I.M., Yaglom A.M., Fortschr. Phys **5**, 517 (1957)

[16] Abreu M.C. *et al.* (NA38 collab.), Phys. Lett. **B192**, 163 (1987);
Z. Phys. **C38**, 117 (1988)

[17] Grossiord J.Y. *et al.* (NA38 collab.), Nucl. Phys. **A498**, 249 (1989)

[18] Baglin C. *et al.* (NA38 collab.), Phys. Lett. **B220**, 471 (1989)

[19] Pisarski R. D., [hep-lat/0203271]

[20] Svetitsky B. and Yaffe L. G., Nucl. Phys. **B210**, 423 (1982)

[21] Itzykson C., Drouffe J. M., *Statistical Field Theory. Vol. 2: Strong Coupling, Monte Carlo Methods, Conformal Field Theory, Snd Random System*, Cambridge University Press (1989)

[22] Metropolis N., Rosenbluth A.W., Rosenbluth M.N., Teller A.H. and Teller E., J. Chem. Phys. **21**, 1087 (1953)

[23] Kennedy A. and Pendleton B, Phys. Lett. **B156**, 393 (1985)

[24] Cabibbo N. and Marinari E., Phys. Lett. **B119**, 387 (1982)

[25] Hoek J., Teper M. and Waterhouse J., Phys. Lett. **B180**, 112 (1986);
Nucl. Phys. **B288**, 589 (1987)

[26] Teper M., Newton Inst. NATO-ASI School Lectures, July 1997, [hep-lat/9711011]

[27] Petronzio R. and Vicari E., Phys. Lett. **B248**, 159 (1990)

[28] Adler S., Phys. Rev. **D37**, 458 (1988)

[29] Creutz M, Phys. Rev. **D36**, 515 (1987);
Brown F. and Woch T., Phys. Rev. Lett. **58**, 2394 (1987)

[30] Kennedy A., Nucl. Phys. B (Proc. Suppl.) **30**, 96 (1993);
Wolff U., Nucl. Phys. B (Proc. Suppl.) **17**, 93 (1990);
Adler S., Nucl. Phys. B (Proc. Suppl.) **9**, 437 (1989)

[31] Berg B., Phys. Lett. **B104**, 475 (1981)

[32] Teper M., Phys. Lett. **B162**, 357 (1985);
B171, 81,86 (1986);
Ilgenfritz E.M., Laursen M.L., Muller-Preubker M., Schierholz G. and Schiller H., Nucl. Phys. **B268**, 693 (1986);
Hoek J.,Teper M. and Waterhouse J., Nucl. Phys. **B288**, 589 (1987);
Smit J. and Vink J.C., Nucl Phys. **B284**, 234 (1987);
Phys. Lett. **B194**, 433 (1987);
Nucl. Phys. **B298**, 557 (1988)

[33] Campostrini M., Di Giacomo A., Panagopoulos H. and Vicari E., Nucl. Phys. **B329**, 683 (1990)

[34] Di Giacomo A., Maggiore M. and Olejnik S., Nucl. Phys. **B347**, 441 (1990)

[35] Polikarpov M.I. and Veselov A.I., Nucl. Phys. **B297**, 34 (1988)

[36] Bonnet F., Fitzhenry P., Leinweber D.B., Stanford M.R, Williams A.G., Phys. Rev. **D62**, 094509 (2000)

[37] Falcioni M., Paciello M., Parisi G., Taglienti B., Nucl. Phys. **B251**, 624 (1985);
Albanese M. *et al.*, Phys. Lett. **B192**, 163 (1987)

[38] Hetrick J.E. and de Forcrand P., Nucl. Phys. Proc. Suppl. **63**, 838 (1998)

[39] Bernard C. and DeGrand T., [hep-lat/9909083]

[40] DeGrand T. [MILC collaboration], Phys. Rev. **D60**, 094501 (1999)

[41] Bali G.S. and Schilling K., Phys. Rev. **D46**, (1992) Vol. 6

[42] Hoek J., Teper M. and Waterhouse J., Phys. Lett. **B180**, 112 (1986);
Nucl. Phys. **B288**, 589 (1987)

[43] Campostrini M. *et al.*, Phys. Lett. **B212**, 206 (1988)

[44] Basak S. and De A.K., Phys. Lett. **B430**, 320 (1998)

[45] Landau L.D., Phys. Z. Sowjun. **11**, 26 (1937);
Zh. Éksp. Teor. Fiz. **7**, 19 (1937);
Phys. Z. Sowjun. **11**, 545 (1937);
Zh. Éksp. Teor. Fiz. **7**, 627 (1937)

[46] Eugene S.H., *Introduction to Phase Transitions and Critical Phenomena*, Oxford Science Publications (1990)

[47] Zinn-Justin J. *Quantum Field Theory and Critical Phenomena*, UK, Oxford University Press (1989)

[48] Chandler D., *Introduction to Modern Statistical Mechanics*, Oxford University Press (1987)

[49] Pisarski R.D., Phys. Rev. **D62**, 111501 (2000)

[50] 't Hooft G., Nucl. Phys. **B153**, 141 (1979)

[51] Polyakov A.M, Phys. Lett. **B72**, 477 (1978)

[52] Susskind L., Phys. Rev. **D20**, 2610 (1979)

[53] Fukugita M., Kaneko T. and Ukawa A., Phys. Lett. **B154**, 185 (1985)

[54] Bacilieri P. *et al.*, Phys. Rev. Lett. **61**, 1545 (1988)

[55] Brown F.R., Christ N.H., Deng Y., Gao M. and Woch T.J., Phys. Rev. Lett. **61**, 2058 (1988)

[56] Kogut J. *et al.*, Phys. Rev. Lett. **51**, 869 (1983)

[57] Kaczmarek O., Karsch F., Laermann E. and Lütgemeier M., Phys. Rev. **D62**, 034021 (2000)

[58] Gavai R.V., Karsch F. and Petersson B., Nucl. Phys. **B322**, 738 (1989)

[59] Svetitsky B. and Yaffe L.G., Nucl. Phys. **B210**, 423 (1982)

[60] Gliozzi F. and Provero P., Phys. Rev. **D56**, 1131 (1997)

[61] Fiore R., Gliozzi F. and Provero P., Phys. Rev. **D58**, 114502 (1998)

[62] Engels J. and Scheideler T., Nucl. Phys. **B539**, 557 (1999)

[63] Fortunato S., Karsch F., Petreczky P. and Satz H., Nucl. Phys. (Proc.Suppl.) **94**, 398 (2001)

[64] Fiore R., Papa A. and Provero P., Nucl. Phys. (Proc.Suppl.) **106**, 486 (2002)

[65] Fiore R., Papa A. and Provero P., Phys. Rev. **D63**, 117503 (2001)

[66] Papa A. and Vena C., Int. J. Mod. Phys. **A19**, 3209 (2004)

[67] Pelissetto A. and Vicari E., Phys. Rept. **368**, 549 (2002)

[68] Blöte H.W.J. and Swendsen R.H., Phys. Rev. Lett. **43**, 779 (1979)

[69] Janke W. and Villanova R., Nucl. Phys. **B489**, 679 (1997) and references therein

[70] Caselle M., Hasenbusch M. and Provero P., Nucl. Phys. **B556**, 575 (1999)

[71] Caselle M., Hasenbusch M., Provero P. and Zarembo K., Nucl. Phys. **B623**, 474 (2002)

[72] Fiore R., Papa A. and Provero P., Nucl. Phys. (Proc. Suppl.) **119**, 490 (2003)

[73] Fiore R., Papa A. and Provero P., Phys. Rev. **D67**, 114508 (2003)

[74] Falcone R., Fiore R., Gravina M. and Papa A., Nucl. Phys. **B785**, 19 (2007)

[75] Falcone R., Fiore R., Gravina M. and Papa A., Nucl. Phys. **B767**, 385 (2007)

[76] Blöte H.W.J. and Swendsen R.H., Phys. Rev. Lett. **43**, 779 (1979)

[77] Janke W. and Villanova R., Nucl. Phys. **B489**, 679 (1997) and references therein.

[78] Gavai R.V., Karsch F. and Petersson B., Nucl. Phys. **B322**, 738 (1989)

[79] Karsch F. and Stickan S., Phys. Lett. **B488**, 319 (2000)

[80] Polyakov A.M., Phys. Lett. **B72**, 477 (1978) Susskind L., Phys. Rev **D20**, 2610 (1979)

[81] Meisinger P.N., Miller T.R., Olgivie M.C., Phys. Rev. **D65**, 034009 (2002); Phys. Rev. **D65**, 056013 (2002)

[82] Wirstam J., [hep-lat/0106141]

[83] Bialas P., Morel A., Petersson B., Petrov K., and Reisz T., these proceedings

[84] Dumitru A. and Pisarski R.D., Nucl. Phys. (Proc. Suppl.) **106**, 483 (2002)

[85] Dumitru A. and Pisarski R.D., Phys. Lett. **B504**, 282 (2001)

[86] Kronfeld A.S., Nucl. Phys. (Proc. Suppl.) **17** 313 (1990)

[87] Lüscher M. and Wolff U., Nucl. Phys. **B339**, 222 (1990)

[88] Agostini V., Carlino G., Caselle M. and Hasenbusch M. Nucl. Phys. **B484**, 331 (1997)

[89] Fisher M.E. and Berker A.N., Phys. Rev. **B26**, 2507 (1982)

[90] Nadkarni S., Phys. Rev. **D33**, 3738 (1986)

[91] Dumitru A.and Pisarski R.D., Phys. Rev. **D66**, 096003 (2002)

[92] Adler S.L., Phys. Rev. **D23**, 2901 (1981)

[93] Boyd G., Engels J., Karsch F., Laermann E., Legeland C., Lutgemeier M. and Petersson B., Nucl. Phys. **B469**, 419 (1996)

[94] Datta S. and Gupta S., Nucl. Phys. **B534**, 392 (1998)

[95] Grossman B., Gupta S., Heller U.M. and Karsch F., Nucl. Phys. **B417**, 289 (1994)

[96] Baker M., James S., and Zachariasen F., Phys. Rep. **209**, 73 (1991)

[97] 't Hooft ., in *High Energy Physics, Proceedings of the EPS International Conference, Palermo, 1975, Italy*, edited by A. Zichichi, (Editrice Compositori, Bologna 1976); 't Hooft G., Physica Scripta **25**, 133 (1982)

[98] Mandelstam S., Phys. Rep. **C23**, 245 (1976)

[99] Abrikosov A.A., Sov. Phys. JETP **32**, 1442 (1957)

[100] Nielsen H.B. and Olesen P., Nucl. Phys. **B61**, 45 (1973)

[101] Baker M., Ball J.S. and Zachariasen F., Phys. Rept. **209**, 73 (1991)

[102] Ripka G., [hep-ph/0310102]

[103] Bali G.S., Quark confinement and the hadron spectrum III 17-36, Newport News 1998 [hep-ph/9809351]

[104] Bringoltz B. and Teper M., PoS **LAT2005**, 175 (2006)

[105] Cea P. and Cosmai L., Nucl. Phys. Proc. Suppl. **47**, 318 (1996)

[106] Liao J. and Shuryak E.V., Phys. Rev. **C53**, 054907 (2007)

[107] Dirac P.A.M., Proc. R. Soc. London **A133**, 60 (1931)

[108] Mandelstam S., Phys. Rept. **23**, 245 (1976);
't Hooft G., Nucl. Phys. **B190**, 455 (1981)

[109] Chagdaa S. and Laermann E., PoS **LAT2007**, 172 (2007)

[110] Kaczmarekand O. and Zantow F., PoS **LAT2005**, 192 (2006)

[111] Petreczky P. and Petrov K., Phys. Rev. **D70**, 054503 (2004)

[112] Kaczmarek O., Karsch F., Petreczky P. and Zantow F., Phys. Lett. **B543**, 41 (2002)

[113] Pennanen P. and Michael C. [UKQCD Collaboration], [hep-lat/0001015]

[114] Liao J. and Shuryak E., arXiv:0706.4465 [hep-ph]

[115] Di Giacomo A., Maggiore M., and Olejnìk Š., Phys. Lett. **B236**, 199 (1990)

[116] Di Giacomo A., Acta Phys. Pol. **B25**, 215 (1994)

[117] Campostrini M., Di Giacomo A., Maggiore M., Panagopoulos H., Vicari E., Phys. Lett. **B225**, 403 (1989)

[118] Flower J.W. and Otto S.W., Phys. Lett. **B160**, 128 (1985)

[119] Cea P. and Cosmai L., Phys.Rev. **D52**, 5152 (1995)

[120] Bali G.S, Schilchter C., Schilling K., Phys. Rev. **D51**, 5165 (1995)

[121] Bolder B., Struckmann T., Bali G.S, Eicker N., Lippert Th., Orth B., Schilling K., Ueberholz P., Phys. Rev. **D63**, 074504 (2001)

[122] Bali G.S. and Schilling K., Phys. Rev. **D46**, 2636 (1992)

[123] Bali G.S. and Schilling K., Phys. Rev. **D47**, 661 (1993)

[124] Bali G.S., Schilling K. and Wachter A., Phys. Rev. **D56**, 2566 (1997)

[125] Bali G., Bolder B., Eicker N., Lippert Th., Orth B., Ueberholz P., Schilling K., Struckmann T. [SESAM - TχL Collaboration], Phys. Rev. **D62**, 054503 (2000)

[126] see *e. g.* Foley J.D. *et al.*, Computer Graphics: Principles and Practice, Addison Wesley Publ. Company 1996 London.

[127] 't Hooft G., Nucl. Phys. **B72**, 461 (1974);
Nucl. Phys. **B75**, 461 (1974)

[128] Witten E., Nucl. Phys. **B160**, 57 (1979)

[129] Teper M., Phys. Rev. **D59** 014512 (1999)

[130] Das S.R., Rev. Mod. Phys. **59**, 235 (1987)

[131] Teper M., [hep-th/0412005]

[132] Polyakov A.M., *Gauge Fields and Strings* (Harwood, 1987).
J. Polchinski, [hep-th/9210045]

[133] Maldacena J., TASI 2003 Lectures on AdS/CFT, [hep-th/0309246];
Aharony O., Gubser S., Maldacena J., Ooguri H. and Oz Y., Phys. Rept. **323** (2000) 183 [hep-th/9905111]

[134] Nambu Y., Phys. Rev. **D10**, 4262 (1974);
Phys. Lett. **B80**, 372 (1979);
Arvis J.F., Phys. Lett. **B127**, 106 (1983)

[135] Polchinski J., *Cambridge, UK: Univ. Pr. (1998) 402 p*

[136] Olesen P., Phys. Lett. **B160**, 144 (1985)

[137] Athenodorou A., Bringoltz B., Teper M., Phys. Lett.**B656**, 132 (2007)

[138] Lüscher M., Symanzik K. and Weisz P., Nucl. Phys. **B173**, 365 (1980);
Lüscher M., Nucl. Phys. **B180**, 317 (1981)

[139] Lüscher M. and Weisz P., JHEP **0407**, 014 (2004);
JHEP **0207**, 049 (2002)

[140] Polchinski J. and Strominger A., Phys. Rev. Lett. **67**, 1681 (1991)

[141] Drummond J.M., [hep-th/0411017]; [hep-th/0608109];
Hari Dass N.D. and Matlock P., [hep-th/0606265]; [hep-th/0611215]

[142] Lucini B., Teper M., Wenger U., JHEP 0406:012,2004

[143] Teper M., Phys. Lett. **B183**, 345 (1987);
Phys. Lett. **B185**, 121 (1987)

[144] Albanese M. *et al.*, Phys. Lett. **B192**, 163 (1987);
Phys. Lett. **B197**, 400 (1987)

[145] Perkins D., *Introduction to High Energy Physics* (Addison-Wesley 1972)

[146] De Forcrand Ph., Schierholz G., Schneider H. and Teper M., Phys. Lett. **B160**, 137 (1985)

[147] Lüscher M., Symanzik K. and Weisz P., Nucl. Phys. **B173**, 365 (1980)

[148] Berg B. and Billoire A., Nucl. Phys. **B221**, 109 (1983);
Fox G.C., Gupta R., Martin O. and Otto S., Nucl. Phys. **B205**, 188 (1982);
Lüscher M. and Wolff U., Nucl. Phys. **B339**, 222 (1990);
Kronfeld A.S., Nucl. Phys. B (Proc. Suppl.) **17** (1990) 313

Acknowledgements

Un doveroso e sentito ringraziamento al Prof. Alessandro Papa, supervisore attento e disponibile. Grazie per la pazienza accordata e per i preziosi consigli forniti. Proverò a ricercare la semplicità, qualsiasi cosa "farò da grande"...

Un dolcissimo abbraccio a Mario.
Diciamo pure che senza di te, non sarebbe stato lo stesso.

Diffusi baci ed abbracci a:
Fiamma, perché senza troppa enfasi, sei la mia vita
Luca, perché sei la mia vicina anima "gemella"
Giuliano, perché non avrei avuto casa senza di te, sarei rimasta senza fissa dimora
Giangi, per tutti i libri scambiati e le più truci discussioni
Evelin, per le dolci e salate pause
Pietro, per gli aiuti informatici tempestivi
Sandro, perché hai visto il fisico lì dove io non vedevo niente
Maria Fernanda, gracias a ti he empezado a amar este nuevo idioma
Fazius, perché non c'è gusto senza qualche dissapore
Antonio, perché sei capitato nella mia vita